Stem cells and neoplasia: a study of acquired melanocytic naevi

Anita Bonthuys

(BNTANI001)

Supervisors: Prof. S. Kidson and Prof. G. Todd

Thesis presented for the degree of Master of Science in Medicine

Division of Cell Biology

Department of Human Biology

Faculty of Health Sciences

University of Cape Town

July 2012

Declaration

I, Anita Bonthuys, hereby declare that the work on which this thesis is based is my original work (except where acknowledgements indicate otherwise) and that neither the whole work nor any part of it has been, is being, or is to be submitted for another degree in this or any other university. I empower the University of Cape Town to reproduce for the purpose of research either the whole work or any portion of the contents in any manner whatsoever.

_____

_____

Acknowledgements

The following people have been instrumental in making this work a reality. Thank you.

Prof. Sue Kidson, for giving me the opportunity to explore the field of cell biology, to grasp numerous new techniques and to discover a great love for laboratory based research. Your immense passion for science and the enthusiasm with which you approach every question has been both stimulating and inspiring. Thank you for your never-ending patience, your belief in my abilities, allowing me the opportunity to advance my career and for imparting a small part of your knowledge to me.

Prof. Gail Todd, for your clinical guidance, insight and enthusiasm surrounding this work. Thank you for allowing me into your department and for the hours of teaching I was able to be a part of. Thank you for developing my clinical abilities and for showing me how to think laterally and completely.

Prof. Dhiren Govender, thank you for providing the specimens used in this project and for your collaboration in this work. It made this thesis possible and I thank you.

Robea, for the hours spent guiding me through laboratory techniques, your immense patience and encouragement. Most importantly, thank you for your friendship.

Morea, for your guidance in just about every aspect of my immunofluorescence work. For the hours spent teaching me fixation, sectioning and staining techniques; for the discussions surrounding antibody optimisation, and being able to share my frustrations when things did not work out, and joy when things did. You have been a great colleague and friend, and I thank you immensely for everything I have shared with you over the past two years.

Toni, for your guidance in just about everything. For your friendship and your lively personality.

Susan Cooper, for your hours of technical assistance on the microscope and our many conversations.

Dr Dirk Lang and Dr Liz van der Merwe, for your assistance with immuno- techniques, providing of materials and guidance when things weren't going according to plan.

Every single member of the SK and Redox labs, for your friendship, encouragement, advice and help on just about every front. Special thanks to Vicky, for your endless encouragement and always offering to help; Britta for your advice, guidance and colour you add to the lab; and Mubeen, for the many hours we have spent together

in the lab, your sense of humour, interest in my work and patience in helping me with the technical side of things. It has been a great pleasure to work with and learn from you.

The MRC, NRF and UCT for financial support during the past three years.

Heather McLeod, for sectioning of samples.

Lauren and Danielle, for the iPS.

And lastly, Mike. Thank you for allowing me to follow this dream. For believing I can achieve just about anything I put my mind to, and for your utmost patience while I completed this work. Thank you for your support and love.

Table of contents

List of Abbreviations

µg	Microgram
µl	Microlitre
µM	Micromolar
°C	Degree Celsius
BIN	Benign intradermal naevus
BMP	Bone morphogenic protein
CHO	Chinese hamster ovary
cm	Centimetre
CO_2	Carbon dioxide
DAPI	4´,6-diamidino-2-phenylindole
Dct	Dopachrome tautomerase
DMEM	Dulbecco's modified Eagles medium
DNA	Deoxyribonucleic acid
DSC	Dermal stem cell
EDNRB	Endothelin receptor type B
EDTA	Ethylenediaminetetraacetic acid
FBS	Foetal bovine serum
FFPE	Formalin-fixed and paraffin-embedded
FoxD3	Forkhead box D3
G0	Gap zero phase or resting phase
G1	Gap 1 phase or post-mitotic phase
GFP	Green fluorescent protein
Gp100	Melanocyte protein Pmel 17 or silver
GSH	Groote Schuur Hospital
H&E	Haematoxylin and Eosin
hES cells	Human embryonic stem cells
HIER	Heat induced epitope retrieval
HLA	Human leukocyte antigen
HMB45	Human melanoma black
HMG	High mobility group
hNCC	Human neural crest stem cell
HNK1	Human natural killer-1, LEU7 or CD57
HPF	High power field
HREC:REF	Human research ethics committee reference

ICC	Immunocytochemistry
IF	Immunofluorescence
iMEF	Inactivated mouse embryonic fibroblasts
iPA6	Inactivated PA6 cells
iPS cells	Induced pluripotent stem cells
Ki-67	Proliferation marker
LIF	Leukaemia inhibitory factor
MART-1	Melanoma antigen recognized by T cells
MEF	Mouse embryonic fibroblast
Melan-A	MART-1 (melanoma antigen recognized by T cells)
mg	Milligram
min	Minute
MITF	Micropthalmia-associated transcription factor
ml	Millilitre
mm	Millimetre
mM	Millimolar
NANOG	Homeobox protein NANOG
NCC	Neural crest stem cells
NESTIN	Type VI intermediate filament
NHLS	National health laboratory service
P75	Low-affinity nerve growth factor receptor
PA6	Bone marrow-derived stromal cell line
Pax3	Paired box 3
PBS	Phosphate buffered saline
PIER	Proteolytic induced epitope retrieval
PNS	Peripheral nervous system
OCT4	POU class 5 homeobox 1 (also known as POU5F1, OCT3, OCT3/4),
PDGFB	Platelet derived growth factor B
PDGFRβ	Platelet derived growth factor β receptor
RNA	Ribonucleic acid
SKP	Skin-derived precursor
S100	Family of calcium channel binding proteins
SAGE	Serial analysis of gene expression
SOX2	SRY (sex determining region Y)-box (SOX) transcription factor 2
SOX8	SRY (sex determining region Y)-box (SOX) transcription factor 8
SOX9	SRY (sex determining region Y)-box (SOX) transcription factor 9

SOX10	SRY (sex determining region Y)-box (SOX) transcription factor 10
STAT3	Signal transducer and activator of transcription 3
TRP1	Tyrosinase related protein 1
TRP2	Tyrosinase related protein 2 (also known as Dopachrome tautomerase)
TWIST	Twist-related protein 1
SMAD	Intracellular signal-transduction proteins
TE	Trypsin/EDTA
U	Unit
UCT	University of Cape Town
UVA	Ultraviolet A
UVR	Ultraviolet radiation
Wnt	Wingless Type

List of Figures

List of Tables

Abstract

Melanocytic neoplasia is a multifaceted process involving a complex interplay of genetic and environmental factors. Despite recent advances, the aetiology and pathogenesis of melanocytic neoplasms remains unclear and the anatomical location and state of differentiation of the initiating cell remains to be elucidated. Traditional models propose melanoma arises from an epidermal melanocyte which passes through defined stages of increasing atypia due to the accumulation of mutational events. The newly proposed tumour stem cell hypothesis, however, advocates melanoma may arise from a mutated tissue-resident precursor cell, and not from a terminally differentiated melanocyte. The overall aim of this study was to investigate whether benign naevi contain cells with a stem cell-like phenotype, and to examine the question of whether these might be stem cell precursors of malignant melanoma. Ten formalin-fixed and paraffin embedded human naevus biopsy samples, of five different naevus subtypes, were systematically re-evaluated by direct immunofluorescence first, to understand the lineage of a "naevus" cell, and second, to evaluate whether melanocytic naevi may originate from a precursor cell and not via de-differentiation from an epidermal melanocyte. For phenotypic characterisation, results were highly suggestive of a melanocytic lineage with 85.36% of naevus cells staining positively for the melanocyte specific differentiation antigen, Melan-A, as determined by a semi-quantitative analysis. Yet, these cells showed important morphological variations and were distinct from differentiated epidermal melanocytes. Furthermore, although studies have suggested regional variations in naevi and a possible Schwann cell lineage, there was no evidence in support of a Schwann cell phenotype of naevus cells in this study. Secondly, precursor markers were identified in all naevus subtypes analysed, thereby convincingly demonstrating the presence of precursor cells within naevus tissue. The majority of positively labelled cells localised to the epidermal compartment (72.72%) and this was similar for all three markers analysed: OCT4 (77.22%), NANOG (63.72%) and p75 (57.15%). Interestingly, dysplastic naevi showed a large proportion of OCT4+ cells (5.81%), which was by far the greatest proportion of any precursor marker identified in this study. As dysplastic subtypes are associated with an increased risk of melanoma development, this may imply an increased stem cell component confers this risk. Thirdly, analysis with the proliferation marker Ki-67 revealed the epidermal compartment contained the majority of dividing naevus cells (76.17%), thereby supporting an epidermal origin of naevi. Since the majority of precursor cells identified were within the epidermal compartment, this may suggest precursor cells drive naevus development, in support of the tumour stem cell hypothesis. In addition, the predominance of these precursor cells within the interfollicular epidermis may aid in identifying a potential stem cell niche. However, no precursor cells were noted in the normal intervening interfollicular epidermis or dermis of naevi, or in the epidermis or dermis of normal human skin, as may have been expected. In conclusion, the presence of stem cell markers in naevus tissue supports the hypothesis that at least some naevus cells may arise from stem cells, and not from differentiated melanocytes.

1. Introduction

1.1 The melanocyte

Melanocytes are dendritic, pigment-producing cells that are located in the basal layer of the epidermis, the hair bulb and the uveal tract of the eye where they play a role in protection against the harmful effects of ultraviolet radiation, as well as skin, coat and eye pigmentation. Melanocytes are also found in the inner ear, heart and meninges where they are thought to be important in the normal development and functioning of these organ systems, as abnormalities of melanin and/or melanocytes are associated with functional impairments, such as hearing loss, atrial arrhythmias and neurodegenerative conditions respectively. Although the specific functions of melanin in these organs remain under investigation, melanin is thought to function as a biological reservoir for substances with cationic properties, such as calcium, iron, copper and magnesium, allowing their storage release and exchange (Nordlund et al, 2006; Tolleson et al, 2005), to play a role in the metabolism of certain oto- and neuro-toxic drugs (Larsson, 1993; Nordlund et al, 2006; Hu et al, 2002), as well as having a proposed vasomotor function (Savin, 1965). Additional roles for melanin in the skin are therefore under investigation.

In human skin, melanocytes reside in the basal layer of the epidermis at a frequency of around one in every ten basal cells. They extend cytoplasmic projections, known as dendrites, laterally and upward between surrounding keratinocytes. Approximately 36 keratinocytes associate with a single melanocyte, forming the "epidermal-melanin unit" (Fitzpatrick and Breathnach, 1963). This organisational relationship forms an important structural unit, allowing for adequate melanin transfer. It also forms an important functional unit whereby keratinocytes regulate melanocyte proliferation, dendricity and rate of melanin production and transfer. This is mediated via direct cell contact by cell-to-cell adhesion molecules, as well as paracrine signalling molecules such as cytokines, growth factors and hormones. Melanocytes produce the pigment melanin in membrane-bound organelles known as melanosomes and transfer these melanosomes via their dendrites to associated keratinocytes. Transferred melanosomes aggregate on the sun-exposed surface of the keratinocyte nucleus, forming an umbrella-like array that protects the underlying DNA from ultraviolet radiation. It is the characteristics of these melanosomes, such as number, size, and degree of melanisation, type of melanin, distribution and rate of degradation in the keratinocytes which determines human skin colour and susceptibility to ultra-violet radiation (UVR), while the absolute number of melanocytes is similar for both sexes and all races. Abnormalities of melanocyte development and/or migration, or in the processes of pigment production and/or transfer, leads to a wide range of hyper- or hypo-pigmentary disorders, and alters susceptibility to sun induced malignancies.

1.2 Melanocyte embryology and development of the neural crest

The embryological origin of melanocytes has been widely studied and current opinion holds that melanocytes are derived from the neural crest, a discrete embryonic structure of vertebrates, first described in the chick

embryo by Wilhem His in 1868. At the time of neural tube formation, a subpopulation of cells at the roof of the neural tube delaminates from the neuroepithelium and, under the influence of bone morphogenic protein (BMP) and Wnt signalling, undergoes subsequent epithelial to mesenchymal transition to form the neural crest. Neural crest stem cells (NCCs) are a transient, highly migratory population of multipotent stem cells and give rise to diverse derivatives, including peripheral neurons, glial cells, adrenal medulla, cardiac cells and melanocytes. Whether NCCs reflect a population of cells with multiple differentiation abilities (Dupin et al, 2007; as reviewed by Le Douarin et al, 2008), or whether the neural crest is composed of a variety of different, yet already committed cells (as reviewed by Achilleos and Trainor, 2012; Andersson, 1997; Gilbert, 2000) remains under debate.

Neural crest cells migrate and differentiate along two known pathways (Figure 1): (i) early delaminating neural crest cells follow the ventral pathway of migration and give rise to the developing peripheral nervous system (PNS) and its supporting Schwann cells; and (ii) late migrating cells follow the dorsolateral pathway of migration and give rise to melanocytes. Melanocyte migration is supported by a number of experiments in avian and mouse embryos, which demonstrate that melanoblasts emerge from the dorsal neural crest and migrate dorsolaterally between the ectoderm and dermamyotome before moving ventrally to reach the basal layer of the epidermis and hair follicles (reviewed in Adameyko et al, 2009). These so-called founder melanoblasts then undergo clonal expansion to populate the overlying epidermis and cycling hair follicles.

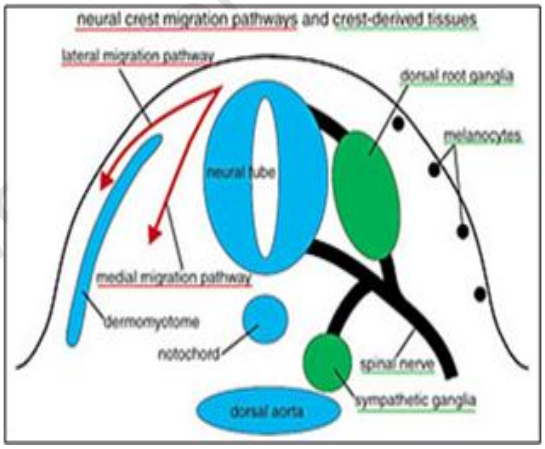

Figure 1: Diagrammatic representation of neural crest migration pathways in the developing embryo (red arrows) and their associated progeny (green underline) (Sakai and Wakamatsu, 2005).

Neural crest formation, and the subsequent migration and differentiation of NCCs along one of the above pathways, is marked by the expression of various transcription factors which form a highly organized transcriptional regulatory network. Transient, premigratory NCCs have been shown to express forkhead box D3 (FOXD3), paired box 3 (PAX3) and the SRY (sex determining region Y)-box (SOX) transcription factors SOX8, SOX9 and SOX10 (as reviewed by Le Douarin et al, 2008; Thomas et al, 2008), all of which have been designated as cell-type-specific effectors and regulate neural crest survival, proliferation, migration and

differentiation by activating downstream transcription factors. Of these, SOX10 plays an important role in the developing PNS in the control of Schwann cell differentiation and myelination (reviewed by Ernfors, 2010). Expression is maintained in mature Schwann cells where it plays a key role in preserving a functional myelinating phenotype (Bremer et al, 2011). SOX10 is also expressed in migrating melanoblasts and has been shown to be strongly and widely expressed in normal human skin melanocytes (Agnarsdottir et al, 2010). SOX10, together with PAX3, regulates the promoter of Micropthalmia-associated transcription factor (MITF), a transcription factor relatively specific for melanocyte lineage (discussed below). In addition, SOX10 activates the tyrosinase enhancer, thereby directly contributing to tyrosinase gene expression in developing melanocytes (Murisier et al, 2007).

Micropthalmia-associated transcription factor is a member of the Myc-related family of basic helix-loop-helix leucine zipper transcription factors and is considered the master regulator of melanocyte fate determination. It is consistently the first marker identifying melanoblasts in the developing embryo (reviewed by Ernfors, 2010) and expression is maintained in normal human skin melanocytes (Levy et al, 2006). As mentioned above, MITF is activated by cell-type-specific effectors, such as PAX3 and SOX10 and has a number of melanocyte-specific transcriptional targets, including tyrosinase (TYR), tyrosinase-related protein 1 (TRP1), tyrosinase-related protein 2 (TRP2), PMEL17 (silver or gp100) and Melan-A (also known as MART-1, melanoma antigen recognized by T cells) (discussed in section 1.5 below).

A further important marker of neural crest development is the low-affinity nerve growth factor receptor, p75 (also known as p75NTR, p75NGFR and CD271). P75 is one of the receptors for the neurotrophins, a family of growth factors important in survival and differentiation of diverse cell types within the developing neural crest and PNS (Lewin and Baarde, 1996). In the neural crest, p75 is expressed in NCCs prior to commitment to either melanoblast or Schwann cell fate and thus does not distinguish between glial and melanocyte lineages at the level of the neural crest. P75 expression is retained in committed Schwann cell precursors and in mature Schwann cells of peripheral nerves (Liang and Johansson, 1998). As melanocyte precursors migrate from the neural crest, they acquire the expression of melanocyte specific markers and lose the expression of p75. This receptor has not been shown to be re-expressed in mature melanocytes (Trejo et al, 2002) and thus, in melanocytes, p75 expression is specific for a precursor phenotype.

1.3 A novel pathway of melanoblast migration

As discussed above, precursor cells exit the neural crest and travel along one of the aforementioned pathways. The exact course and anatomical relationships of these migrating cells, however, has not been clearly demonstrated. Also, it has been observed that some ventral melanoblasts appeared to populate the skin at earlier time points than can be explained by the arrival of migrating precursor cells of the late-migrating dorsolateral pathway (Fox, 1949). To better understand melanoblast migration, Ademeyko et al (2009) analysed the

expression of key transcription factors, MITF and SOX10, in chick embryo NCCs. Neural crest cells of the dorsolateral pathway showed positive MITF and SOX10 expression, as would be expected. Similarly, migrating NCCs of the ventral pathway showed positive SOX10 expression and occurred in close association with developing peripheral nerves. Surprisingly, however, some of these ventrally migrating cells co-expressed MITF, which suggests precursor cells in association with developing peripheral nerves may be an alternate source of skin melanocytes. To test this hypothesis, ablation experiments were performed on chick embryos using a green fluorescent protein (GFP) expressing construct for NCC tracing. Results showed that ablation of both the dorsal and ventral pathway resulted in a dramatic loss of cutaneous melanocytes; however, ablation of the dorsal pathway alone did not quantitatively affect numbers of melanoblasts in the ventral limb bud. Lineage tracing of GFP NCCs showed neural crest-derived Schwann cell precursors of the ventral pathway as an origin of skin melanocytes. This provides new evidence for a ventral pathway of melanoblast migration, and importantly, implies a common progenitor cell of both Schwann cells and skin melanocytes persists after exiting the neural crest. It could be hypothesised that some progenitor cells may persists in adult tissues and retain a multipotent phenotype; and, when stimulated could give rise to either melanoblasts or cells of a Schwann cell lineage.

1.4 Neural crest development using experimental models of human origin

As human embryos are difficult to obtain, there is little information on neural crest pathways in human development. To address this issue, Thomas et al (2008) cultured NCCs from human embryos (hNCC), Carnegie stages (C) 10 and C14. They found that cultured hNCCs remained euploid and morphologically unchanged after more than 20 passages. Using a serial analysis of gene expression (SAGE) technique, they reported the expression of classical transcription factors FOXD3, PAX3, SOX9, SOX10 and TWIST1, as well as signalling molecules or the membrane-bound receptors NESTIN, p75, endothelin receptor type B (EDNRB), platelet-derived growth factor B (PDGFB) and platelet derived growth factor receptor β (PDGFRβ). Of particular interest, they noted that the transcriptional profile of some hNCCs was similar to that of human embryonic stem (hES) cells and showed positive expression of pluripotency markers SOX2, NANOG and POU class 5 homeobox 1 (POU5F1, OCT3, OCT4; hereafter referred to as OCT4). This suggests that a subset of neural crest stem cells retains expression of pluripotency markers and thus, the simultaneous expression of SOX2, NANOG and OCT4 is not sufficient to confer an embryonic stem cell identity. In agreement with this, a number of studies have derived neural crest-like cells from postnatal tissue niches which, when cultured, contain a subset of cells with expression profiles consistent with both embryonic and neural crest lineage. These subsets of cells have been identified as NCCs which may retain stem cell properties and include skin-derived precursor cells from mouse and human dermal papilla (Fernandes and Miller, 2009; Li et al, 2009; Toma et al, 2005), epidermal NCCs from the mouse hair follicle bulge (Sieber-Blum et al, 2006; Sieber-Blum and Hu, 2008), palatum-derived NCCs of Wistar rats (Widera et al, 2009) and NCCs derived from mouse corneal limbus (Brandl et al, 2009). It is possible therefore that most migrating NCCs undergo progressive differentiation and

eventual fate restriction, while a subset of NCCs may reside in certain postnatal niches and retain a multipotent phenotype. It is also possible that this subpopulation consists of committed NCCs which are able to re-attain a multipotent fate if required or if subject to micro-environmental alterations, including *in vitro* conditions.

1.5 Fate of melanoblasts on reaching the dermis

Following the migration of neural crest cells into the dermis, by either the dorsolateral or ventral pathways as discussed above, melanocyte precursors migrate ventrally to reach the basal layer of the epidermis and hair follicles. In humans, immunohistochemical staining has shown that melanoblasts first appear in the dermis at 6-8 weeks gestational age (Gleason et al, 2008; Holbrook et al, 1989) and express melanocyte specific markers MITF, Melan-A and human melanoma black (HMB45) (Melan-A is specific to skin and retinal melanocytes and thus a useful marker for melanocytic tumours, while HMB45 is a pre-melanosomal, transmembrane protein of undetermined function which detects melanoblasts/early melanocytes and melanoma cells, but not normal melanocytes). These precursor cells then migrate into the epidermis by 10 weeks gestational age, where they are observed to localise to the basal layer and have pre-melanosomes as seen by direct electron microscopy and their reaction with reduced silver (Zimmerman and Becker, 1959). Interestingly, the number dermal melanocytes, as detected by MART-1 and MITF staining, outnumbered those that ultimately localised to the epidermis and this likely results from programmed cell death, or apoptosis, as is consistent with normal developmental biology. The suggestion, however, that some dermal precursors may be retained within the dermis and persist into adult life cannot be excluded.

1.6 Disorders of melanocytes: hyperpigmentary and proliferative disorders

The final destination for melanocyte migration within the skin is the basal layer of the epidermis. Here, melanocytes produce the pigment melanin which confers skin colour and protects the skin from ultraviolet radiation as discussed previously. There are two broad categories of melanocytic disorders: those resulting in an increase in skin pigmentation, due to an increase in pigment and/or an increase in melanocyte number; and those resulting in a decrease in skin pigmentation, due to an absence or decrease in melanocyte number and/or function (Freedberg et al, 2003).

Disorders of melanocytes which result in areas of increased pigmentation are broadly sub-grouped into simple hyperpigmentary disorders, which include lesions such as the common freckle and solar lentigo, and neoplastic disorders, which comprise benign melanocytic naevi and malignant melanoma. The simple hyperpigmentary disorders result from an increase in melanin synthesis and transfer to basal keratinocytes. This gives the clinical appearance of a well-defined, level area of increased pigmentation, and is generally dependent on local environmental factors, such as solar radiation. There is usually little or no proliferation of melanocytes and, if proliferation does occur, this is limited and melanocytes retain their linear arrangement along the basement membrane, preserving their normal anatomical relationships with neighbouring keratinocytes (Figure 2b).

These melanocytes have a normal dendritic phenotype which allows transfer of melanin to surrounding keratinocytes and/or other cells, such as dermal macrophages (melanophages).

Proliferative or neoplastic disorders on the other hand are characterized by an abnormal proliferation of cells and an associated disruption in normal anatomical relationships with surrounding keratinocytes and the underlying basement membrane. This proliferation is typically independent of local environmental signals. Neoplastic cells are not limited to the epidermal compartment, but may also be located in the dermis or both (Figure 2c). Neoplastic cells are often deficient in melanogenesis and may not exhibit dendrites, so that when melanin is produced, it is typically retained in their cytoplasm.

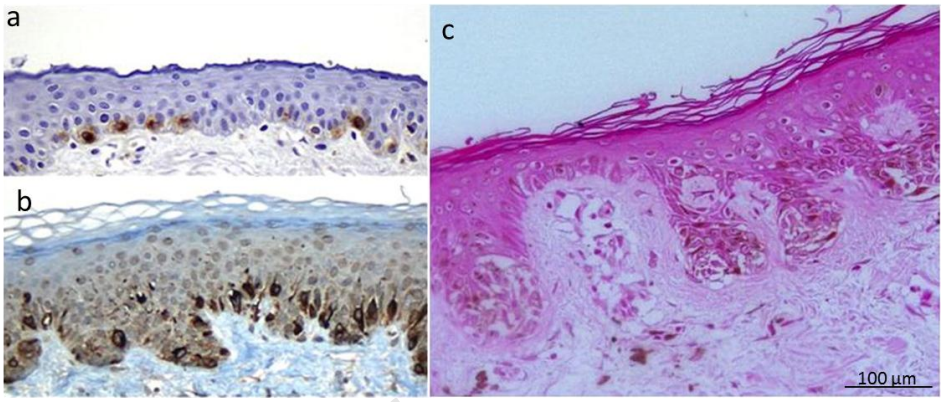

Figure 2: Histological features of simple hyperpigmentary and neoplastic disorders of melanocytes: 2a: Normal skin showing solitary melanocytes along the dermo-epidermal junction at a frequency of about 1 melanocyte to 4-10 basal keratinocytes. b: Melanocytic hyperplasia occurring in sun-damaged skin showing a limited proliferation of basal melanocytes which preserve their normal anatomical relationships with the basement membrane and surrounding keratinocytes, as well as exhibit a dendritic phenotype (images: Carlson et al, 2009). c: Neoplastic proliferation of melanocytes, occurring in clusters or nests. There is an associated loss of normal relationships with neighbouring keratinocytes and basement membrane. Dendrites are not seen (own image).

1.6.1 The "multiple-hit" hypothesis of neoplasia

Neoplasia, in general, is thought to arise from a complex interplay of genetic and environmental factors. The basic steps are initiation, promotion, progression and, occasionally, resolution. Initiation involves a mutational event, which primes the cell to respond abnormally to normal growth signals, or previously sub-threshold signals. These mutations are within oncogenes, which promote growth, or within tumour suppressor genes, which then allow the cell to proceed through the cell cycle unchecked. This so-called primed cell is now susceptible to further insult, usually environmental, and promotion occurs when this primed cell is activated and begins to proliferate. Abnormal proliferation is sustained by the underlying initiating mutation, and eventual autonomy from surrounding signals leads to neoplastic growth, invasion and metastasis (Cotran et al, 1994; Freedberg et al, 2003; Rippey, 1994). For some tumours, such as colon carcinoma, the sequential steps contributing to carcinogenesis are well documented and widely accepted. However, the exact processes in naevus and melanoma development are less well understood.

1.6.2 Benign melanocytic naevi

The melanocytic naevus, or common mole, is a benign neoplastic proliferation thought to arise from epidermal melanocytes. Common (banal) naevi appear as small, round to oval nodules with uniform colour and a regular border. They characteristically first appear around one year of age, peak in number during the second or third decade of life and then decrease or disappear by the seventh to ninth decade (Kincannon and Boutzale, 1999). Banal naevi are broadly sub-grouped according to their histological characteristics as outlined in Table 1.

Naevus Subtype	Histological Characteristics
Junctional	Epidermal component only
Compound	Epidermal and dermal components
Intradermal	Dermal component only
Blue Naevus	Various subtypes, generally consist of a dermal aggregation of cells which retain their dendrites and resemble epidermal melanocytes, show active melanin synthesis, and clinically appear to have a bluish tinge due to dermal melanin accumulation
Epithelioid or Spindle-cell Naevus ("Spitz Naevus")	Clinical and histopathological features may resemble melanoma
Halo Naevus	Banal naevus surrounded by a halo of depigmentation, can be junctional, compound or intradermal
Dysplastic or Atypical Naevus	Clinically irregular lesions, usually larger than banal naevi, and show inconsistencies of colour, border and shape. Histologically, they are characterized by cytological and/or architectural atypia
Congenital Naevus	Naevus apparent at birth which may extend to the subcutaneous fat and contain other hyperproliferative components such as hairiness or thickened verrucous overlying epidermis

Table 1: Classification of benign melanocytic naevi (adapted from McKee et al, 2005)

1.6.2.1 Histological features of benign melanocytic naevi

Histologically, benign neavi consist of small, well-circumscribed proliferations or "nests" of cells, termed "naevomelanocytes", which may be located in the epidermis, dermis or both. These so called "naevomelanocytes" or "naevus" cells are thought to represent a type of melanocyte but the exact relationship between the two cell types is still under debate, and will be further discussed below. Nests at the dermo-epidermal junction are round to oval in shape, tend to localise to the tips of the rete ridges and are usually equidistant from one another (see Figure 21a, 21b, Results section 3.3.1). As nests descend through the dermis, they may be seen to decrease in size and discrete nests may be replaced by singly dispersed cells, features referred to in histological terms as "maturation". Naevus cells in the deeper dermis may also show a smaller, spindle-shaped morphology, wavy or s-shaped nuclei and align in vertical cords within loosely woven collagen bundles. In addition, these cells may stain negatively for melanocyte markers Melan-A and HMB-45, stain positively for Schwann cell antigens S100 or p75 (Barnhill et al, 2004; Freedberg et al, 2003) and may not express tyrosinase activity or contain melanosomes (Mishima, 1965; Winnepenninkx and van den Oord, 2004). Naevi exhibiting these features are referred to as neurotised or neural naevi as these features are typical of peripheral nerve sheath elements and neural tumours, such as neurofibromas. Dysplastic naevi generally show

varying degrees of architectural and/or cellular atypia, with merging of epidermal nests and fusion of adjacent rete ridges (see Figure 21e, 21f, Results section 3.3.1). The cytological atypia may resemble a melanoma.

1.6.2.2 Existing theories on the aetiopathogenesis of melanocytic naevi

As briefly mentioned above, the precursor cell, and subsequent pathogenesis, of a "naevus" cell remains to be fully understood and has, in fact, been debated for over one hundred years. The term "melanocytic naevus", itself, implies a relationship exists between a melanocyte and a naevus cell and in agreement with this a number of authors argue for a naevus cell as originating from an epidermal melanocyte, which has undergone specific alterations in cellular transcription pathways leading to abnormalities in proliferation, differentiation and senescence. Others, however, propose a naevus cell as a distinct cellular lineage. Since most available data on melanocytic naevi consists of static, cross-sectional analyses from naevus biopsy specimens, the step wise evolution of naevi remains undefined and evidence to support existing hypotheses is limited. A number of hypotheses have been proposed and these will be outlined below.

Unna first proposed the theory of "*Abtropfung*" in 1893, whereby it was hypothesised that melanocytic naevi develop from a differentiated epidermal melanocyte with the subsequent "dropping off" of these cells into the dermis. This theory describes the sequential development of junctional, compound and, finally, intradermal naevi. Evidence in support of this hypothesis is the observation that the majority of naevi in childhood are junctional and/or compound, while those arising in adolescents and young adults are predominantly intradermal (McKee et al, 2005). This remains the most widely accepted theory to date and is the hypothesis on which Clark's model of melanoma progression, the best accepted model of melanoma development, is based (Figure 3 below). Many years later, following the observation that naevus cells in the epidermis and superficial papillary dermis resemble epithelial cells and demonstrate positive tyrosinase activity, while those in the middle and deep dermis show features consistent with neurotisation, as discussed previously, Masson (1951) proposed the "*Dual origin of naevi*", where he suggested that the junctional component of naevi arises from epidermal melanocytes, while the intradermal component arises from Schwann cells.

In opposition to the theory of an epidermal origin of naevi, Kawamura (1956) introduced the concept that naevus cells may result from embryonically misdirected cells of the neural crest. He proposed these misdirected cells retain the ability to differentiate along both melanocytic and Schwannian lineage, which may well result in the dual phenotype of cells observed in certain naevi. Following this, Mishima (1965) proposed the term "nevoblast", where he described an already committed neural crest-derived precursor cell, of either melanocyte or Schwannian lineage, resident in the post-natal dermis which, when recruited, proliferates to give rise to a collection of "naevus" cells.

The concept of naevi arising from a dermal precursor cell and not an epidermal melanocyte was further supported by Cramer (1984) who proposed the theory of "*Hochsteigerung*" or, literally, "upward climb". Here, Cramer proposed that naevi may originate from neural crest stem cells which are arrested in normal embryonic migratory pathways. It was hypothesised that neural crest stem cells may migrate along developing peripheral nerve sheaths, first into the dermis and then into the epidermis. If these multipotent precursor cells are retained within the dermis due to incomplete migration and, if subject to genetic or environmental aberrations, they may give rise to "naevus cells". In agreement with this, studies have convincingly shown that melanocytes first appear in the dermis before populating the overlying epidermis (Gleason et al, 2008; Hulley et al, 1991). And, as discussed previously, it has recently been demonstrated that a substantial number of skin melanocytes are derived from multipotent Schwann cell precursors of developing peripheral nerves (Ademeyko et al, 2009). Persistence of some precursor cells within the dermis may occur and thus be a potential postnatal niche of neural crest stem cells.

Lastly, the concept of a melanocytic naevus as a hamartoma has been proposed. A hamartoma is a benign, focal malformation of normal tissue elements, which grow at the same rate as surrounding tissue, but grow in a disorganised mass, and are commonly found incidentally in the lung. Other organs affected include the heart, central nervous system, skin and kidney, and these are seen in various genetic syndromes, such as tuberous sclerosis. The demonstration, however, that some naevi are clonal (Hui et al, 2001), and do not simply represent an increased proliferation of normal melanocytes and associated epidermal structures, has limited the acceptance of this hypothesis. Congenital naevi exhibit distinct histological features and have been considered by many to be true hamartomas. For this reason congenital naevi are not considered within the scope of this thesis.

1.6.3 Malignant melanoma

Melanoma is a malignant proliferation of cells thought to arise from epidermal melanocytes. Four distinct subtypes exist, as outlined in Table 2. Unlike benign naevi, a melanoma is characterised histologically by cellular and architectural atypia. Nests at the dermo-epidermal junction are often elongated or irregular in shape, and distort the rete ridges. Maturation of cells in the deep dermis is often not observed (as described for naevi) and melanocytes may be seen to invade adnexal structures. Inflammatory infiltrates are often seen, and associated clinical features, such as ulceration, may be present. Malignant cells may acquire the potential to metastasize, whereby they migrate from the primary tumour and grow autonomously at a distant site. This characteristic is a hallmark of malignant cells and is thought to represent the final step in melanoma evolution.

Melanoma Subtype	Clinical and histological Characteristics
Superficial Spreading Melanoma	The most common subtype, accounting for approximately 70% of all melanomas. Occurs most commonly on the lower legs of females and upper backs of males. It generally presents in the fourth and fifth decade.
Nodular Melanoma	The second most common subtype of melanoma, accounting for approximately 15-30% of all melanomas. The trunk, head and neck are frequent anatomical sites.
Acral Lentigenous Melanoma	The most common form in dark skinned individuals and relatively infrequent in fair skins. Typically occurs on the palms, soles and beneath the nail plate. This type of melanoma is usually diagnosed in older patient, with a median age at onset of 65 years.
Lentigo Maligna Melanoma	The least common subtype, accounting for approximately 4-15% of all melanomas. Typically occurs on sun exposed areas of the head and neck, commonly occurring on the nose and cheeks. It is uncommon before the age of 40 years and the median age at diagnosis is 65 years.

Table 2: Classification of malignant melanoma (adapted from Freedberg et al, 2003).

1.6.3.1 The aetiopathogenesis of melanoma: are naevi and melanoma a continuum of the same process?

Like melanocytic naevi, the cell of origin and subsequent pathogenesis of a melanoma remains to be fully understood. The most widely accepted model for the aetiopathogenesis of melanoma was described by Clark in 1984. This hypothesis proposes that melanomas arise from epidermal melanocytes which pass through stages of increasing atypia due to the accumulation of mutational events (Figure 3). This model depicts an epidermal melanocyte which, following a mutational event, proliferates to form a benign naevus. Additional genetic or environmental insults allow for the progression of a benign naevus to a dysplastic naevus, and finally a melanoma. The resultant melanoma first exhibits a radial growth phase, where cells are limited to the epidermis and superficial dermis, before exhibiting a vertical growth phase where cells invade the deeper dermis. Cells finally acquire the ability to migrate out of the dermis, resulting in a metastatic melanoma, the concluding step in melanoma evolution (Clark et al, 1984; Herlyn et al, 1985, 1987). This hypothesis is in agreement with Unna's theory of naevus development (discussed previously) and provides a model on which melanomas are staged today. This theory is based on the concept that naevi are direct precursor lesions to melanoma; and indeed, the presence of numerous naevi, dysplastic naevi and large (>20cm) congenital naevi are identified as risk factors for the development of a melanoma. This model is also based on the pathological risk of melanoma, where those limited to the epidermis, or "in situ" tumours, are considered low risk due to "early" detection, while high risk correlates with depth of dermal invasion and thought to represent a later stage of tumour evolution.

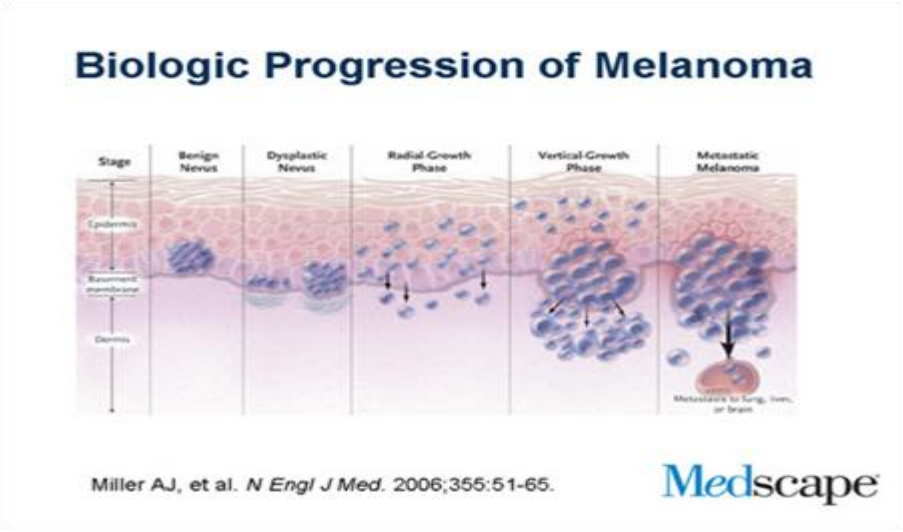

Figure 3: Biologic Progression of melanoma: Hypothesised evolution and progression of an epidermal melanocyte to a metastatic melanoma.

This step-wise theory of carcinogenesis is a well accepted and plausible model of melanoma development, and it neatly ties together the evolution of benign naevi and melanoma. However, clinical information does not always support this hypothesis. It has previously been reported that a number of melanomas appear to arise *de novo*, in previously appearing normal skin. In fact, it has been reported that 70-80% of cutaneous melanomas do not evolve from an identified precursor lesion (Kelly et al, 1997; Lucas et al, 2003).

The difficulty in understanding melanoma aetiology and pathogenesis is that, like naevi, most available data consists of static, cross-sectional analyses. In addition, the natural history of naevi is difficult to study. Many atypical or suspicious naevi, which may well have progressed to malignant melanoma with time, are removed to reduce the risk of melanoma transformation and thus the true rate of melanoma evolution in a pre-existing naevus may be under-represented. Similarly, in patients presenting with established melanoma, ascertaining the presence or absence of a precursor lesion is usually dependent on patient history alone. It is often difficult to objectively establish whether the lack of a precursor lesion was simply due to the patient not noticing a pre-existing naevus, or whether the presence of a noted pre-existing naevus was in an actual fact a melanoma from the outset. A more objective method would be to determine the presence or absence of naevus tissue within a melanoma biopsy, but whether the naevus preceded the melanoma, or whether the melanoma developed areas of well-differentiated, naevus-like areas cannot be evaluated. The possibility of both lesions arising simultaneously should also be considered.

1.6.3.2 The natural history of naevi: clues to melanoma evolution?

In an attempt to better understand the aetiology and pathogenesis of melanoma, and to obtain more information on the natural history of naevi, Tucker et al (2002) prospectively followed 844 members of melanoma-prone families for a period of 25 years, forming the best longitudinal study on the natural history of naevi to date.

Sequential documentation of skin lesions was performed by regular clinical examinations and serial photographs. Suspicious or changing lesions were biopsied and the histology reviewed. This study reports three central results with regards to the natural history of naevi and melanoma evolution.

Firstly, individuals of melanoma-prone families were found to have several hundred naevi (some exceeding 500) and multiple clinically atypical naevi. The vast majority of these banal and dysplastic naevi remained stable or regressed over time. This suggests that multiple naevi and dysplastic naevi are important phenotypic markers for individuals who are at risk for melanoma development, independent to their potential risk as a precursor lesion. It has been proposed that the increased risk of melanoma in these individuals is due to an inherited susceptibility to melanocyte proliferation which confers the initiating step in melanoma evolution. In support of this hypothesis, several studies have demonstrated a significant correlation between naevus counts in parents and their children, or between siblings, independent of their sun exposure patterns (Graham et al, 1999; Green and Swerdlow, 1989; Weicker et al, 2003), implying a genetic susceptibility to naevus development, independent of environmental factors. Also, distinct patterns of naevus morphology may be observed in a single individual, resulting in a "signature naevus", where the majority of naevi are morphologically alike. This would suggest these naevi have a similar underlying genetic aberration. In agreement with this, genetic analyses of naevus subtypes have identified activating mutations in components of cellular transcription pathways which, in turn, lead to the altered expression profile of multiple transcription factors which may drive the neoplastic phenotype. A number of candidate genes have been proposed, including cyclin-dependent kinase inhibitor 2A (CDKN2A), BRAF, melanocortin-1-receptor (MC1R) and MYC (details beyond the scope of this discussion). Studies have further shown various exogenous oncogenes can drive melanocytes to acquire malignant and/or invasive characteristics *in vitro* (Grichnik et al, 2006). An alternative theory proposes that the increased risk of melanoma development in these individuals with multiple naevi may simply reflect an increased probability of malignancy due to a higher number of melanocytes in their skin (Green and Swerdlow, 1989).

A second important finding by Tucker et al (2002) in their long-term follow up of melanoma-prone families was the prospective detection of 86 new melanomas in 37 individuals. Fifty-one of these melanomas were found to have an identified precursor lesion, based on either the presence of naevus tissue within the melanoma biopsy and/or the presence of a benign lesion, documented photographically, at an earlier time point. Thirty-two of these precursor lesions were dysplastic naevi. This study thus provides convincing evidence that, independent to their presence as phenotypic risk markers for melanoma, banal and dysplastic naevi also represent potential direct precursor lesions for melanoma development.

Importantly, however, it must be noted that over one third (40.7%) of these melanomas did not arise in an identified precursor lesion. This is the third noteworthy finding by Tucker et al (2002). Histological and photographical evidence confirmed these melanomas arose *de novo* in previously appearing normal skin. This

supported the findings of an earlier study where Kelly et al (1997) followed a cohort of 278 patients with 5 or more dysplastic naevi for a mean period of 42 months. Clinical examinations and serial photographs were recorded as described for Tucker et al (2002). This group reports the prospective detection of 20 new melanomas in 16 patients, with only 3 melanomas arising in a documented precursor lesion. Fifteen of the 20 melanomas (75.0%) did not have an identified precursor lesion and were shown to arise *de novo*.

1.6.4 An alternative route of melanoma development: the tumour stem cell hypothesis

As previously discussed, it has long been accepted that initiating mutations could arise and drive a fully differentiated epidermal melanocyte along the aforementioned step-wise process of melanoma evolution. It has recently been proposed, however, that these mutations may actually occur in a tissue resident precursor cell and not in a fully differentiated melanocyte. This "initiated" progenitor cell may then be primed to respond abnormally to surrounding environmental signals (Grichnik, 2008; Grichnik et al, 2006; Ross et al, 2011). This hypothesis is known as the tumour stem cell hypothesis (further discussed in section 1.6.4.3) and is based on the *in vitro* observation of a sub-population of cells with stem-like features within tumour cultures. Stem cells have been identified in cultures of several malignancies including haematological (Bonnet and Dick, 1997; Wulf et al, 2001), breast (Al-Hajj et al, 2003), brain (Kondo et al, 2004; Singh et al, 2003, 2004), pancreatic (Li et al, 2007), colon (O'Brien et al, 2007; Ricci-Vitiani et al, 2007), lung (Ho et al, 2007) and melanoma. Evidence in support of the tumour stem cell model of melanoma development will be discussed below.

1.6.4.1 Stem cells: a brief overview

Stem cells are slow proliferating cells characterised by the ability to maintain their undifferentiated state through self renewal and to give rise to differentiated cell types (Figure 4). Embryonic stem cells are pluripotent cells derived from the inner cell mass of blastocyst-stage embryos. A group of "core" pluripotency transcription factors have been identified in both human and mouse embryonic stem cells and include OCT4, SOX2 and NANOG (Orkin, 2005).

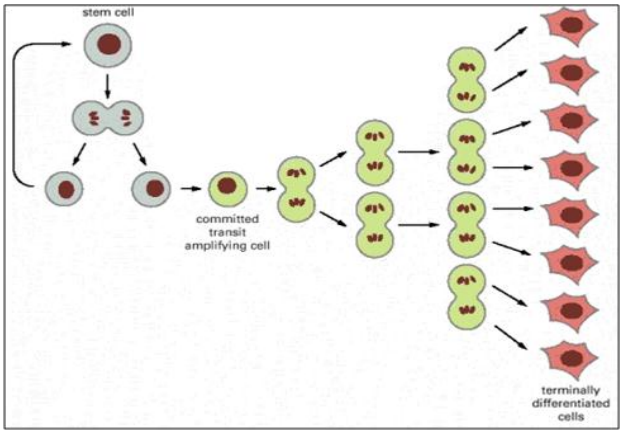

Figure 4: Stem cell biology: Stem cells are able to self renew (blue) as well as give rise to transit amplifying cells (green) which undergo eventual terminal differentiation (red) (Alberts et al, 2002).

These transcription factors trans-activate downstream genes which in turn encode transcription factors, signal transduction components and chromatin modifying enzymes that promote self renewal. OCT4 (OCT3/4 or POU5f1) belongs to the POU transcription factor family (Nichols et al, 1998). The downregulation of OCT4 in both mouse and human ES cells causes cell differentiation (Niwa et al, 2000; Darr et al, 2006). SOX proteins are a group of transcription factors widely found in the animal kingdom. They contain a high-mobility group (HMG) domain and belong to the HMG box superfamily. SOX2 is essential in maintaining self-renewal of undifferentiated embryonic stem cells. OCT4 forms a trimeric complex with SOX2 on target regulatory elements to collaborate in transcriptional control of the expression of a number of genes involved in embryonic development. NANOG belongs to the NANOG homeobox family and binds DNA via a conserved homeodomain motif. NANOG has been identified as a marker for undifferentiated human ES cells and thought to be fundamental in maintaining pluripotency. However, its exact role in these cells is not yet fully understood. It is thought to interact with SMAD1, interfering with the recruitment of co-activators to the active SMAD transcriptional complexes and blocking bone morphogenetic protein-induced mesoderm differentiation. OCT4, SOX2 and NANOG co-activate a number of genes, often at apparent overlapping sites, suggesting these factors act in a co-ordinate manner to control the transcriptional program of pluripotency.

Totipotent	**Ability to form all lineages of organism; in mammals only the zygote and first cleavage blastomeres are totipotent.**
Pluripotent	**Ability to form all lineages of body. Example: embryonic stem cells**
Multipotent	**Ability to form multiple cell types of one lineage. Trait of adult stem cells. Example: hematopoietic stem cells**
Unipotent	**Form one cell type only. Example: spermatogonial stem cells**
Plasticity	**Ability of precursor cell to generate cells of other lineages**

Table 3: Definition of terms (adapted from Jaenisch and Young, 2008)

1.6.4.2 Evidence for stem cells in postnatal skin

During embryogenesis, stem cells undergo a process of selective determination, differentiation and eventual fate restriction as their differentiation potential, or plasticity, becomes increasingly limited (Table 3). In adult tissues, integrity is thought to be maintained by tissue-resident stem cells and these precursor cells have been identified in a wide range of human tissues, including the skin. The best described stem cell niche in postnatal skin is the permanent mid-portion of the hair follicle known as the bulge region which, in mice, has been shown to house melanocyte stem cells, giving rise to mature melanocytes in the hair bulb during normal hair cycling (Amoh et al, 2005; Nishimura et al, 2002; Sieber-Blum et al, 2004; Wong et al, 2006). Specific markers for these precursor cells have yet to be identified, but studies have shown that quiescent precursor cells in the hair follicle bulge downregulate melanocyte specific markers Mitf, TRP1, TRP2 (Dct) and Tyrosinase (Nishimura et al,

2010). This makes the detection of melanocyte precursor populations difficult. This stem cell niche has also been shown to give rise to epithelial stem cells (Blainpan and Fuchs, 2009) as well as neurons, glial and smooth muscle cells (Amoh et al, 2005), indicating either a highly plastic stem cell population, or a stem cell niche housing multiple stem cell lineages. Maintenance of the interfollicular epidermis was shown to involve many small "units of proliferation" (Blainpan and Fuchs, 2009) scattered throughout the interfollicular epidermis, suggesting an independent interfollicular niche of keratinocyte stem cells. To date, the presence of melanocyte stem cells in the interfollicular epidermis has not been definitively demonstrated, but is hypothetically possible and is supported by the observation of repigmentation of glabrous skin following UVA treatment in conditions such as vitiligo (Davids et al, 2009).

A dermal reservoir for melanocyte stem cells has also been proposed, based on the theory that the dermis would be less exposed to physiological or chemical stress than the epidermis (Li et al, 2009). A novel population of dermal stem cells, termed skin derived precursors (SKP), was first described by Toma (2001) where dissociated mouse dermis was shown to be capable of generating free-floating spheres, resembling neurospheres. Further studies have demonstrated a neural crest origin of SKPs and have been shown to be capable of differentiating along glial, neuronal, mesenchymal and melanocytic lineages (Fernandes et al, 2004, 2008; Wong et al, 2006). Li et al (2009) isolated a similar multipotent dermal precursor from human foreskin, termed dermal stem cells (DSC), which expressed additional embryonic stem cell markers OCT4 and NESTIN, not previously shown in SKPs. This group further demonstrated, via a three-dimensional skin equivalent model, the sphere forming dermal stem cells migrated from the epidermis to the dermis, differentiating into mature HMB45-positive melanocytes. This study demonstrated, for the first time, the existence of a dermal reservoir of melanocyte stem cells. A defined, spatially restricted niche for these melanocyte precursors has not yet been reported.

Belicchi et al (2004) described a population of pluripotent cells in human skin which expressed the neural crest stem cell marker CD133 and differentiated into neurons, astrocytes and glial cells. CD133 has also been identified in endothelial cells and mast cell precursors. Interestingly, mast cells have been shown to insert into the hair follicle following bone marrow transplantation and Grichnik (2008) has proposed it may be possible that both mast cells and melanocytes are derived from a circulating CD133+ precursor, and further, that this may be the mechanism resulting in spontaneous repigmentation of grey hair. Whether this may also be used to explain eruptive naevi, circulating naevus cells or the observation of naevus cells in lymphoid tissues remains uncertain.

1.6.4.3 The tumour stem cell hypothesis in the evolution of melanocytic naevi and melanoma

As discussed above, the *in vitro* observation of a sub-population of cells with stem-like features within tumour cultures has led to the hypothesis known as the tumour or cancer stem cell hypothesis. The identification of stem cell niches and cells of a precursor phenotype which persist in post-natal tissues has made this hypothesis feasible. The tumour stem cell model advocates some cancers may arise from a tissue resident precursor cell

which has undergone a mutational event and not from a fully differentiated cell as previously accepted. It is hypothesised that this mutated precursor cell responds abnormally to local environmental signals and, when recruited, may result in a genomically unstable transit amplifying population (refer to Figure 4) which forms the bulk of the tumour. These cells may then initiate differentiation and, depending on the nature of the underlying mutation, or on the presence of cumulative mutations, varying degrees of differentiation may be reached. Self-limiting defects may allow the cells to retain normal cellular functions and responses to local environmental signals, resulting in a neoplasm more similar to normal tissue and hence growing in a benign manner, while more severe defects, or cumulative defects, may result in autonomy of surrounding signals, a limitless replicative potential, the ability to invade local tissues and/or metastasise and hence, malignancy. Of importance, this model suggests that only a subpopulation of self-renewing tumour cells drive tumour formation. This is in contrast with the stochastic model of tumour development, which advocates that all cells within a tumour are capable of tumour generation. In addition, the resultant transit amplifying population may carry varying numbers of mutations and/or reach varying degrees of differentiation, both of which may result in a heterogeneous population of cells within a single tumour mass, a well described finding in tumour biopsies and cultures (discussed in 1.6.4.4 below).

This tumour stem cell hypothesis provides an attractive model of tumour development in general. It can be used to explain tumour dormancy, as precursor cells would exist unstimulated for long periods of time before being recruited and giving rise to mutated progeny. It can simplify the concept of "de-differentiation", the process whereby a cancer cell is said to progress from a cell resembling a fully differentiated cell, to one resembling a precursor phenotype (i.e. a reversed process of differentiation), a process which has not be fully explained to date. It is well accepted that cells resembling their differentiated counterparts tend to behave in a more benign manner, while those losing this phenotype, known as "un-differentiated" or anaplastic cells, tend to behave in a far more malignant manner and carry a worse prognosis. For this reason, "un-differentiated" cells were thought to represent a later stage in cancer development. However, this process of "de-differentiation", and why a cell would revert to a precursor phenotype, has not been adequately described. The tumour stem cell hypothesis can also be used to explain metastases. Here, metastases can be explained by stem cell biology alone, including smaller size and differences in adherence. It is further been proposed that these highly migratory embryonic cells retain their ability to migrate and, if these tumour stem cells circulate, they may give rise to distant metastases. Lastly, the tumour stem cell hypothesis may explain the poor regression rates observed in certain malignancies. It is proposed that rapidly dividing and differentiated cells are destroyed by chemotherapeutic strategies and the immune system response, while the slow-dividing stem-like cells, which feed the malignancy, may be overlooked (Grichnik et al, 2006). This may also be used to explain late local recurrence or metastasis after a "disease free interval", as malignancy may be harboured in these slow-dividing, yet self renewing cells.

The tumour stem cell model also proves an attractive hypothesis in naevus and melanoma development specifically. Firstly, it can be used to explain the multiple subtypes of lesions observed. Melanocytic neoplasms demonstrate numerous different, yet repeatable, patterns both clinically and histologically which allows for classification of these neoplasms into specific subtypes. They display variations in colour, size, morphology and distribution, yet show reproducible patterns within each specific subtype. It has been proposed that each distinct pattern represents a distinct underlying mutation, developmental phase or local signalling environment (Grichnik, 2008) (Figure 5). Similarly, precursor cells higher in the dermis and epidermis would be exposed to normal epidermal environmental cues and develop along melanocytic lines, while those deeper in the dermis would be removed from epidermal stimuli and/or exposed to altered stimuli in the dermal environment and may revert to a phenotype resembling Schwann cells.

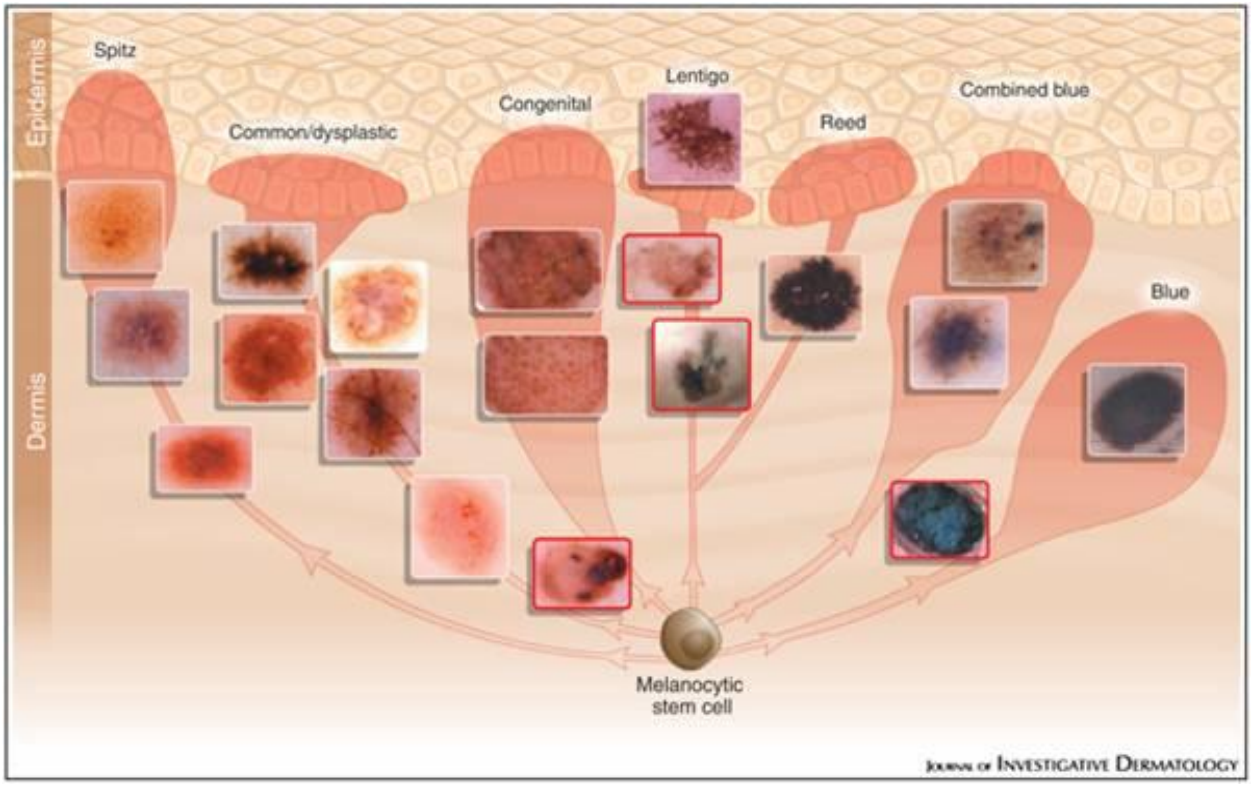

Figure 5: Theoretical growth patterns of melanocytic neoplasms: A mutated dermal precursor cell (brown) attempting normal developmental pathways to the epidermis. Varying clinical and histological subtypes would result depending on the mutation and/or local environmental influences (Grichnik, 2008).

The tumour stem cell model, however, is based on a static cross-sectional analysis of neoplastic tissues and the temporal development of these neoplasms cannot be accurately concluded. It is entirely possible that these precursor-like cells result from differentiated cells which have undergone a mutational event, reverting to a stem-like phenotype. Thus, the "cancer stem cell hypothesis" does not imply that the "cell of origin" is a true stem cell. Understanding the relationship between cancer stem cells and adult stem cells still needs to be fully explored.

1.6.4.4 Evidence for the tumour stem cell model in melanocytic naevi and melanoma

In considering the tumour stem cell model in melanoma development, a number of studies have shown data in support of this hypothesis. Melanomas have been shown to exhibit phenotypic heterogeneity, both *in vivo* and *in vitro*, suggesting an origin from a cell with multi-lineage differentiating abilities. Fang et al (2005) report a sub-population of melanoma cells which propagate as non-adherent spheres and individual cells which are able to differentiate into multiple cell types, including melanocytes, adipocytes, osteocytes and chondrocytes, imitating the plasticity of neural crest stem cells. Grichnik et al (2006) studied melanoma cell lines and their ability to efflux Hoechst 33342 dye, a technique known to enrich for stem cells in many tissues, to separate cell populations. The cells with the greatest ability to efflux the dye were small in size, less melanised and gave rise to larger cell forms. They exhibited lower proliferative rates, but had the greatest ability to expand in culture. These findings are in keeping with stem cell biology. Neural crest stem cell markers CD133, nestin (Klein et al, 2007) and HNK1 (Thies et al, 2004) have been described in cutaneous melanoma cultures suggesting the presence of a neural crest precursor phenotype. Schatton and Frank (2008) showed a subset of cells in primary and metastatic melanoma express the neural crest stem cell marker p75 (CD271). These cells displayed a markedly enhanced capacity for self renewal, increased differentiation plasticity and the ability to form tumours and metastasize when injected into mouse models, as compared to p75 negative cells from the same melanomas.

What the above studies interestingly indicate is that not all melanoma cells are equally tumorigenic. Instead, subsets of tumour cells appear to exist which are capable of increased self-renewal and differentiation plasticity. In opposition to the above, Quintana et al (2008) showed efficient tumour formation from single, unsegregated melanoma cells. In a subsequent study, Quintana et al (2010) showed a high proportion of melanoma cells to be tumorigenic (28%) and no specific marker could distinguished tumorigenic from non-tumorigenic melanoma cells. In addition, surface markers appeared to be reversibly expressed by tumorigenic melanoma cells. It has been suggested that the disparity regarding cancer stem cells may result from variations in the methodology used to study such cells, and that the tumour microenvironment and host immune system response may affect the frequency and phenotype of melanoma stem cells (as reviewed by Girouard and Murphy 2011; Gupta et al, 2009 and Kennedy et al, 2007).

1.7 Study rationale, aims and specific objectives

In considering all the above, including evidence for the existence of stem-like cells in melanoma cultures, the disparity with regards to specific cancer stem cell markers and the role of microenvironmental influence on cell phenotype, one cannot exclude the impact of *in vitro* conditions on cell morphology, phenotype and selective outgrowth. To our knowledge, no data exists for the *in vivo* identification and/or characterisation of precursor cells within naevus or melanoma biopsies. This study has therefore selected to analyse human biopsy samples by direct immunofluorescence in order to determine the *in vivo* presence, or absence, of precursor cells. Secondly, although benign naevi are incredibly common, with more than 97% of individuals having at least one

naevus (Kincannon and Boutzale, 1999), are easy to detect clinically, and are commonly removed for cosmetic and/or diagnostic purposes thus being widely available for histological examination, naevi have received very little attention in current literature. Also, the occurrence of "de-differentiated" cells in some melanomas, and the current lack of understanding as to the overlap between "de-differentiated" and precursor or stem-like cells in general, may cloud the issue should precursor cells be found within melanoma tissue. As a result, in this study it is proposed that the benign melanocytic naevus is an underutilised and model system with which to study tumour stem cell biology. Melanocytic naevi may well provide critical information on the role of stem cells and/or melanocytes as a possible initiating event in both benign and malignant disorders. This knowledge may thus assist in advancing the understanding of such disorders and facilitate refining of classification, diagnosis and treatment strategies.

1.7.1 Broad aims

The broad aims of this study are to provide a detailed phenotypic characterisation of a naevus cell, and to examine the hypothesis that melanocytic naevi may originate from a pluripotent or neural crest-like stem cell and not via de-differentiation from a mature epidermal melanocyte.

1.7.2 Objectives

- To determine the *in situ* expression and distribution of key melanocyte markers in acquired melanocytic naevi and to establish whether these markers are typical of mature epidermal melanocytes or of a precursor phenotype.
- To determine the *in situ* expression and distribution of key Schwann cell markers in acquired melanocytic naevi and to establish whether these markers are typical of mature myelinating Schwann cells or of a precursor phenotype.
- To determine the *in situ* expression and distribution of neural crest markers in acquired melanocytic naevi.
- To determine the *in situ* expression and distribution of stem cell markers in acquired melanocytic naevi.
- To establish whether the five selected subtypes of acquired melanocytic naevi (junctional, compound, intradermal, dysplastic and blue naevi) are similar or different with regards to cellular composition and distribution of precursor cells, if present. And to examine whether the presence of precursor cells is related to an increased risk of malignant transformation, as determined by "high-risk" dysplastic subtypes.
- To determine, if present, the proliferating compartment of naevi; and thus identify a potential compartment of origin of melanocytic neoplasms and/or a potential niche for melanocyte stem cells within the skin.

1.7.3 Approach and selection of markers

Melanocytic naevi have been shown to display features of both melanocyte and Schwann cell lineage. The cell of origin, and subsequent pathogenesis, of a "naevus" cell thus remains to be fully understood. In order to fully characterise a naevus cell phenotypically, markers of melanocyte and Schwann cell lineage were selected. Melan-A (MART-1) is a melanocyte differentiation antigen which is specific to melanocytes of normal skin, melanomas and retinal pigment epithelium, but is not expressed in other tissues. Antibodies against this antigen are widely used in anatomical pathology in order to detect cells of melanocyte lineage as it is a highly sensitive and specific marker (Sheffield et al, 2002; Snyder and Paulino, 2002). S100 is a large family of calcium channel binding proteins. In the skin, S100 is expressed in melanocytes, Langerhan's cells and dermal dendritic cells. It is considered the most sensitive marker for differentiated melanocytes, yet its lack of specificity limits its use as a single diagnostic marker (Sheffield et al, 2002; Snyder and Paulino, 2002).

As discussed previously, p75 is expressed in NCC prior to commitment to either melanoblast or Schwann cell fate. P75 continues to be expressed in myelinating Schwann cells where it would be expected to be co-expressed with S100. It is not expressed in normal skin melanocytes, and thus a p75 positive but S100 negative (p75+/S100-) cell, not in association with dermal nerves, would suggest a cell of neural crest phenotype. OCT4 and NANOG are transcription factors important in maintaining pluripotency of embryonic stem cells. They are highly expressed in undifferentiated embryonic stem cells and expression decreases gradually after embryoid body formation. Both markers have been identified in certain malignant tissues of embryonic origin, as well as foetal gonads, ovary and testis. Tai et al (2005) examined human normal tissue arrays for the expression of OCT4. One weakly OCT4-positive cell was unconvincingly demonstrated in the basal layer of the epidermis and thought to represent an epidermal stem cell. At present, there is no convincing data for the demonstration of OCT4 and/or NANOG positive cells in normal human skin.

Ki-67 is a proliferation marker expressed throughout all stages of the cell cycle except G0, when it cannot be detected. It localises to the nucleus where it is predominantly located in the perinucleolar region in the G1 phase, and in the later phases, provides a more diffuse pattern by dispersing throughout the nuclear matrix. It was thus utilised to determine the proliferating compartment of naevi.

2. Materials and Methods

2.1 Tissue culture

Positive "tissue" controls for OCT4 and NANOG immunostaining were generated from cultured mouse embryonic stem (mES) cells and human induced pluripotent stem cells (iPS) respectively. All tissue culture was carried out in a Bio-Flow Biological Safety Cabinet Class II. All surfaces, microscopes, bottles, tubes, gloves and instruments were sterilised by wiping with a 70% ethanol solution immediately prior to working with them. Gloves were worn at all times. Cells were incubated in a Forma Scientific water-jacketed incubator (Thermo Scientific, USA) at 37^{o}C, 5% CO_2.

2.1.1 Culture of mouse embryonic fibroblasts (MEF) feeder layers

Mouse embryonic fibroblasts (MEFs) from 14 day old mouse embryos were harvested according to standard procedures by Robea Ballo (Evans and Kaufman, 1981; Martin, 1981). All cells used were at passage 2 and were cultured in MEF medium consisting of Dulbecco's modified Eagles medium (DMEM) (Highveld Biological, South Africa) supplemented with 10% foetal bovine serum (FBS) (Gibco, USA), 100 U/ml penicillin (Sigma-Aldrich, USA), 100 µg/ml streptomycin (Sigma-Aldrich, USA), 1% non-essential amino acids (Gibco, USA) and 0.1 mM β-mercaptoethanol (Merck, Germany). Cells were cultured in 10 cm dishes (Corning Inc., USA) and medium was changed every 3-5 days depending on cell density. Cells were passaged when reaching 90% confluence using a 0.05% trypsin/EDTA (TE) solution, were split 1:3 and seeded into 10 cm plates. MEFs were not used beyond passage 5.

2.1.2 Mitotic inactivation of MEFs

Mitomycin C inhibits cell division by cross-linking DNA and is widely used as a chemotherapeutic agent by virtue of its antitumour and antibiotic activity. In cell culture systems it is used for mitotic inactivation, inhibiting cell division, yet allowing continued cell metabolism. MEFs at passage 3-4 were inactivated using mitomycin C (Sigma-Aldrich, USA). Briefly, MEF medium was removed from plates and cells were washed in 1x PBS. Cells were then incubated in MEF medium containing 10 µg/ml of mitomycin C for 3 hours at 37°C. Following inactivation cells were thoroughly washed in 1x PBS to remove all traces of mitomycin C, trypsinised and resuspended in MEF medium. Cells were subjected to repeat trituration in order to generate a single cell suspension and counted using a haemocytometer (Marienfeld, Germany). Cells were seeded in a 6 well plate at a density of 5 x 10^5 cells/well in MEF medium, in preparation for use with mouse embryonic stem (mES) cell cultures. Inactivated MEFs (iMEFs) were seeded a minimum of 24 hours prior to mES cell seeding in order to allow for adequate formation of a feeder layer. Inactivated MEFs were used for a total of 7 days following inactivation. Excess iMEFs were frozen down (section 2.1.8).

2.1.3 Mouse embryonic stem cell (mES cell) culture

Mouse ES cells (stocks prepared by Allison Patterson in the Kidson laboratory) were thawed and seeded in 35 mm dishes containing a feeder layer of iMEFs. Cells were grown in mES cell medium containing DMEM (Highveld Biological, South Africa) supplemented with 15% FBS (Gibco, USA), 100 U/ml penicillin (Sigma-Aldrich, USA), 100 µg/ml streptomycin (sigma-Aldrich, USA), 1% non-essential amino acids (Gibco, USA), 0.1 mM β-mercaptoethanol (Merck, Germany) and 1% Leukaemia inhibitory factor (LIF) (courtesy of the Department of Immunology, UCT). LIF is a cytokine which has been isolated from the conditioned medium of certain feeder layers and is important in suppressing mES cell differentiation by its interaction with the transcription factor STAT3 (Matsuda et al, 1999). In this study, LIF was acquired from the conditioned medium of the CHO-cell line and diluted 1:400 in PBS to result in a working stock solution. Medium was changed every 1-3 days depending on colony density.

Mouse ES cells were expanded every 2-4 days according to colony density, size and morphology (as recommended by Robertson, 1987). Colonies were lifted using 300 µl of dispase (5 mg/ml) (Sigma-Aldrich, USA) per 35 mm dish as it was found to selectively lift mES cell colonies before disrupting the underlying feeder layer. A single cell suspension was generated by repeat trituration before sub-culturing. From each 35 mm dish one third was seeded on an existing feeder layer of iMEFs to expand the mES cultures and subsequently passaged as above. The remaining two thirds were either: (i) placed in a 10 cm dish on an existing feeder layer of inactivated PA6 cells for neurosphere generation (section 2.1.7), (ii) one third placed in 500 µl Tripure (Roche Diagnostics, USA) for RNA extraction (not detailed here), and one third frozen down to restore stocks, or (iii) two thirds embedded in HistoGel™ (Richard-Allan Scientific, USA) for immunofluorescence (section 2.2.3.2[b]).

2.1.4 PA6 cell culture

PA6 cells are derived from newborn mouse calvaria (Kodama et al, 1982). Cells were grown in PA6 medium, consisting of DMEM supplemented with 10% FBS, 100 U/ml penicillin and 100 µg/ml streptomycin. The PA6 cell line used in this study showed a loss of contact inhibition and cells were inactivated using mitomycin C according to the above protocol (section 2.1.2, PA6 medium was substituted for MEF medium). Although this technique has been described (Schwartz CM et al, 2005) it had not been used previously in our laboratory. Mitomycin C inactivation of PA6 cells was verified by a growth curve (section 2.1.5).

2.1.5 Verification of mitomycin C inactivation of PA6 cells

A defined number of inactivated PA6 (iPA6) cells (2×10^5) were seeded onto numerous 35 mm plates and cultured in PA6 medium (section 2.1.4) for growth rate analysis. Cells were counted on either day 2, 3, 6 or 9 post-seeding and a growth curve constructed. Cell counts were performed as described above (section 2.1.2),

and showed a slight drop off in cell number and importantly, no increase in cell number, thus validating the inactivation of PA6 cells by mitomycin C.

2.1.6 Determining the seeding density of iPA6 cells

Since PA6 cells have not been routinely inactivated, the concentration of iPA6 cells required to generate a stable 80-90% confluent feeder layer needed to be determined. Here, iPA6 cells were seeded onto numerous 35 mm dishes in the following concentrations (i) 1 x 10^5, (ii) 2 x 10^5, (iii) 3 x 10^5, (iv) 4 x 10^5 and (v) 5 x 10^5 and cultured in PA6 medium (section 2.1.4). Cells were visualised over the next 7 days and an optimal seeding density of between 2 x 10^5 and 3 x 10^5 was noted to result in an 80-90% confluent feeder layer. For the remaining iPA6 work, a seeding density of 2.5 x 10^5 per 35 mm dish was used, and was adjusted proportionately for 6 cm and 10 cm plates.

2.1.7 Generation of neurospheres from mES cells

Inactivated PA6 cells were seeded at the above density onto 10 cm plates and allowed to recover overnight in PA6 medium (section 2.1.4). Sub-cultured mES cells were seeded on the iPA6 feeder layers and grown in DMEM supplemented with 1% FBS, 10% Knock Out Serum Replacement (Gibco, USA), 100 U/ml penicillin and 100 µg/ml streptomycin. At 10-14 days following seeding of mES cells, colonies had started to lift and formed neurospheres in suspension as described by Kitajima et al (2005). Medium containing neurospheres was removed using a wide-bore pipette and gently centrifuged. The resultant neurosphere pellet was resuspended by gentle trituration, taking care not to fracture the neurospheres, and whole neurospheres were transferred to the inverted lid of a 6cm dish (TPP, Europe) which was contained within a 10cm dish (Corning Inc., USA). Medium was replaced every 3-4 days by removing 4-5ml of medium from the edge of the dish, taking care not to remove any neurospheres. Fresh medium was then added.

Neurospheres propagated by "budding off" (refer Results, Figure 18) and dishes were sub-cultured by removing medium containing neurospheres in a wide-bored pipette and placing in a new 6 cm dish. After a further 14 days of propagation, neurospheres were either (i) embedded in HistoGel™ for immunofluorescence analysis (section 2.2.3.2 [b]), (ii) frozen down for stock (section 2.1.8) or (iii) resuspended, after careful trituration, in 1 ml Tripure (Roche Diagnostics, Germany) for RNA extraction (not detailed here).

2.1.8 Freezing down of cells

Neurospheres, MEFs, iMEFs, PA6s and iPA6s were frozen down for storage and later use. This ensured adequate stocks for future research, as well as a constant availability of inactivated feeder layers for immediate use when required. Briefly, cells were washed in 1x PBS and lifted with TE. The resultant cell suspension was centrifuged to generate a cell pellet and resuspended in DMEM with 20% FBS and 10% dimethyl sulfoxide

(Merck, Germany). This was then placed in cryogenic tubes (Greiner bio-one, Germany), cooled slowly overnight in a cotton wool lined box at -80°C and transferred to liquid nitrogen storage the following day.

2.1.9 Mycoplasma analysis and treatment

Mycoplasma, an intracellular bacterium, is a common contaminant in cell culture and may induce cellular changes, including chromosome aberrations, changes in cellular metabolism and cell growth. Cultured cells were thus tested routinely for mycoplasma infection using a Hoechst (Sigma-Aldrich, USA) nuclear stain and standard operating procedure as outlined by Chen (1977). Cells were viewed under the appropriate channel using a Zeiss Axiovert 200M microscope and images were captured using the Zeiss Axiocam HR monochrome camera. Cells infected with mycoplasma were treated with 10 µg/ml Ciprobay (Highveld Biological, South Africa) every 12 hours in fresh medium for 3 days and then re-stained with Hoechst as above. No cell line testing positive for mycoplasma was used in this study.

2.1.10 Microscopy of cultured cells

Cells were periodically photographed for record purposes. Cells were visualized using an Olympus CKX41 Microscope (Olympus, Japan) and photographed using a Canon Powershot S50 (Canon, Japan).

2.1.11 Human induced pluripotent stem cell (iPS) culture

Samples for optimisation of immunofluorescence protocol for pluripotency marker NANOG used human induced pluripotent stem cells (iPS) which were kindly donated by Lauren Watson and Danielle Smith, Human Genetics, University of Cape Town.

2.2 Immunofluorescence

2.2.1 Study samples

Biopsy samples of melanocytic naevi from human skin were obtained from the archives of the National Health Laboratory Services (NHLS), courtesy of Professor D. Govender, NHLS, Groote Schuur Hospital (GSH). These samples were previously obtained from patients who had undergone a biopsy of a pigmented lesion, which was subsequently histologically confirmed as a benign melanocytic naevus and archived in the NHLS archives. All samples were formalin-fixed and paraffin-embedded at the time of biopsy. Each sample was given a histopathological diagnosis of a benign melanocytic naevus by a qualified anatomical pathologist. A total of ten samples were included in this study. Five subtypes of acquired melanocytic naevi (two samples within each subtype) were included: junctional, compound, intradermal, dysplastic and blue naevi.

Study samples were kindly sectioned by Heather McLeod, Department of Anatomical Pathology, GSH, as described in section 2.2.3.1(b). A total of 15 sections were obtained from each naevus sample, generating one section per slide. Slides were labelled sequentially 1 through to 15.

2.2.2 Patient clinical information

Patient folders were made accessible in order to access relevant clinical information. Details regarding age, sex, anatomical site, change in appearance, personal or family history of melanoma and subsequent re-presentation for naevus/melanoma biopsy were noted for correlation with immunofluorescence findings (refer Results, Table 6). Full ethical approval to access patient folders was obtained from the Human Research Ethics Committee, UCT, (HREC:REF 553/2010) as well as provincially from the Western Cape Department of Health (RP 159/2011) (Appendix B).

2.2.3 Control samples

Naevus biopsy samples were formalin-fixed and paraffin embedded (FFPE) at time of initial biopsy and IF protocols were thus optimised for FFPE tissues. Positive controls for Melan-A (epidermal melanocytes), S100 (epidermal Langerhan's cells), Ki-67 (suprabasal keratinocytes) and p75 (epineurium and perineurium of dermal nerves) are found in normal skin and therefore control skin biopsies were used to optimise the IF protocol for these antibodies in FFPE tissues. Positive controls for OCT4 and NANOG are not reliably present in normal human skin and optimisation of these antibodies was performed using cultured mES and iPS cells respectively (discussed in section 2.2.3.2 below). Optimised protocols for antibodies in FFPE tissues are detailed in Table 4.

2.2.3.1 Control skin biopsies

Human skin biopsies were obtained from the Department of Plastic Surgery, Groote Schuur Hospital. These samples consisted of excess tissue which was donated following a scheduled surgical procedure. Informed consent was obtained prior to the procedure in all cases. Samples used in this study were obtained from reduction mammoplasties of middle aged females, of both African and Caucasian skin types. Specimens were placed in sterile specimen bags and transported directly to the Department of Human Biology laboratory on ice. All subsequent work was performed in a Bio-Flow Biological Safety Cabinet Class II and gloves were worn at all times. A 2 mm punch biopsy was made and this was placed in the lid of a 10 cm dish and washed in PBS to remove all traces of blood. This was then transferred to a 15 ml centrifuge tube (TPP, Germany) and fixed in 10 ml of 4% formaldehyde for 30 minutes.

2.2.3.1 (a) Paraffin embedding of control samples

Following fixation in 4% formaldehyde in PBS, skin biopsy samples were placed in tissue cassettes and processed according to a standard protocol for tissue processing (Boenisch et al, 2001) Briefly, samples were placed in an automatic tissue processor (Shandon Scientific, England) for overnight processing where they were dehydrated through a series of increasing grades of ethanol and then cleared in xylol prior to wax impregnation. The following day, samples were embedded in a wax "tissue block" (Kunz Instruments, Denmark) in preparation for sectioning.

2.2.3.1 (b) Sectioning of control samples

Tissue blocks were sectioned at 4 µm using a microtome (Reichert-Jung, RSA). Sections were mounted on Thermoscientific Superfrost Plus slides (Menzel-Glaser, Germany). These slides were utilised to ensure adequate adherence of the section to the slide during subsequent antigen retrieval steps. Sections were then placed at 60°C overnight and transferred to 37°C for a further 3 hours. Sections were stored in air-tight slide boxes at 4°C to prevent excessive drying prior to staining.

2.2.3.2 Control samples generated from cultured cells

2.2.3.2 (a) Immunocytochemistry (ICC)

Positive expression of selected markers in cultured cells was first confirmed by ICC. Cells grown on a coverslip in a 35 mm plate were washed in 1x PBS and fixed in 4% formaldehyde (Merck, Germany) in PBS for 30 minutes, then washed three times in 1x PBS, 10 minutes each. Cells were blocked for one hour at room temperature in 500 µl of blocking solution, containing 1x PBS, 5% FBS and 0.01% Triton X (BDH Chemicals Ltd, RSA). The block was aspirated and samples incubated with 300 µl primary antibodies at 4^{o}C overnight in a humidified chamber. Primary antibodies were diluted in 1% FBS in 1x PBS according to manufacturers recommendations, and further optimised by serial dilution if required. Primary antibodies and their dilutions were identical to those used for immunofluorescence analysis and are outlined in Table 4. The following day, cells were rinsed three times in 1x PBS, 5 minutes each, and incubated for 1 hour at room temperature in the dark with secondary antibodies (Jackson ImmunoResearch, USA), where antibodies and dilutions were also identical to those used for immunofluorescence analysis and outlined in Table 4. Cells were rinsed as above and mounted using mowiol and viewed under the appropriate channel using a Zeiss Axiovert 200M microscope and images were captured using the Zeiss Axiocam HR monochrome camera.

2.2.3.2 (b) Formalin-fixation and paraffin-embedding of cultured cells

Cultured mES cells and neurospheres were used to optimise the IF protocol for OCT4 and p75 in FFPE samples respectively. Unfortunately human iPS could not be generated in sufficient quantity to allow for FFPE of these cells and NANOG was optimised in cultured cells only.

Cultured mES cells and neurospheres (section 2.1.3 and 2.1.7 respectively) were subject to gentle trituration to generate a single cell suspension. Cells were washed three times in 1x PBS and fixed in 4% formaldehyde in PBS for 10 minutes. Cell pellets were washed, re-centrifuged and embedded in HistoGel^{TM} (Richard-Allan Scientific, USA). HistoGel^{TM} is a specimen processing gel which encapsulates small, friable and cytological specimens, while not interfering with staining processes. HistoGel^{TM}, which is solid at room temperature, was heated in a microwave oven for 30 seconds, or until liquid, and 500 µl of heated solution was added to the cell pellet using a wide-bore pipette. The cell pellet was gently resuspended in the liquid and transferred via a wide-bore pipette to a modified Eppendorf tube, which had been modified by cutting of the tip of the tube and placing

the Eppendorf tube upside down on its closed lid. This resulted in the contents settling in the lid of the inverted tube and allowed for easy removal of the HistoGel™ pellet once solidified. The tube was cooled on ice to allow the HistoGel™ to solidify. The HistoGel™ -pellet was then carefully removed by opening the lid. The resultant cylindrical HistoGel™ -pellet was dislodged from the lid using tissue forceps and placed in filter paper and into a tissue cassette for further processing, wax impregnation and tissue sectioning as described in section 2.2.3.1 above.

2.2.4 Optimisation of immunofluorescence protocol in FFPE control tissues

2.2.4.1 Antigen retrieval:

It is well recognized that formaldehyde fixation of tissues induces artefact by cross-linking of protein amino acid residues which may lead to masking of tissue antigens. Many antigen retrieval techniques have been devised to unmask these hidden antigen epitopes and recover immunoreactivity. Methods include (i) enzymatic digestion, known as proteolytic induced epitope retrieval (PIER) and (ii) heating of tissues by various methods, known as heat induced epitope retrieval (HIER). Methods include the use of a water bath, pressure cooker or microwave oven.

In this study, all antibodies were optimised for HIER using a pressure cooker. Melan-A, Ki-67, S100, p75 and NANOG were optimised using a 10mM Citrate buffer (pH 6.0). Briefly, slides were placed in a plastic Coplin jar, containing 50 ml Citrate buffer solution. A maximum of 4 slides per Coplin jar was used to allow for adequate buffer-to-slide ratio. This was then placed in a pre-heated pressure cooker for 20 minutes. Following this, the samples were removed from the pressure cooker and allowed to cool within the buffer for a further 20 minutes to allow for re-forming of antigenic sites. OCT4 was optimised using a 1 mM EDTA buffer (pH 8.0) and similarly heated in a pressure cooker for 5 minutes, followed by a 5 minute cooling period.

2.2.4.2 Blocking solution

The blocking solution consisted of a 1% Bovine Serum Albumin (BSA) (Roche Diagnostics, USA) in 1x PBS. All samples were blocked for 1 hour at room temperature in a humidified incubation chamber.

2.2.4.3 Primary and secondary antibody dilutions

For all samples, primary and secondary antibodies were diluted in 1% BSA in 1x PBS. Primary antibodies were incubated overnight at 4°C in a humidified incubation chamber. Secondary antibodies were incubated for 2 hours at room temperature in a humidified incubation chamber in the dark. Optimised protocols for antibodies used are detailed in Table 4.

Primary Antibody (Dilution)	Description	Cellular Localisation	Antigen retrieval	Secondary Antibody (Dilution)
Mouse monoclonal to **Melan-A** (Santa Cruz Biotechnology Inc, USA) (1:25)	Raised against recombinant Melan-A. Recognises the 20 kD Melan-A or MART-1 protein in human, mouse and rat.	Cytoplasm	HIER, Citrate buffer (Ph 6.0) 20 minutes	Donkey anti-mouse Cy3 (1:1000)
Rabbit polyclonal to **S100** (Dakopatts A/S, USA) (1:100)	Recognises human S100A and B.	Cytoplasm	HIER, Citrate buffer (Ph 6.0) 20 minutes	Donkey anti-rabbit Alexa-488 (1:500)
Mouse monoclonal to **p75** (BioTrend, Germany) (1:100)	Recognizes a cyteine-rich repeat located in the NGFR molecule. Cross reacts with human, monkey, pig, cat, raccoon and mouse.	Cell surface and cytoplasm	HIER, Citrate buffer (Ph 6.0) 20 minutes	Donkey anti-mouse Cy3 (1:1000)
Rabbit polyclonal to **Ki-67** (Abcam, USA) (1:200)	Raised against a synthetic peptide derived from within residues 1200-1300 of human Ki-67. Cross reacts with human, mouse and horse.	Nucleus	HIER, Citrate buffer (Ph 6.0) 20 minutes	Donkey anti-rabbit Alexa-488 (1:500)
Rabbit polyclonal to **OCT4-ChIP Grade** (Abcam, USA) (1:200)	Raised against a synthetic peptide derived from within residues 300 to the C-terminus of Human OCT4. Cross-reacts with human, mouse and Rhesus monkey.	Nucleus	HIER, EDTA buffer (Ph 8.0) 5 minutes	Donkey anti-rabbit Alexa-488 (1:500)
Rabbit polyclonal to **NANOG- ChIP Grade** (Abcam, USA) (1:200)	Raised against a synthetic peptide, corresponding to amino acids 29-49 of human NANOG. Does not cross-react..	Nucleus	HIER, Citrate buffer (Ph 6.0) 20 minutes	Donkey anti-rabbit Cy3 (1:1000)

Table 4: Optimised immunofluorescence protocols in FFPE samples. Primary and secondary antibodies, and their respective dilutions, were identical for immunocytochemistry (ICC) analysis but no antigen retrieval step was required.

2.2.5 Immunofluorescence of naevus study samples

Slides were place on a heating block (Kunz Instruments, Denmark) for 15 minutes or until wax thoroughly melted. Slides were then cleared in xylol and rehydrated through a series of alcohols to tap water as according to standardized protocols (full protocol, Appendix c). Heat induced epitope retrieval (HIER), using a pressure cooker, was utilised to unmask antigenic sites (section 2.2.4.1). Samples were washed three times in phosphate buffered saline (PBS) and placed in a humidified incubation chamber, blocked with 1% BSA for 2 hours and incubated with primary antibodies overnight at 4^{o}C as detailed in Table 4. The following day, samples were rinsed three times in PBS and incubated with secondary fluorescent-conjugated antibodies for 1 hour at room temperature in a humidified incubation chamber in the dark. Secondary antibodies were diluted in 1% BSA at ratios shown in Table 4. Following incubation with secondary antibodies, samples were washed three times in

1x PBS in the dark and mounted with mowiol. Sections were allowed to dry for 1 hour at room temperature in the dark and then placed at 4°C until viewing using the Zeiss microscope as detailed below (section 2.2.9).

2.2.6 Dual labelling

A double-staining or dual labelling IF protocol was developed which was identical for all steps outlined in section 2.2.5 above. Samples were incubated with a cocktail of primary antibodies, including Melan-A and Ki-67 (1:25 and 1:200 respectively) and Melan-A and S100 (1:25 and 1:100 respectively); and the correct final concentrations for each antibody was ensured. For the secondary incubation step, a similar cocktail of secondary antibodies - donkey anti-mouse Cy3 and donkey anti-rabbit Alexa (1:1000 and 1:500 respectively) was applied and subsequent steps as per section 2.2.5 above.

2.2.7 Internal and external controls in naevus sample analysis

Positive and negative controls were included in each section analysed, as outlined in Table 5. These controls were used to ensure optimal staining procedures in every section analysed regardless of day or time of IF processing. An autofluorescent control was performed to detect the tissues normal autofluourescence and "fixative-induced" fluorescence as a result of the above fixation, processing, antigen retrieval and blocking steps. Once the IF protocol for each antibody had been determined, optimised and verified, the external and autofluorescence controls were omitted. These were, however, performed periodically throughout the study to ensure ongoing adequate technique. No change in technique for any of the antibodies was required.

Control Type	Method	Rationale
Internal Positive Control	Study sample incubated with primary and secondary antibodies. Cells known to positively express epitope examined for positive staining: epidermal melanocytes (melan-A), Langerhan's cell (S100), basal and suprabasal keratinocytes (Ki-67), dermal nerves (p75), occasional pluripotent cells in adipose tissue, sebaceous glands and hair follicles (OCT4 and NANOG).	Exclude **false negative** result due to inadequate binding of primary or secondary antibody.
Internal Negative Control	Study sample incubated with primary and secondary antibodies. Cells known to negatively express epitope examined: for example epidermal keratinocytes (melan-A).	Exclude **false positive** results due to non-specific binding of primary or secondary antibody.
External Negative Control	Control sample incubated with secondary antibody only.	Exclude **false positive** results due to non-specific binding of secondary antibody in absence of primary antibody.
Auto-fluorescence Control	Omission of primary and secondary antibodies.	Exclude **false positive** results due to normal autofluorescence or "fixative induced" fluorescence following fixation, processing and HIER.

Table 5: Procedural controls used in the analysis of FFPE naevus samples.

2.2.8 DAPI staining

DAPI (4',6-diamidino-2-phenylindole), is a fluorescent stain that binds strongly to A-T rich regions in DNA. It is thus an important nuclear stain and is used extensively in fluorescence microscopy. In this study, DAPI was utilised to verify the nuclear positioning of OCT4 and NANOG staining. Following incubation of secondary antibodies and subsequent washes samples for OCT4 and NANOG were incubated with DAPI (Sigma-Aldrich, USA) (1:50, diluted in 1% BSA in 1x PBS) for 20 minutes in a humidified incubation chamber in the dark. Following incubation, samples were washed 3 times in 1x PBS and mounted as per section 2.2.5 above.

2.2.9 Viewing and image capturing

Slides were viewed under the appropriate channel using a Zeiss Axiovert 200M microscope and images were captured using the Zeiss Axiocam HR monochrome camera and Zeiss Axiovision 4.8 software program. For each run of each sample, the exposure time was optimised and subsequently set so that intensity of staining could be compared throughout the sample. This was not able to be standardised across samples due to differing staining intensity on different days, so intensity of staining is not comparable across samples.

2.2.10 Haematoxylin and Eosin stain (H&E)

All naevus samples were sectioned and numbered section 1-15. The middle section of each biopsy series, section 8, was subject to standard protocol for H&E staining and the other sections subject to IF analysis detailed above. Each H&E section was viewed using a Zeiss AxioSkop M microscope and images were captured using the Zeiss Axiocam HRc camera and Zeiss Axiovision 4.7 software program. The distribution of naevus cells recorded using a Zeiss Axiocam HR monochrome camera. Fluorescent images were correlated with corresponding H&E images to ensure data analysis was performed on representative areas of naevus cells only.

2.3 Analysis

2.3.1 Qualitative analysis

Ten naevus samples (two samples within each of five different subtypes) were included in the analysis and the expression of six antigens examined by IF. For each antigen, at least two sections were analysed, a minimum of ten sections apart (Figure 6a). In cases where large biopsies were divided into two or three fragments prior to fixation and wax impregnation, a total of four to six sections were analysed (Figure 6b). Qualitative analysis was performed by examining the entire immunolabelled section and noting the overall characteristics of IF staining, including the distribution, morphology and intensity of staining. Dual labelling techniques and serial section analysis allowed for detection of co-expressed markers.

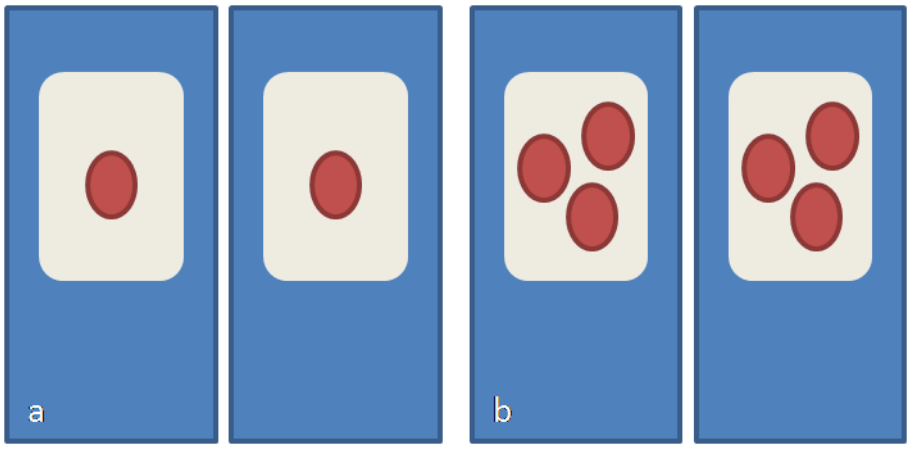

Figure 6: Diagrammatic representation of tissue sections generated from naevus biopsy samples.

2.3.2 Quantitative analysis

Quantitative analysis was performed by determining the proportion of positively labelled naevus cells per total naevus cells counted. For each biopsy sample, two sections (a minimum of ten sections apart) were subject to analysis with one of the six selected antibodies. Ten high power fields (HPF) evenly distributed throughout the bulk of the naevus biopsy which contained areas representative of naevus tissue were evaluated per sample, giving a total of twenty HPFs analysed for each antibody in each section. To determine the relationship between naevus occurrence and epidermal keratinocyte proliferation, the ten naevus samples and ten control skin samples were analysed. Five HPF were selected in each of two sections, a minimum of ten sections apart, in each of the naevus and control skin samples. The number of Ki-67 positive epidermal keratinocytes per unit length (µm) of basement membrane was determined by measuring the length of the basement membrane (section 2.3.3) and manually counting the positively stained cells.

2.3.3 *Image J* analysis software program

Images were analysed using the *Image J* (*Image J*, WCIF) for image analysis software program. The area of sample analysed and basement membrane length could be accurately calculated. Brightness and contrast could be adjusted for better viewing.

3. Results

3.1 Optimisation of immunofluorescence (IF) protocol for selected antibodies

The first objective of this study was to optimise the immunofluorescence (IF) protocol for each antibody selected. As detailed previously, naevus biopsy study samples consisted of archived specimens obtained from the NHLS that had been formalin-fixed and paraffin embedded (FFPE) at the time of naevus biopsy. Consequently, all antibodies required optimisation for use on FFPE tissue. Antibodies selected for analysis included: Melan-A, S100, Ki-67, OCT4, NANOG and p75. Optimised protocols are detailed in Table 4. Of note, antigen retrieval using a citrate buffer resulted in a high degree of background fluorescence when an Alexa-488-conjugated secondary antibody was utilised. A Cy3-conjugated secondary antibody was thus preferentially selected for Melan-A, NANOG and p75 analysis. Dual staining for Melan-A/S100 and Melan-A/Ki-67 necessitated the use of an Alexa-488-conjugated secondary antibody for S100 and Ki-67 analysis despite the increase in background fluorescence. OCT4 showed optimal staining using an EDTA buffer and an Alexa-488-conjugated secondary antibody could be utilised with minimal background fluorescence. Regardless of the secondary antibody selected, all images were captured in both the Alexa-488 (green) and Cy3 (red) channel as composite images were found to better delineate the skin architecture. In addition, DAPI was used for OCT4 and NANOG imaging and here images were captured in all three channels, with DAPI being visualised in the DAPI (blue) channel. DAPI, however, has been omitted from the below composite images to allow for better clarity of image. Only dual labelled cells (OCT4+/DAPI+ and NANOG+/DAPI+) were accepted as being true positive cells.

3.1.1 Optimisation of Melan-A

Results of Melan-A staining in control skin biopsies demonstrated Melan-A positive (Melan-A+) melanocytes within the basal layer of the epidermis (red arrows, Figures 7a, 7b). Staining was cytoplasmic and fine dendrites which projected into the epidermis were clearly visible (insert, Figure 7b). Non-melanocytic cells did not stain positively for Melan-A and no staining was seen in control samples where the primary antibody was omitted (Figure 7c).

3.1.2 Optimisation of S100

Results of S100 staining in control skin biopsies demonstrated S100 positive (S100+) epidermal melanocytes in the basal layer of the epidermis (red arrows, Figures 8a, 8b). S100 positive Langerhan's cells were seen in the suprabasal layers of the epidermis (white arrows, Figures 8a, 8b). S100 staining was cytoplasmic and fine dendritic processes that projected into the epidermis were clearly visible (insert, Figure 8a). Other epidermal cells did not stain positively for S100 and no staining was seen in the control samples where the primary antibody was omitted (Figure 8c).

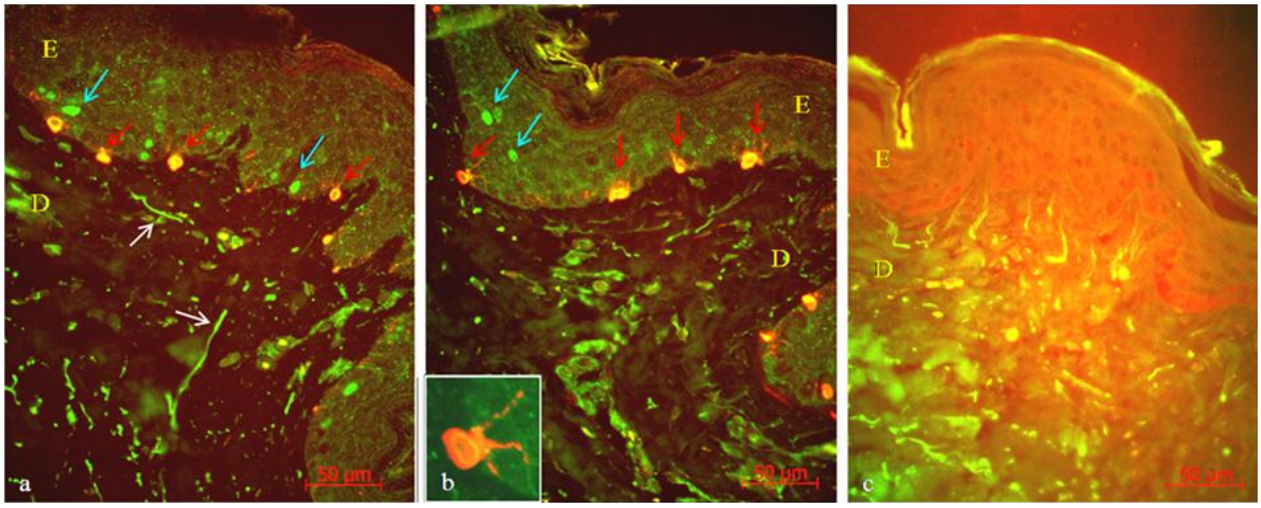

Figure 7: Optimisation of Melan-A immunostaining in FFPE human skin samples: a, b: Melan-A+ melanocytes within the basal layer of the epidermis (red) (red arrows) and Ki-67+ epidermal keratinocytes (green) (blue arrows) using a dual staining technique. Non-specific fluorescence of collagen fibres is seen within the dermis (white arrows). Insert b: Cytoplasmic staining and clear dendrites. c: No Melan-A staining in sample where primary antibody omitted. E: indicating epidermis. D: indicating dermis.

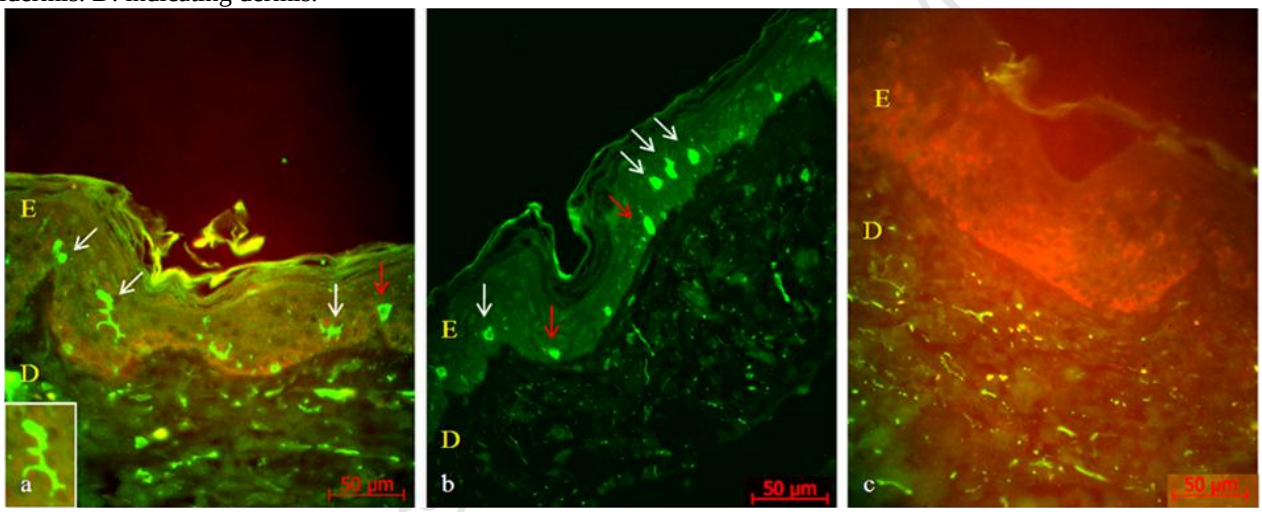

Figure 8: Optimisation of S100 immunostaining in FFPE human skin samples: a, b: S100+ basal melanocytes (red arrows) and suprabasal Langerhan's cells (white arrows) (both green). Insert a: Cytoplasmic staining and clear dendrites. c: No S100 positivity in section where primary antibody was omitted. E: indicating epidermis. D: indicating dermis.

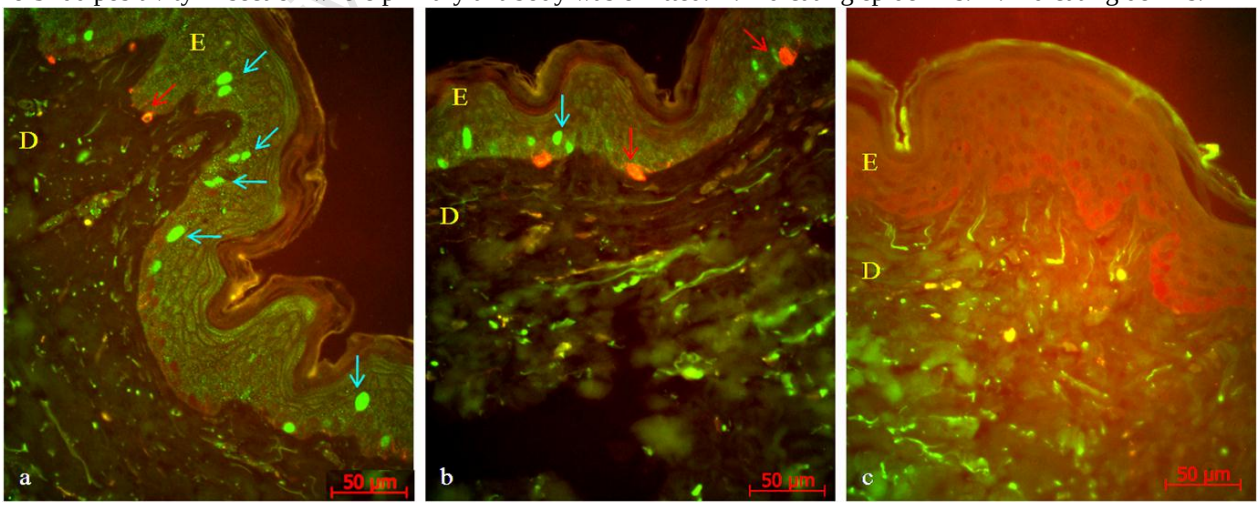

Figure 9: Optimisation of Ki-67 immunostaining in FFPE human skin samples: a, b: Ki-67+ keratinocytes in the suprabasal layer of epidermis (green) (blue arrows), predominantly paired, and Melan-A+ melanocytes in the basal layer of the epidermis (red) (red arrows). c: No Ki67+ cells in control where primary antibody omitted. E: indicating epidermis. D: indicating dermis.

3.1.3 Optimisation of Ki-67

To identify proliferating cells, and to establish whether it is possible to detect dividing melanocytes, a dual labelling technique for Melan-A and Ki-67 was performed on control samples of normal human skin. Results demonstrated Ki-67 positive (Ki-67+) keratinocytes within the basal and suprabasal layers of the epidermis (blue arrows, Figures 9a, 9b), with positive staining cells often occurring in pairs. No staining was seen in the control samples where the primary antibody was omitted (Figure 9c). Two sections of normal human skin, both obtained from the same individual, each showed a dual positive (Melan-A+/Ki-67+) melanocyte in the basal layer of the epidermis (arrows, Figures 10a, 10d).

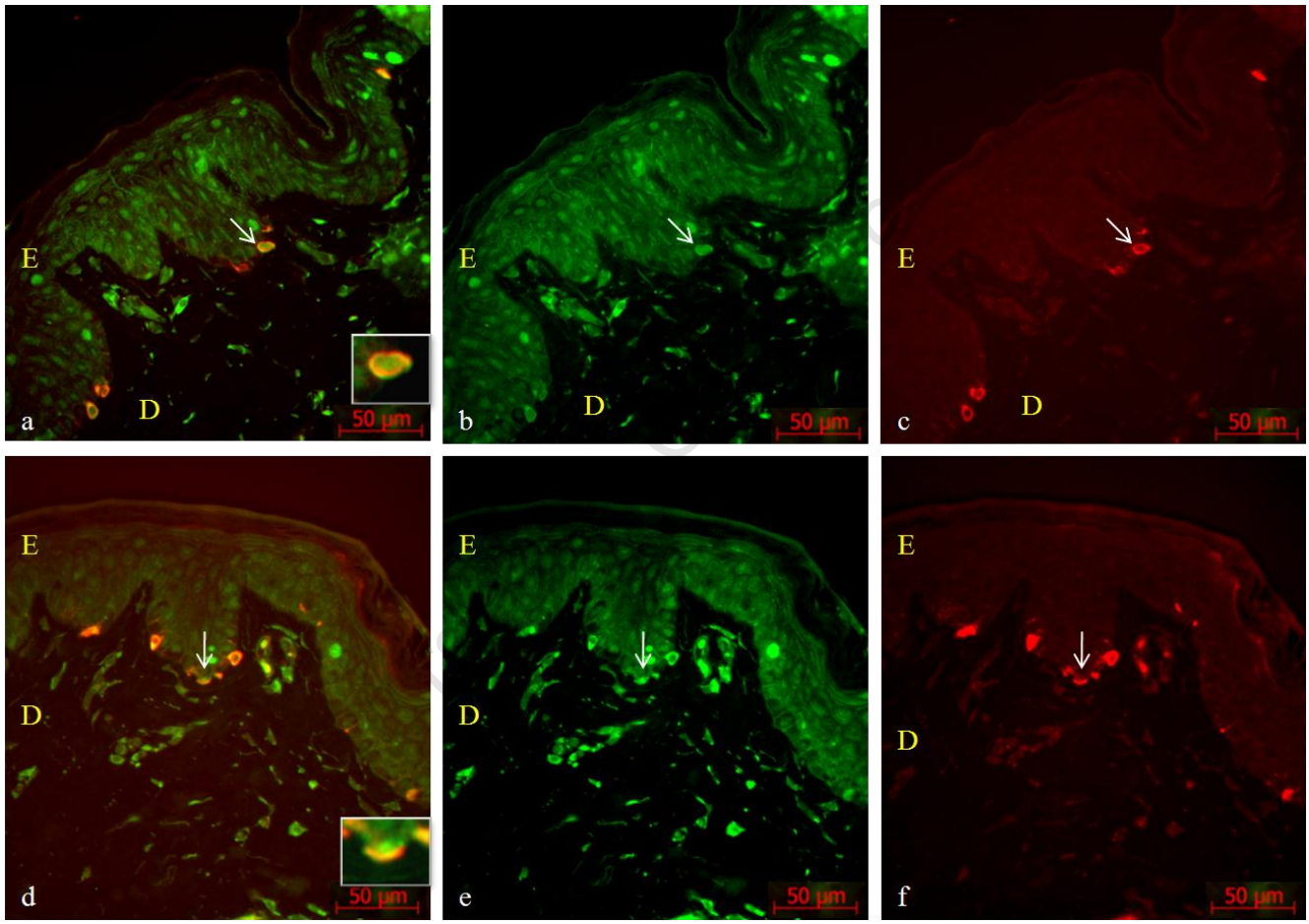

Figure 10: Dual labelling for Melan-A (red) and Ki-67 (green) in FFPE human skin samples: a, d: Composite images showing Melan-A+/Ki-67+ epidermal melanocytes (arrows). Insert a, d: Co-localisation of signals, enlarged view. b, e: Single channel images showing Ki-67+ melanocytes (arrows). c, f: Single channel images showing Melan-A+ melanocytes (arrows). E: indicating epidermis. D: indicating dermis.

3.1.4 Optimisation of OCT4

The objective of this experiment was to generate a positive "tissue" control for OCT4 immunostaining. Mouse ES cells were cultured as described in materials and methods (section 2.1.3) and formed well defined colonies. Colonies are typically small in size and display a rounded, defined bright edge under light microscopy (Figures

11a, 11b). As colonies matured and began to differentiate, they exhibited a larger size and a flattened, less well-defined edge (Figures 11c, 11d); features consistent with a loss in pluripotent phenotype (Robertson et al, 1987).

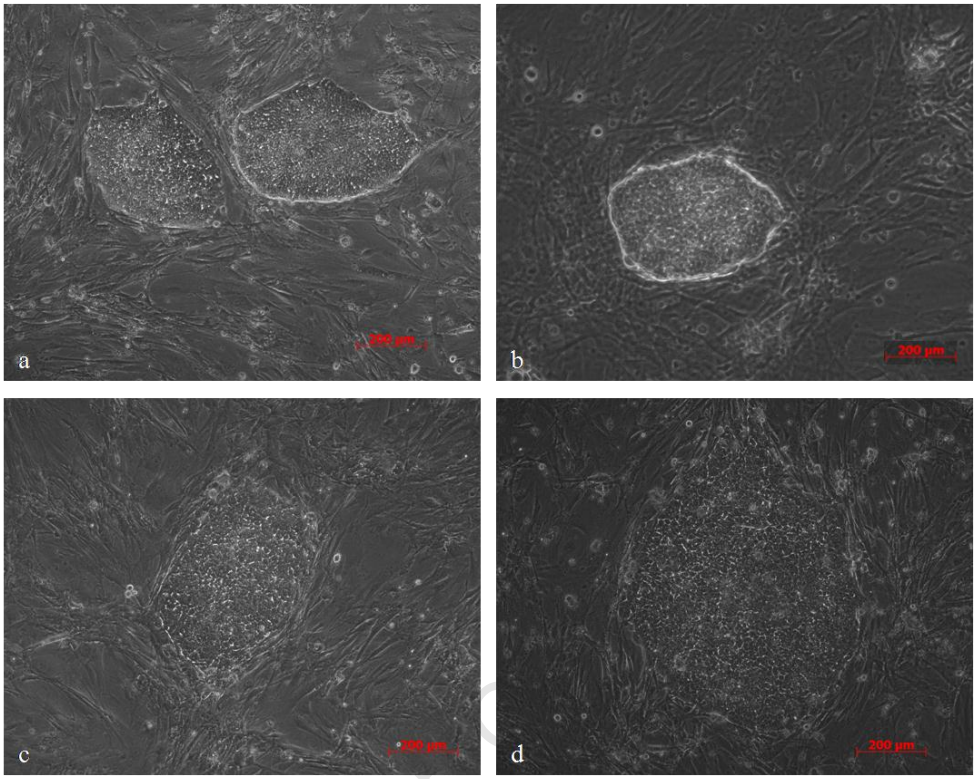

Figure 11: Morphology of mES colonies under light microscopy. a, b: Small, rounded, well-defined pluripotent colonies with a bright border. c, d: Flattened, poorly defined colonies which have started to differentiate and expand into the surrounding feeder layer.

Cultured mES cell colonies were then subject to immunofluorescence analysis and showed positive OCT4 expression in the nuclei of mES cells (Figure 12a). Nuclear localisation was confirmed by co-localisation with the nuclear stain DAPI (not shown here). Some nuclei did not show OCT4 positivity (white arrows Figure 12a). Underlying iMEF cells did not stain positively for OCT4 (internal negative control, red arrows Figure 12a) and no OCT4 staining was seen in the control sample where primary antibody was omitted (Figure 12b).

Once colonies were shown to express OCT4, cultured mES cells were lifted with dispase and subject to careful trituration to generate a single cell suspension, and then subject to formalin-fixation and wax impregnation (as detailed in materials and methods, section 2.2.3.2[b]). Results showed OCT4 positive (OCT4+) nuclei of mES cells (Figure 13a, 13b) and no staining was seen in control sections where primary antibody was omitted (Figure 13c).

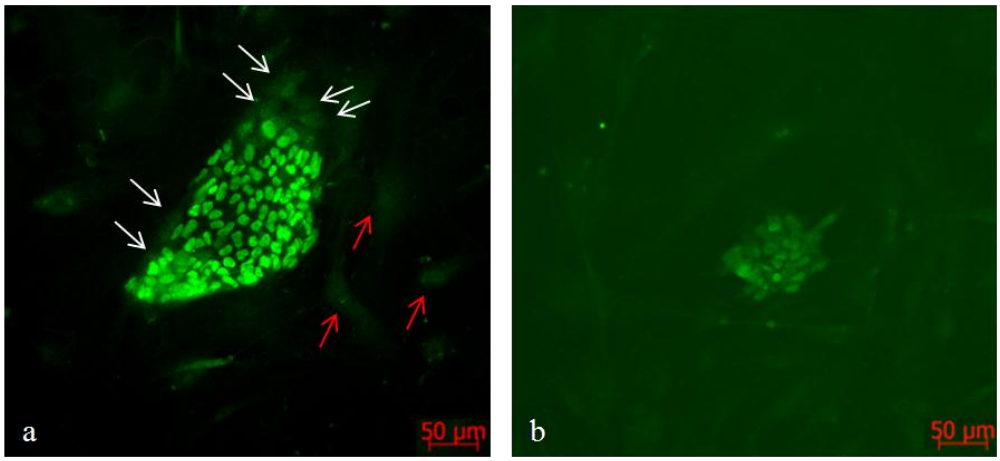

Figure 12: OCT4 expression in cultured mES cell colonies by immunocytochemistry: a: An OCT4+ mES cell colony (green) showing positive nuclear staining. Some nuclei appear elongated and/or flattened in areas of high cell density. Some mES cells did not display OCT4 positivity (white arrows). Background iMEF cells stain negatively for OCT4 and are poorly visualised (red arrows). b: No OCT4+ cells seen in control where primary antibody was omitted.

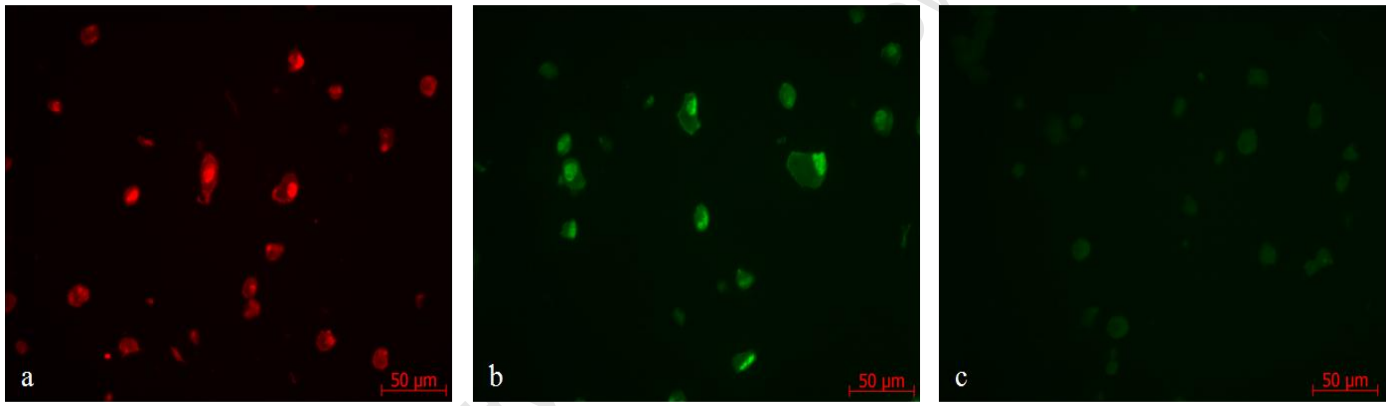

Figure 13: OCT4 expression in FFPE mES cells: a, b: OCT4+ mES cells visualised by Cy3- and Alexa-488-conjugated secondary antibodies respectively (red and green correspondingly), showing nuclear localisation of signal. c: No staining is seen in control sample where primary antibody was omitted.

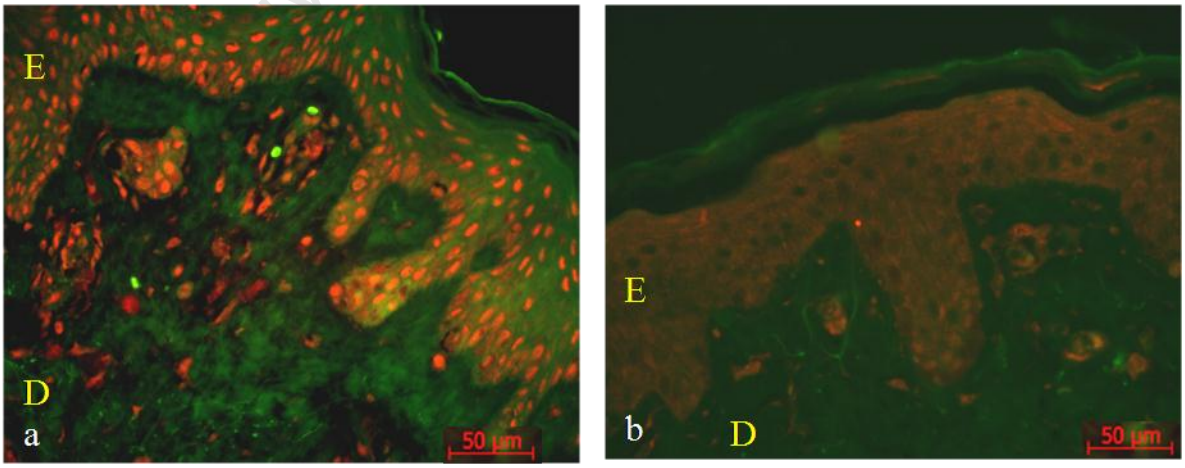

Figure 14: Optimisation of OCT4 immunostaining in FFPE human skin samples: a: OCT4+ epidermal keratinocytes following Citrate mediated antigen retrieval (red). B: Negative epidermal staining when an EDTA buffer was used. E: indicating epidermis. D: indicating dermis.

OCT4 expression was then examined in normal skin biopsies to further optimise the IF protocol for FFPE human skin. The aim was to eliminate non-specific binding of this antibody in processed skin and thus exclude false positive results. When HIER using a citrate buffer was performed, the majority of epidermal keratinocytes appeared positive for OCT4 (Figure 14a), indicating non-specific background staining. This non-specific binding was eliminated when and EDTA buffer was utilised (Figure 14b). Both Citrate and EDTA mediated antigen retrieval resulted in optimal OCT4 immunostaining in cultured mES cells and an EDTA buffer was thus selected for antigen retrieval in naevus samples. Interestingly, although stem cell niches have been described in both the basal layer of the epidermis and in the dermis of murine skin (Amoh et al, 2005; Fernandes et al, 2004, 2007; Li et al, 2009; Nishimura et al, 2002; Sieber-Blum et al, 2004; Toma et al, 2001; Wong et al, 2006), further subsets of OCT4 positive epidermal and/or dermal cells were not seen in normal human skin in this study. No staining was seen in control samples where primary antibody was omitted (not shown here).

3.1.5 Optimisation of NANOG

As for OCT4, the first objective of NANOG optimisation was to generate a positive "tissue" control. The NANOG antibody used in this study did not cross-react with mouse ES cells and thus induced pluripotent (iPS) cells of human origin were used as a positive control (materials and methods section 2.1.11). Immunostaining of human iPS cell colonies (Figure 15a) showed positive NANOG expression in the nuclei of iPS cells. Nuclear staining was diffuse and clear nucleoli were visualised. Nuclear localisation was confirmed by co-localisation of the nuclear stain, DAPI (Figure 15b). Nuclei were not uniformly round or oval in shape and appeared flattened and/or elongated in areas of high cell density. Some nuclei did not show NANOG positivity (white arrows Figure 15a). Underlying iMEF cells did not stain positively for NANOG (internal negative control, yellow arrows Figure 15a) and no staining was seen in control samples where primary antibody was omitted (Figure 15c).

Human iPS colonies could not be generated in sufficient quantities to generated FFPE samples of cultured cells and thus NANOG optimisation for FFPE tissue was carried out in normal human skin biopsies according to manufacturer's recommendations (Abcam, USA). Results of NANOG immunostaining showed a subset of NANOG positive (NANOG+) cells within a sebaceous gland (Figure 16a). In addition, a single NANOG+ cell was seen within the basal layer of the epidermis (Figure 16b) in a second section. No staining was seen in control samples where primary antibody has been omitted (Figure 16c).

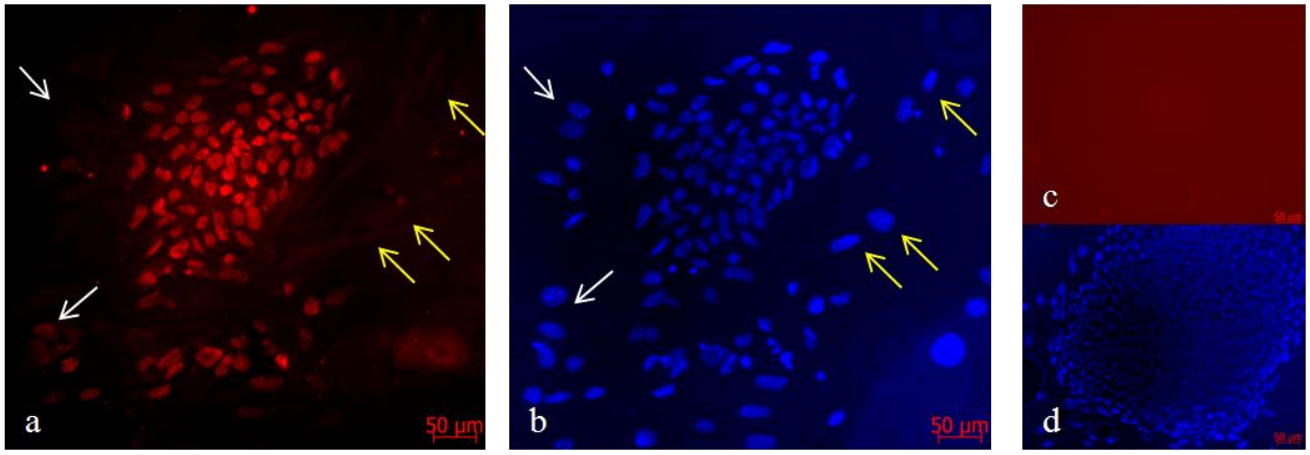

Figure 15: NANOG expression in human iPS cell colonies evaluated by ICC: a: NANOG+ human iPS cell colony (red). Staining is nuclear and nucleoli are clearly visible. DAPI positive nuclei of the same iPS colony are shown in b. Some iPS cells did not show NANOG positivity (white arrows a, b). Similarly, underlying iMEFs acted as an internal negative control and demonstrated positive DAPI signal but did not express NANOG (yellow arrows a, b). c: No staining is seen in control sample where primary antibody was omitted. DAPI positive nuclei of the same iPS colony are shown in d.

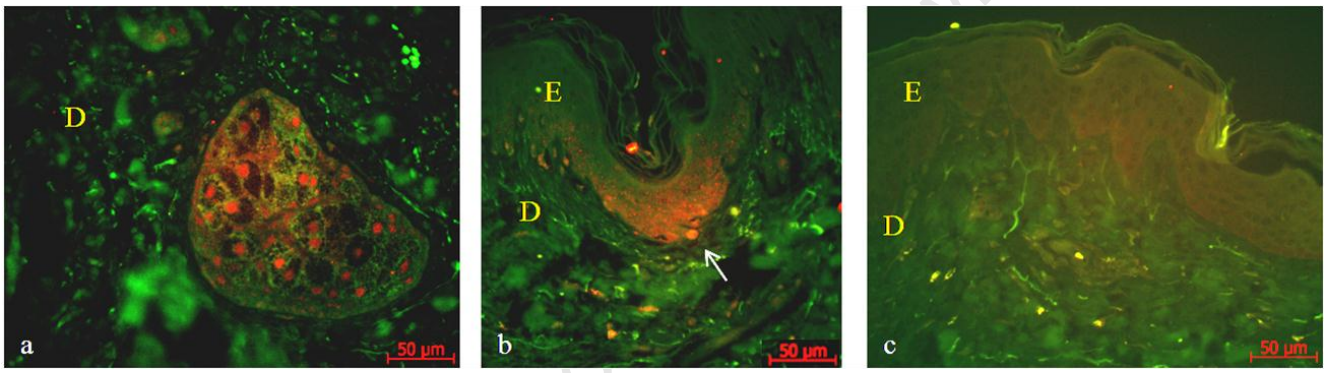

Figure 16: Optimisation of NANOG immunostaining in FFPE human skin samples: a: NANOG+ cells (red) within a sebaceous gland. b: A single NANOG+ cell (red) within the basal layer of the epidermis (arrow). c: No staining in control sample where primary antibody has been omitted. E: indicating epidermis. D: indicating dermis.

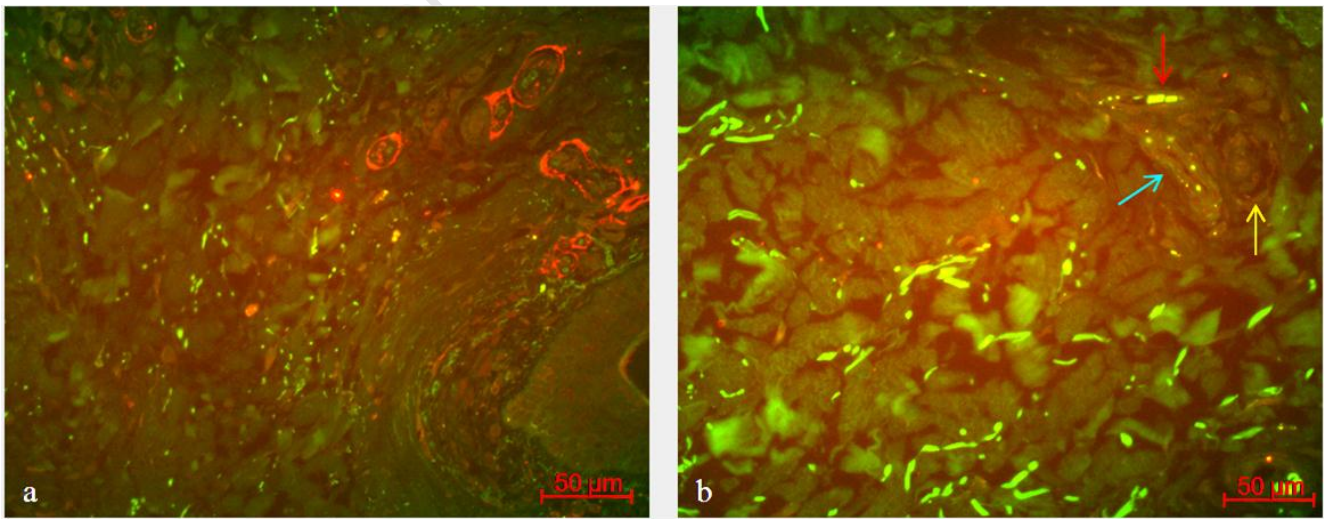

Figure 17: Optimisation of p75 immunostaining in FFPE human skin samples: a: Positive p75 expression in the epineurium and perineurium of dermal nerves (red). b: No staining is seen in control sample where primary antibody has been omitted. A neurovascular bundle is seen in the top right: nerve (yellow arrow), artery (red arrow) (two autofluorescent red blood cells can be seen) and vein (blue arrow).

3.1.6 Optimisation of p75

Results of p75 immunostaining showed positive p75 expression in the epineurium and perineurium of dermal nerves (Figure 17a). P75 positive (p75+) cells were not noted in any other skin compartment (internal negative control) and no staining was seen in control samples where primary antibody was omitted (Figure 17b).

To ensure protocols for optimisation were comparable between cultured cells and FFPE skin samples, p75 was also optimised for cultured neurospheres (materials and methods, section 2.1.7). In brief, mES cells were seeded on iPA6 feeder layers and small, spherical colonies began to lift from the underlying feeder layer by day 14 and float freely in suspension (Figure 18). Once in suspension, neurospheres were seen to propagate by "budding off" from suspended neurospheres (arrow Figure 18a).

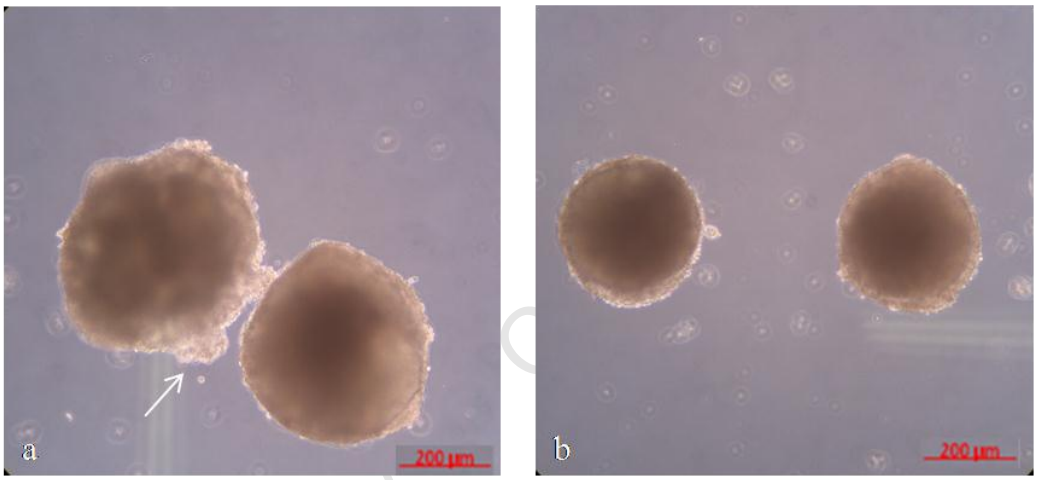

Figure 18: Neurospheres grown in suspension from mES cell colonies: a, b: Neurospheres grew in suspension as tightly adherent spheres and propagated by budding. An early bud can be seen (white arrow, a).

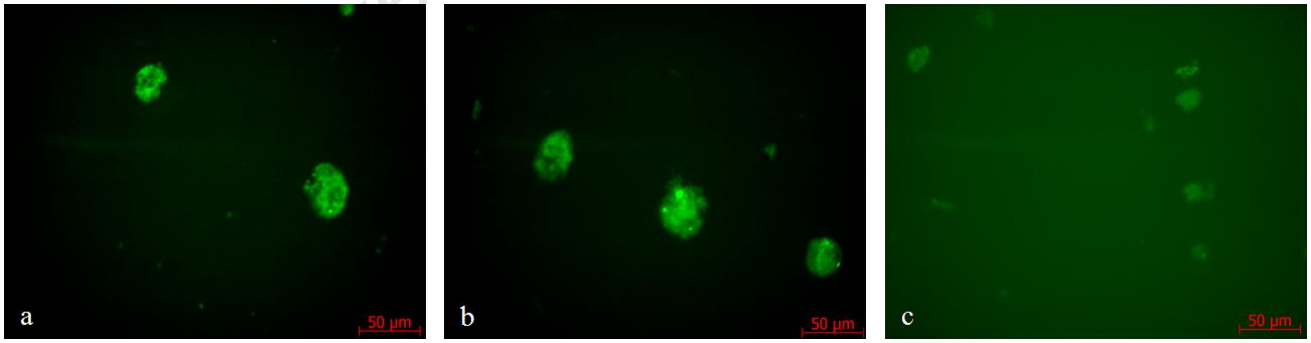

Figure 19: Optimisation of p75 immunostaining in FFPE neurospheres: a, b: p75+ neurospheres (green) which have been FFPE. c: No staining is seen in the FFPE control sample where primary antibody has been omitted.

Cultured neurospheres were first evaluated for p75 expression by ICC (materials and methods, section 2.2.3.2[a]) and showed positive staining for p75. No staining was seen in control samples where primary antibody was omitted (results not shown here). Cultured neurospheres were then subject to formalin-fixation and paraffin embedding to generate FFPE control sections. Using the same protocol as optimised for FFPE normal

skin samples, processed neurospheres showed positive p75 staining (Figure 19a, 19b). Again, no staining was seen in control samples where primary antibody was omitted (Figure 19c).

3.2 Histological analysis of FFPE naevus biopsy study samples

Naevus biopsy samples were obtained from the National Health Laboratory Services (NHLS) archives. All specimens were analysed by a qualified anatomical pathologist at the time of naevus biopsy. Only specimens with a proven histopathological diagnosis of benign melanocytic naevus were included in this study. For each specimen, a single section was analysed using a standard histological stain (Figure 20) and this was utilised to orientate the IF images and to ensure data analysis was performed on representative areas of naevus cells only.

In total, ten naevus specimens were included in this study. Two samples from five different subtypes were included. These consisted of (i) junctional (Figures 20a, 20b), (ii) compound (Figures 20c, 20d), (iii) benign intradermal naevus (BIN) (Figures 20e, f), (iv) blue (including one cellular blue naevus and one epithelioid blue naevus) (Figures 20g, 20h respectively) and (v) dysplastic (Figures 20i, 20j). The characteristics of each naevus are summarized in Table 6 below.

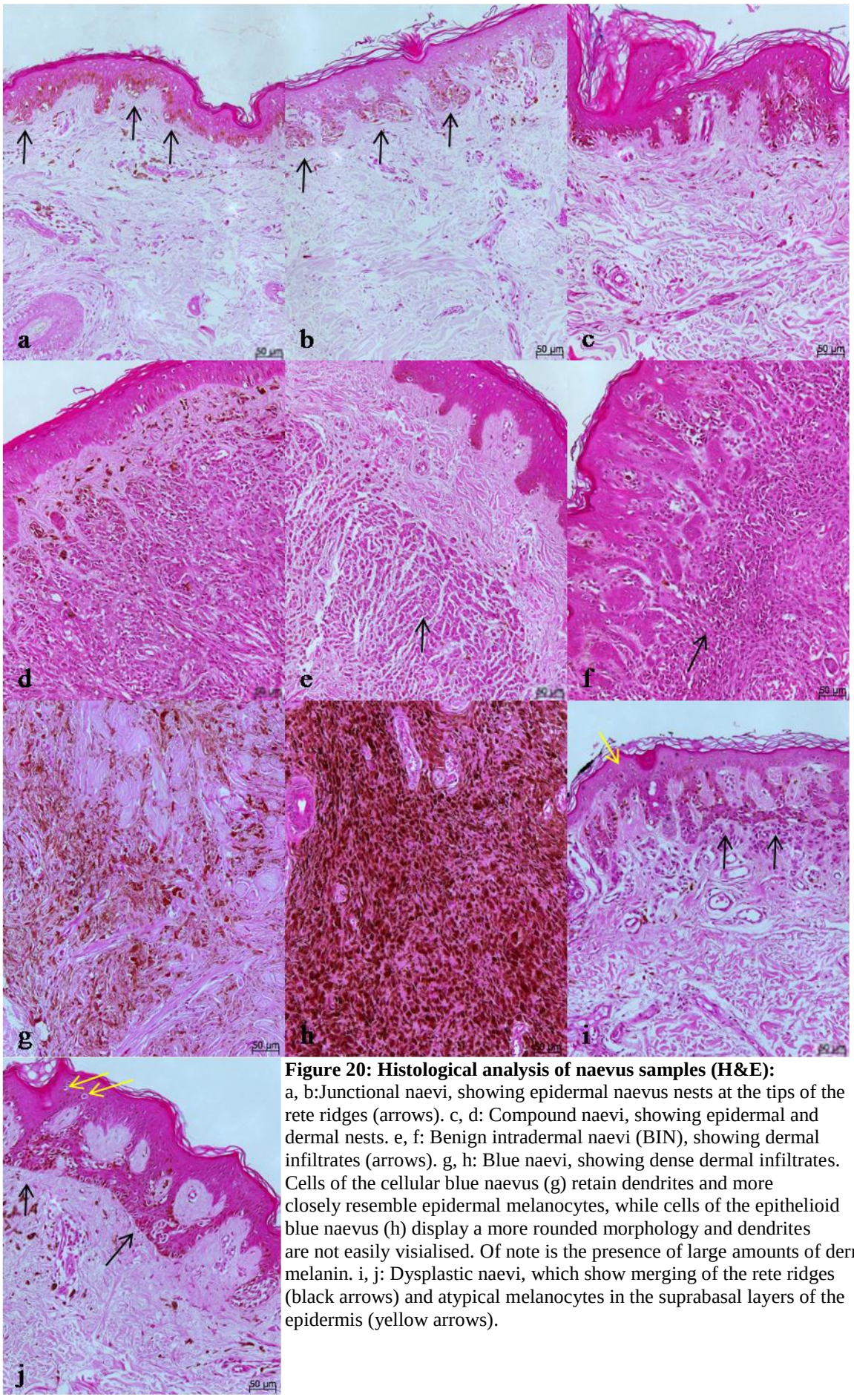

Figure 20: Histological analysis of naevus samples (H&E):
a, b:Junctional naevi, showing epidermal naevus nests at the tips of the rete ridges (arrows). c, d: Compound naevi, showing epidermal and dermal nests. e, f: Benign intradermal naevi (BIN), showing dermal infiltrates (arrows). g, h: Blue naevi, showing dense dermal infiltrates. Cells of the cellular blue naevus (g) retain dendrites and more closely resemble epidermal melanocytes, while cells of the epithelioid blue naevus (h) display a more rounded morphology and dendrites are not easily visialised. Of note is the presence of large amounts of dermal melanin. i, j: Dysplastic naevi, which show merging of the rete ridges (black arrows) and atypical melanocytes in the suprabasal layers of the epidermis (yellow arrows).

Naevus Sample	Histological Subtype	Age at Biopsy (years)	Sex	Site	Diameter (mm)	Clinical Presentation and Reason for Removal	History of naevi / melanoma and other tumours (age)
1	Junctional	-	-	Thigh	5	Uniform pigmentation. Regular border. Biopsied to exclude melanoma.	-
2	Junctional	64	F	Back	3	Uniform pigmentation. Irregular border. Reason for biopsy not recorded.	-
3	Compound	52	F	Thigh	4	Recent change in size and colour (darker). Biopsy to exclude melanoma.	Malignant blue naevus (37), Dermatofibroma (47), Melanoma (52), Benign naevus (52), Endometrial poyps (unknown)
4	Compound	51	F	Foot	10	Dark pigmentation and irregular border. Biopsy to exclude melanoma.	-
5	BIN	48	M	Buttock	6	Removed at time of concomitant melanoma removal.	Melanoma (48)
6	BIN	30	F	Abdomen	3	Increase in size and irregular border. Biopsy to exclude melanoma.	Congenital naevus x2 (23), BIN and dermatofibroma (unknown)
7	Blue	-	-	Forearm	5	No change clinically prior to reoval, regular border. Biopsy to exclude melanoma.	-
8	Blue	30	F	Nose	5	No change clinically prior to biopsy. Biopsy for cosmetic reasons.	-
9	Dysplastic	-	-	-	9	Irregular border. Biopsy to exclude melanoma.	Melanoma- currently being treated and file unavailable.
10	Dysplastic	41	F	Calf	9	Recent change in shape colour (darker). Biopsy to exclude melanoma.	Multiple dysplastic naevi,

Table 6: Patient clinical information and histological subtype of naevus samples: (-) designates unknown fields (not documented in folder or folder not existent).

3.3 Immunofluorescence of benign melanocytic naevi

3.3.1 Analysis of differentiation markers Melan-A and S100

To examine the phenotype of a naevus cell, FFPE naevus samples were examined for the expression of differentiation markers Melan-A and S100 using a dual staining technique. A melanocytic phenotype was characterised by cells being Melan-A+ or by exhibiting dual positivity (Melan-A+/S100+), while cells of a potential Schwann cell phenotype were identified as being S100+ but Melan-A-, and occurring within naevus tissue. Potential Langerhan's cells and dermal dendritic cells could not be excluded. A definitive myelinating Schwann cell phenotype was determined as being positive for both S100 and p75. This was determined by detecting the Melan-A-/S100+ cells in each sample and then staining the sequential section for p75. Expression of p75 by this Melan-A-/S100+ cell was examined (detailed in section 3.3.4 below). The association of a Schwann cell phenotype within naevi showing histological features of neurotisation was also evaluated. In addition, the distribution, orientation, and morphology of naevus cells were assessed in order to provide a general overview of morphology according to naevus subtype, and this also served as a template with which to orientate the sections when evaluating serial sections for Ki-67, p75, OCT4 and NANOG immunostaining.

Results for Melan-A and S100 immunostaining confirmed the histological features of naevi. Typically, epidermal naevus cells occurred as discrete circular nests which localised to the tips of the rete ridges (Figures 21a, 21b). Intervening naevus cells or melanocytes were few-to-none. Some samples showed a continuous proliferation of naevus cells with merging of adjacent epidermal nests and distortion of normal epidermal architecture (Figures 21c, 21d). The nests observed in such dysplastic subtypes were pleomorphic in morphology and fusion of the rete ridges with disruption of the normal epidermal architecture was marked. In addition, in dysplastic subtypes naevus cells were not restricted to naevus nests, but also occurred as single cells scattered haphazardly within the suprabasal layers of the epidermis, in keeping with the histological characteristics of dysplastic naevi (Figures 21e, 21f). Dermal naevus cells formed well circumscribed nests in the superficial/papillary dermis (Figure 21g), while those in the deeper/reticular dermis occurred more often as single cells. Specimen 4 and 6 showed histological features of maturation/neurotisation in H&E analysis and in keeping with this, naevus cells were seen to align vertically in cord-like structures in deeper dermal layers (Figure 21h), as previously described.

Of interest, many naevus cells appeared to lie in pairs or "doublets" (Figure 21i, j). This was seen in all the naevus subtypes analysed and was observed within both the epidermal and dermal compartments. This characteristic "pairing" of naevus cells appeared to be a prominent feature of naevi and, when co-stained with Ki-67, these "paired" cells did not co-express Ki-67 thus recent cellular division could not be used to explain this phenomenon.

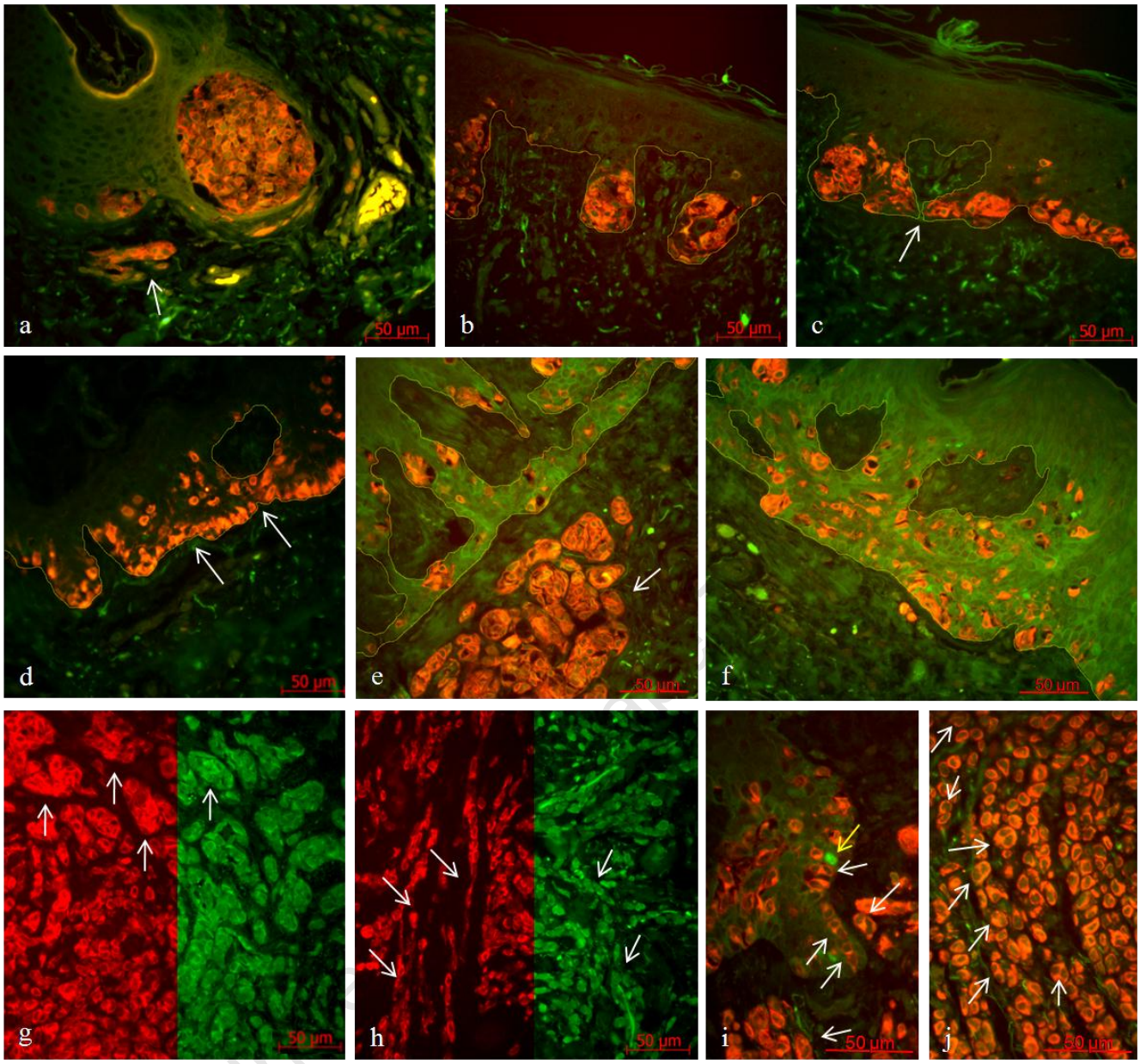

Figure 21: Morphological patterns of naevi visualised by Melan-A (red) immunostaining: a, b: Melan-A+ naevus nests within the epidermis of a compound and junctional naevus respectively. Nests are discrete and localise to the tips of the rete ridges. A naevus nest is also seen within the superficial dermis (arrow, a). c, d: Naevus cells within the epidermis of a junctional and compound naevus respectively, showing merging of epidermal nests (arrows) and disruption of normal epidermal architecture. e, f: Naevus cells within the epidermis of a dysplastic naevus. Epidermal architecture is obliterated and single naevus cells are dispersed throughout the epidermis. Well circumscribed nests are present within the dermis (arrow, e). g, h: Dual labelling technique for Melan-A and S100. Split channel view showing Melan-A+ cells (red) and S100+ cells (green) within the superficial (g) and deep (h) dermis. Discrete nests are present within the superficial dermis (arrows, g), while deeper dermal cells arrange in a vertical orientation, forming cord-like structures (arrows, h). Melan-A expression is retained in the deeper dermal layers, despite morphological features of neurotisation. i, j: Dual labelling technique for Melan-A and Ki-67. Numerous "doublet" or "paired" Melan-A+ (red) naevus cells within the dermis and epidermis of a dysplastic naevus (arrows, i) and a BIN (arrows, j) respectively. Paired cells did not co-stain with Ki-67. A single Ki-67+ keratinocyte (green) (yellow arrow) can be seen in i. Individual naevus cells display a haphazard arrangement with nuclei in variable planes of orientation (21a-j). Yellow line (b, c, d, e and f) indicates the dermo-epidermal junction.

In assessing individual naevus cell morphology and orientation, dual labelled (Melan-A+/S100+) normal epidermal melanocytes localised to the basal layer of the epidermis and showed a regular orientation with their long axis lying along the basement membrane (refer Figure 7). In contrast, naevus cells showed a haphazard proliferation, with nuclei lying in all planes of orientation (refer Figure 21a-j). With the exception of blue naevi, dendrites were predominantly absent and/or obscured in areas of high cell density and naevus cells adopted a more rounded morphology (Figure 21a-j). The blue naevi analysed were of two differing subtypes, an epithelioid blue naevus and a cellular blue naevus. Similarly, these naevi showed Melan-A and S100 dual positivity at all dermal depths, regardless of their morphology. The epithelioid blue naevus (specimen 8) showed a rounded or "epithelioid" morphology and absent dendrites, in keeping with other naevus subtypes (Figure 22a), and were similarly arranged as singular or small aggregates of cells, but not in typical nests. The cellular blue naevus (specimen 7) consisted of intradermal naevus cells with morphology similar to that of epidermal melanocytes and clearly visible dendrites (Figure 22b). Similarly, cells occurred singly, or in small clusters, within the dermis and no typical nests were noted.

In evaluating naevus cell phenotype, Melan-A and S100 immunostaining demonstrated co-expression of Melan-A and S100 in by far the majority of sections analysed. Occasional single staining cells were noted and these appeared to be specific to the epidermal compartment of naevi, where sporadic epidermal cells were noted to be either Melan-A+/S100- (white arrows, Figure 23a, 23c) or Melan-A-/S100+ (yellow arrows, Figure 23b, 23d), while the intradermal component of compound, BIN, blue and dysplastic naevi showed naevus cells which were consistently positive for both markers. Even in samples with features of neurotisation, the deeper dermal cells were found to retain their expression of Melan-A, thus retaining a melanocytic phenotype (refer Figure 21g, h). This differs from previously reported findings (Barnhill et al, 2004; Freedberg et al, 2003). In addition, S100+ but Melan-A- cells did not co-stain with p75 in serial section analysis indicating these S100+/Melan-A- cells cannot be ascribed a myelinating Schwann cell phenotype.

Melan-A and S100 showed a similar sensitivity for normal epidermal melanocytes and naevus cell identification (discussed further below). Although both markers had a comparable sensitivity, Melan-A proved a superior marker with regards to specificity, as expected, as well as cell morphology. Using Melan-A immunostaining, nuclei were more clearly visible, cellular limits more easily definable and dendrites, when present, more easily visualised (Figures 23a, 23c); as compared to S100 immunostaining which resulted in less clear imaging on all three accounts (Figure 23b, d).

Other points of interest include the observation of occasional single dermal melanocytes in the reticular dermis of normal human skin (Figure 24).

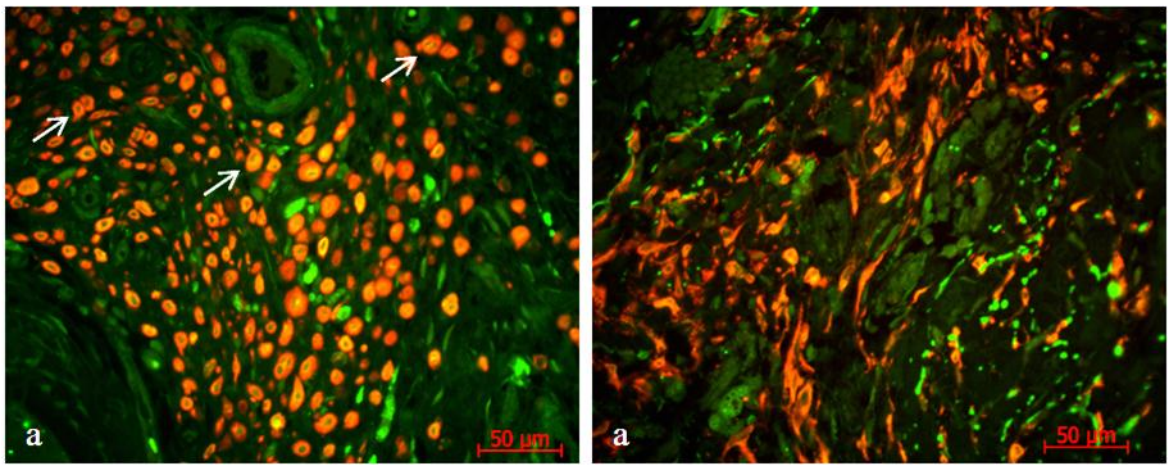

Figure 22: Cellular morphology of blue naevi visualised by Melan-A (red) immunostaining: a: Naevus cells of an epithelioid blue naevus typically showed a rounded morphology with a loss of dendritic phenotype. Again, paired or "doublet" naevus cells are observed (arrows). b: Naevus cells of a cellular blue naevus showing a morphology more in keeping with an epidermal melanocyte. Cells display an elongated cell body and retention of dendritic phenotype.

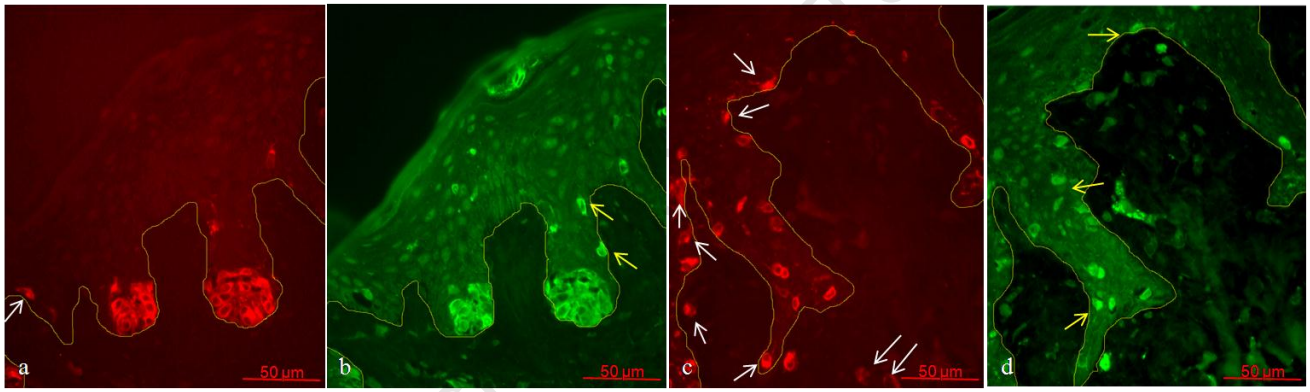

Figure 23: Comparison of Melan-A and S100 immunostaining in FFPE naevus samples: a, c: Melan-A+ naevus cells (red) showing clear nuclei and distinct cellular borders. b, d: The same fields showing S100+ naevus cells (green). Cells borders are less distinct and nuclei less clearly visualised as compared to Melan-A. Not all Melan-A+ cells are S100+ (white arrows). Similarly not all S100+ cells are Melan-A+ (yellow arrows). Yellow lines indicate the dermo-epidermal junction.

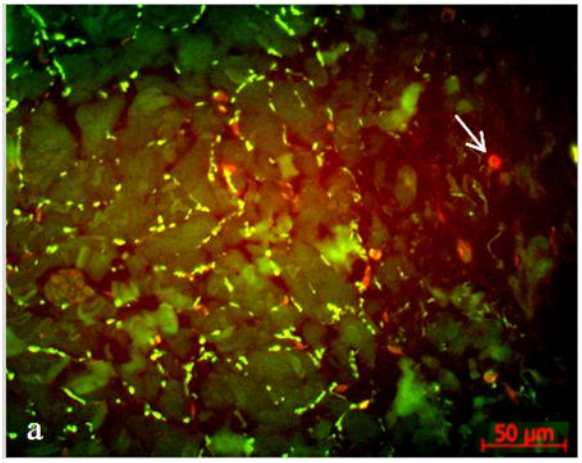

Figure 24: Melan-A+ (red) dermal melanocyte in the reticular dermis of normal human skin.

In an attempt to establish what proportion of naevus cells express Melan-A and/or S100, a semi-quantitative analysis was carried out as detailed in materials and methods (section 2.3.2). In brief, areas representative of naevus tissue, as determined by H&E and Melan-A immunostaining, were identified in ten high power fields (HPFs) of each neavus sample. An area within this was randomly selected and the total number of cells counted. The proportion of Melan-A or S100 positive cells relative to Melan-A or S100 negative cells respectively within the selected areas were then calculated and presented as a percentage of total cells counted (Figure 25a). In this semi-quantitative analysis, 85.36% of naevus cells stained positively for Melan-A and 84.15% for S100. The epidermal compartment of naevi, showed a relatively low proportion of Melan-A and S100 positive cells, as compared to other compartments (64.25% and 56.77% respectively) (Figures 25b, 25c respectively), and this low value was attributed to intervening keratinocytes within the epidermal naevus nests which did not stain positively for either marker and could not be excluded from the selected area due to their location within naevus tissue. The superficial dermal compartment showed the vast proportion of naevus cells staining positively for Melan-A and S100 (96.7% and 97.24% respectively). Similarly, the deep dermis showed Melan-A and S100 staining at 95.12% and 98.45% respectively (Figures 25b, 25c).

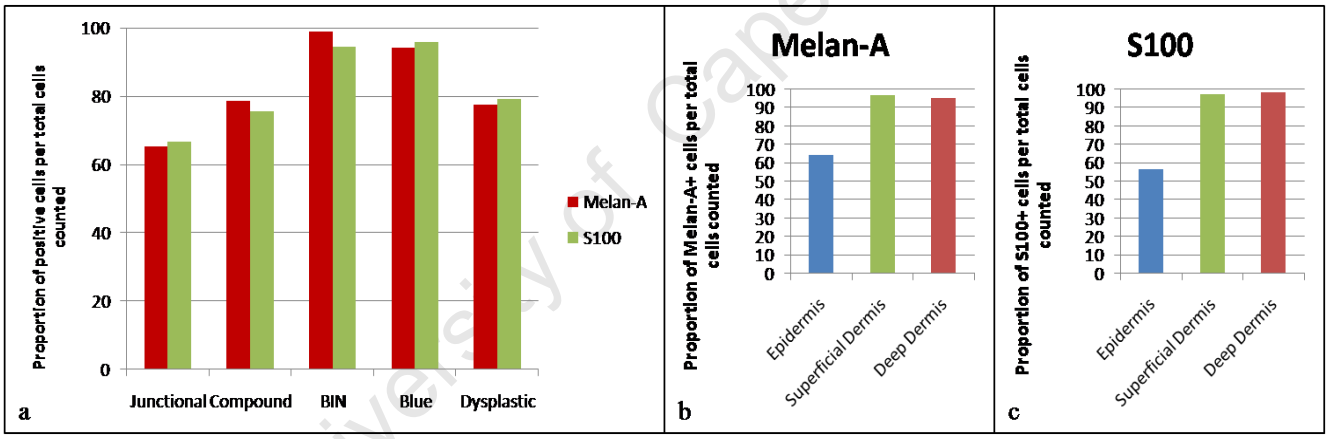

Figure 25: Comparison of Melan-A and S100 immunolabelling in naevus biopsy samples according to naevus subtype (a) and cutaneous compartment (b, c).

3.3.2 Analysis of proliferation marker Ki-67

To determine whether proliferating naevus cells were present in the samples analysed, and to which compartment these cells localised, the proliferation marker Ki-67 was used in a dual labelling technique with Melan-A. Results of Ki-67 immunostaining showed dual labelled (Melan-A+/Ki-67+) cells within all naevus samples analysed (Figure 26), with the exception of one sample (sample 5). Dual labelled cells were most numerous in the epidermal component of naevi, but were occasionally present within the superficial and deep dermis.

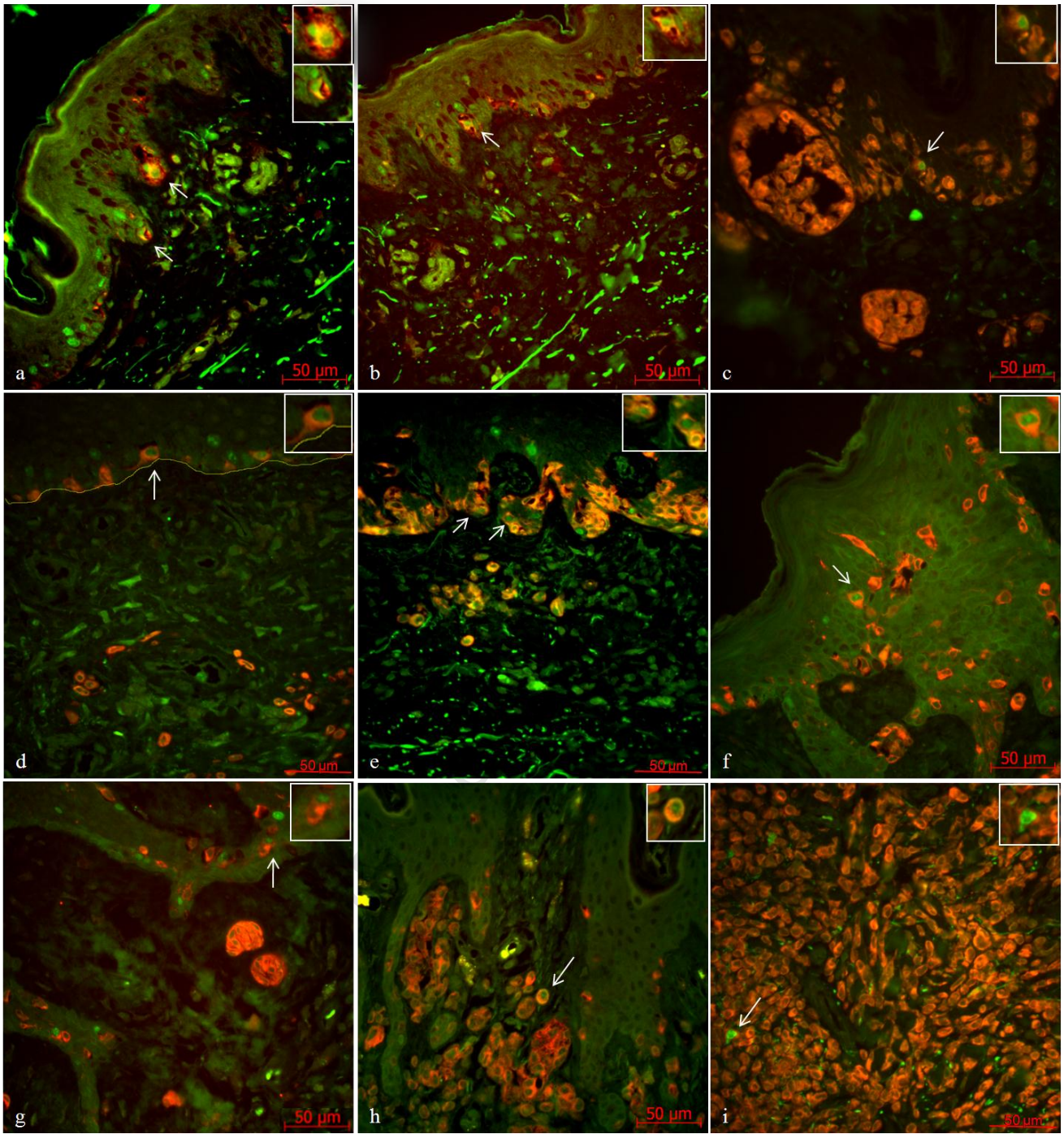

Figure 26: Dual labelling technique for Melan-A (red) and Ki-67 (green) in FFPE naevus biopsy samples: a-g: Melan-A+/Ki-67+ cells within the epidermis of junctional (a, b), compound (c), blue (d) and dysplastic (e, f, g) naevi (arrows). h, j: Melan-A+/Ki-67+ cells within the dermis of a compound and BIN respectively (arrows). Inserts a-i: Dual labelled naevus cells, enlarged views. Yellow line (d) indicates dermo-epidermal junction (dermo-epidermal junctions of other images more easily visualised).

In an attempt to establish what proportion of naevus cells express Ki-67, a semi-quantitative analysis was carried out as detailed in materials and methods (section 2.3.2) and previously described for Melan-A and S100 analysis (section 3.3.1). The proportion of dual labelled (Melan-A+/Ki-67+) naevus cells per total Melan-A+

naevus cells counted was determined and results are shown in Figure 27. Junctional naevi contained the highest proportion of dual labelled naevus cells (1.54%), closely followed by dysplastic naevi (1.26%). Compound, blue and BIN exhibited less dual positivity (0.8%, 0.53% and 0.14% respectively) (Figure 27a). As mentioned above, the epidermal compartment contributed the vast majority of dual labelled cells (Figure 27b). Of the total Melan-A+/Ki-67+ cells counted, the epidermal compartment contained 76.17%, while superficial dermis and deep dermis contributed 14.32% and 9.62% respectively.

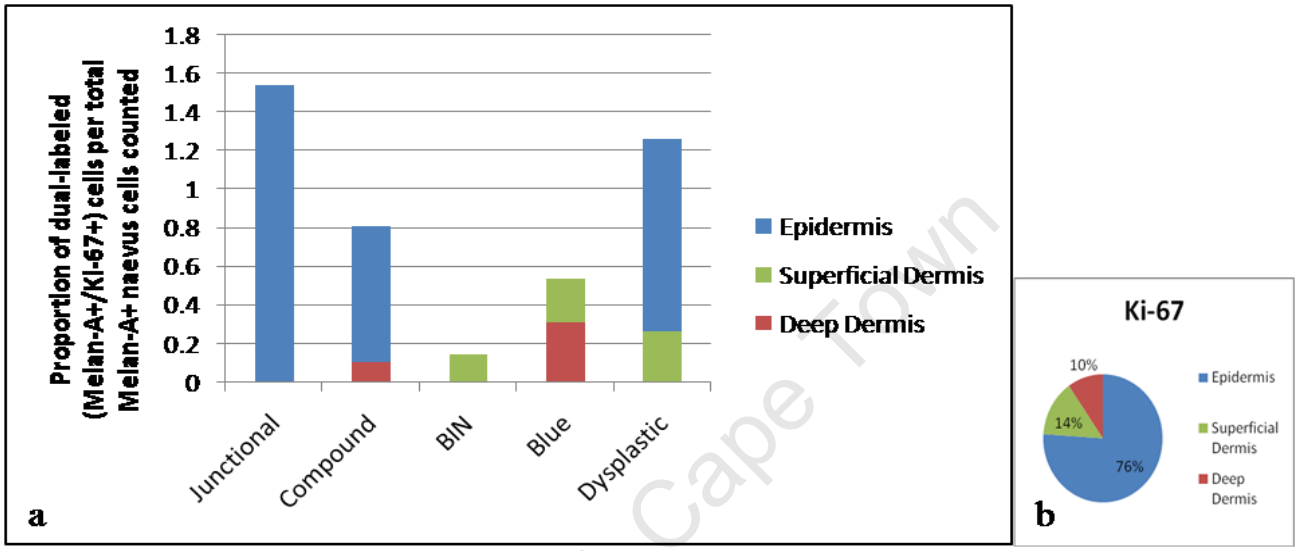

Figure 27: The proportion of dual labelled (Melan-A+/Ki-67+) naevus cells in the epidermis (blue), superficial dermis (green) and deep/reticular dermis (red) relative to the total number of Melan-A+ naevus cells counted, stratified according to naevus subtype (a) and cutaneous compartment (b).

Naevus samples analysed showed a large proportion of Ki-67+ keratinocytes within the epidermis of naevus tissue (Figure 28a, b). This prompted the comparison of Ki-67+ keratinocytes within naevus tissue, as compared to normal skin and described in materials and methods. Briefly, five HPFs in each naevus sample (ten naevus samples) and five HPFs in normal human skin (ten normal skin biopsies) were selected for analysis. Each HPF selected contained epidermal tissue and the total number of Ki-67+ epidermal keratinocytes per field were counted. In addition, the total length of basement membrane was determined for each field and results were expressed as the total number of Ki-67+ epidermal keratinocytes (x) per unit length of basement membrane in microns (x/µm). Results were comparable between naevus tissue and control skin (Figure 29), however, blue naevi surprisingly demonstrated a marked increase in Ki-67 positivity as compared to control skin and other naevus subtypes.

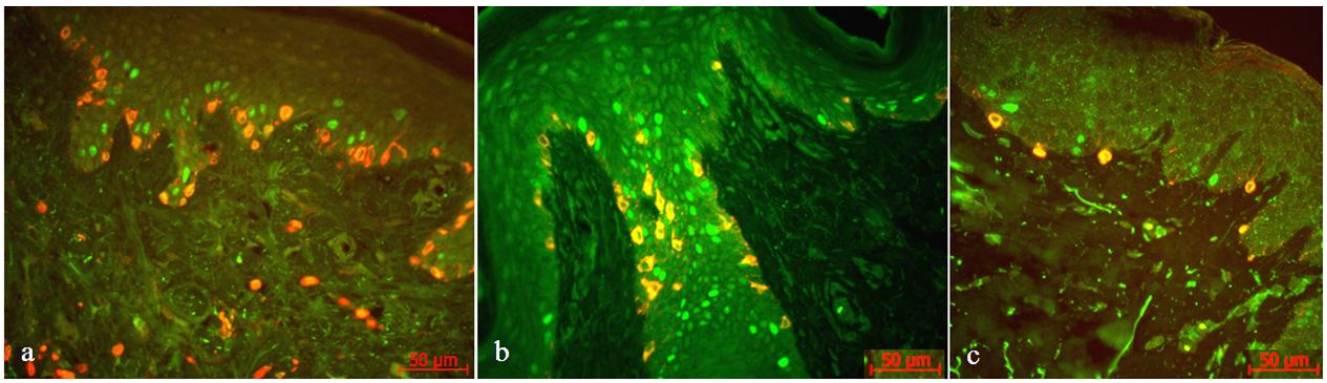

Figure 28: Increased numbers of Ki-67+ epidermal keratinocytes (green) in FFPE naevus samples (a, b) as compared to normal human skin (c).

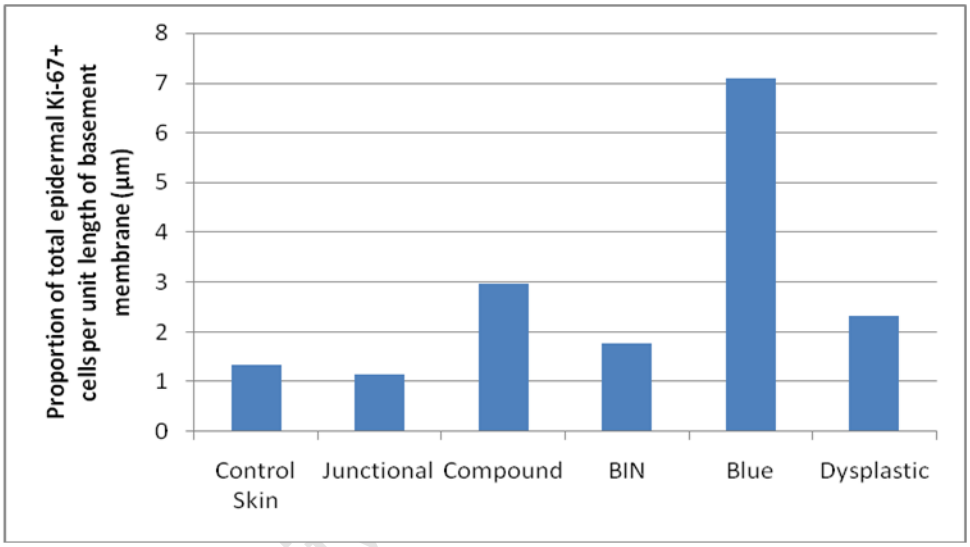

Figure 29: Proportion of total epidermal Ki-67+ cells per unit length of basement membrane (µm) in naevus subtypes and in normal skin.

3.3.3 Analysis of pluripotency markers OCT4 and NANOG

To determine whether pluripotent stem cells are present in naevus tissue, FFPE naevus samples were examined for expression of pluripotency markers OCT4 and NANOG. Nuclear localisation of both markers was confirmed by co-localisation with the nuclear stain DAPI. Only dual labelled cells (OCT4+/DAPI+ and NANOG+/DAPI+) were accepted as being true positive cells.

3.3.3.1 OCT4

Results for OCT4 immunostaining demonstrated the presence of OCT4+ cells within naevus tissue in seven of the ten samples analysed (sample 2, 3, 4, 6, 8, 9 and 10). In naevus tissue with a low cell density, OCT4+ nuclei were of a similar morphology to surrounding keratinocytes, while they appeared elongated and/or flattened in naevus tissue with a high cell density. This observation was similar to that observed for cells in high density mES colonies (refer Figure 12a).

In the epidermal compartment of naevi, OCT4+ cells occurred predominantly in clusters and were located towards the centre of the naevus nests (white arrows Figures 30a-c). These clusters were distributed throughout the length of the involved epidermis and are as prominent at the edge of the lesions as in the centre. This clustered pattern was most marked in dysplastic naevi. OCT4 positive cells were also seen to occur in pairs (yellow arrows Figures 30d-f, 30j) and as single cells (grey arrows Figures 30f, 30h-j). Single OCT4+ cells occurred more commonly at the periphery of the naevus nests where they would be expected to abut the basement membrane. Two single OCT4+ cells were also seen in the basal layer of normal intervening epidermis, adjacent to naevus tissue (red arrows Figure 30a, 30g). No further OCT4+ cells were noted within the epidermis.

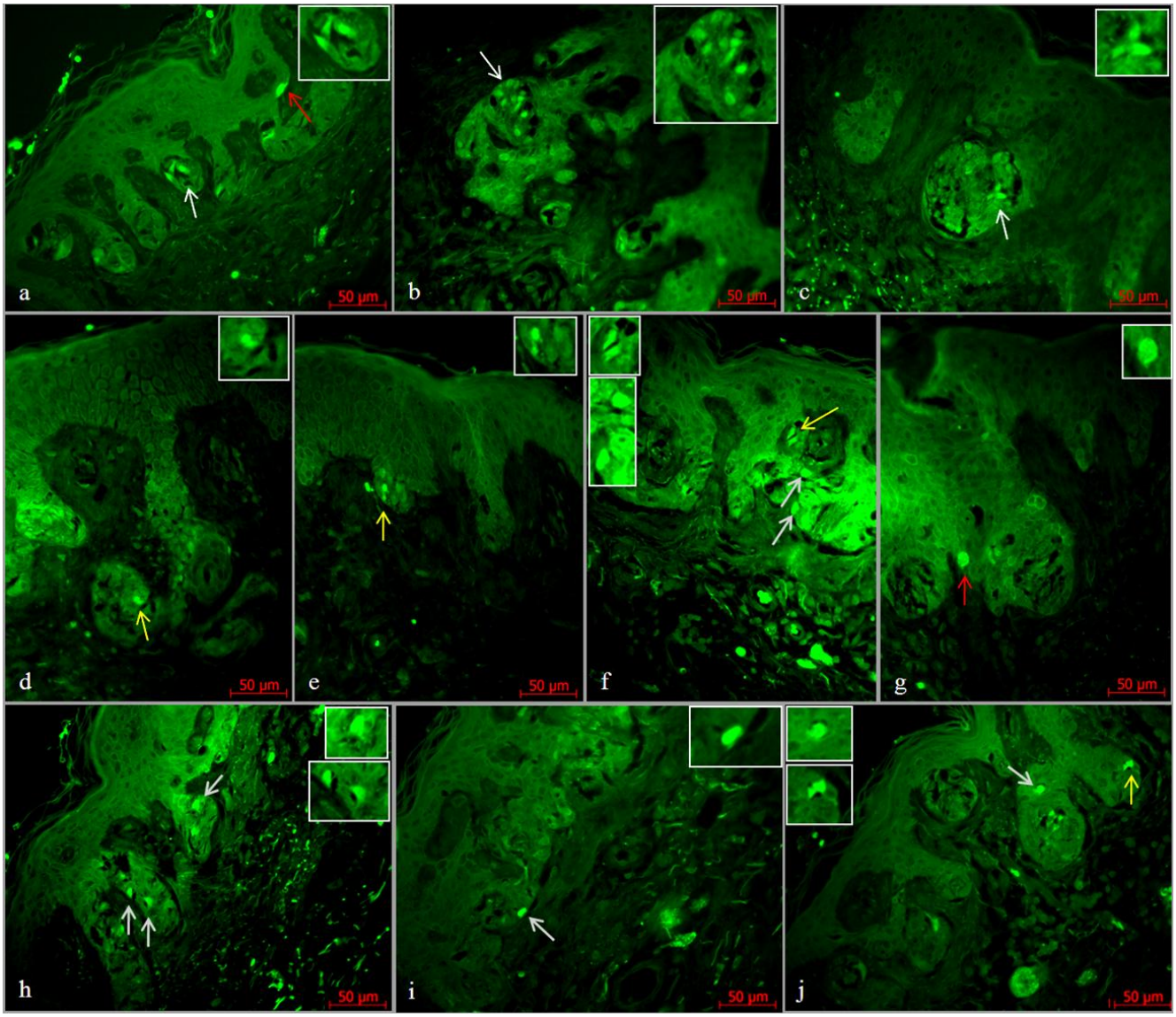

Figure 30: OCT4+ cells (green) within the epidermal compartment of naevi. a-c: Clusters of OCT4+ cells within epidermal naevus nests (white arrows). d-j: OCT4+ cells occurring in pairs (yellow arrows) (d, e, f, j) and as single cells (grey arrows) (f, h, i, j), typically occurring toward the periphery of a naevus nest. a, g: Single OCT4+ cells in the basal layer of normal intervening epidermis (red arrows). Inserts: Enlarged views of OCT4+ cells. Of note: only cells showing dual labelling with DAPI are indicated as being OCT4+ cells.

In the dermal compartment of naevi, OCT4+ cells were only occasionally seen (samples 3, 4, 6, 8 and 10) and when present, localised to the superficial or papillary dermis (arrows Figures 31a-c). Here, OCT4+ cells occurred as pairs or as single cells and not within clusters as seen in the epidermis. Only one sample (sample 8) showed OCT4+ cells within the deeper reticular dermis (arrows Figure 31d).

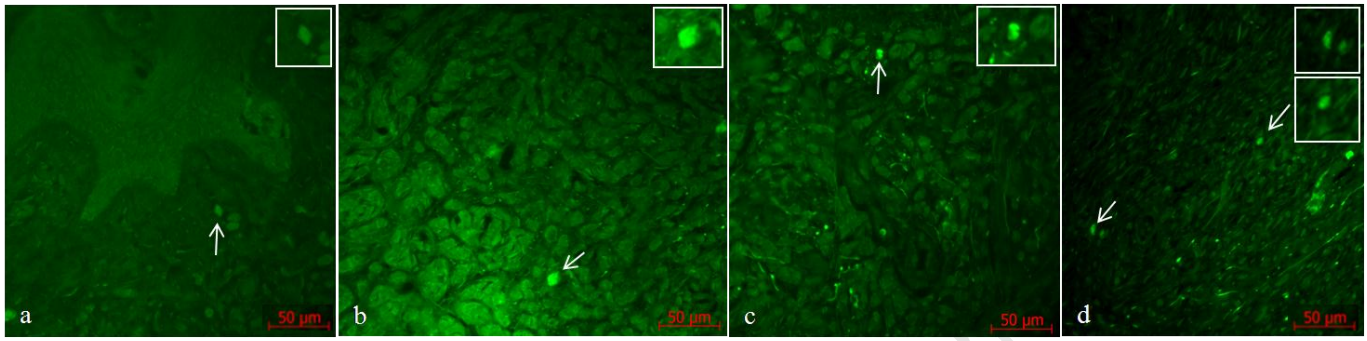

Figure 31: OCT4+ cells (green) within the superficial and deep dermal compartments of naevi: a-c: OCT4+ cells within the superficial dermis of a compound naevus (arrows). d: OCT4+ cells within the deeper reticular dermis of a blue naevus (arrows). Inserts: Enlarged views of OCT4+ cells.

In an attempt to establish what proportion of naevus cells express OCT4, a semi-quantitative analysis was carried out as detailed in materials and methods (section 2.3.2) and previously described for Melan-A and S100 analysis (section 3.3.1). Results are shown in Figure 32. Dysplastic naevi showed the largest proportion of OCT4+ cells (5.81%) as compared with other subtypes analysed (Figure 32a). Compound naevi (2.13%), blue naevi (0.9%), junctional naevi (0.13%) and BIN (0.12%) showed a lower proportion of OCT4+ cells, but importantly, they still showed OCT4 positivity. Of the total number of OCT4+ cells identified, the greatest proportion occurred in the epidermal compartment of naevi (77.22%), while a far smaller proportion occurred in the superficial and deeper dermal compartments (17.73% and 5.05% respectively, Figure 32b).

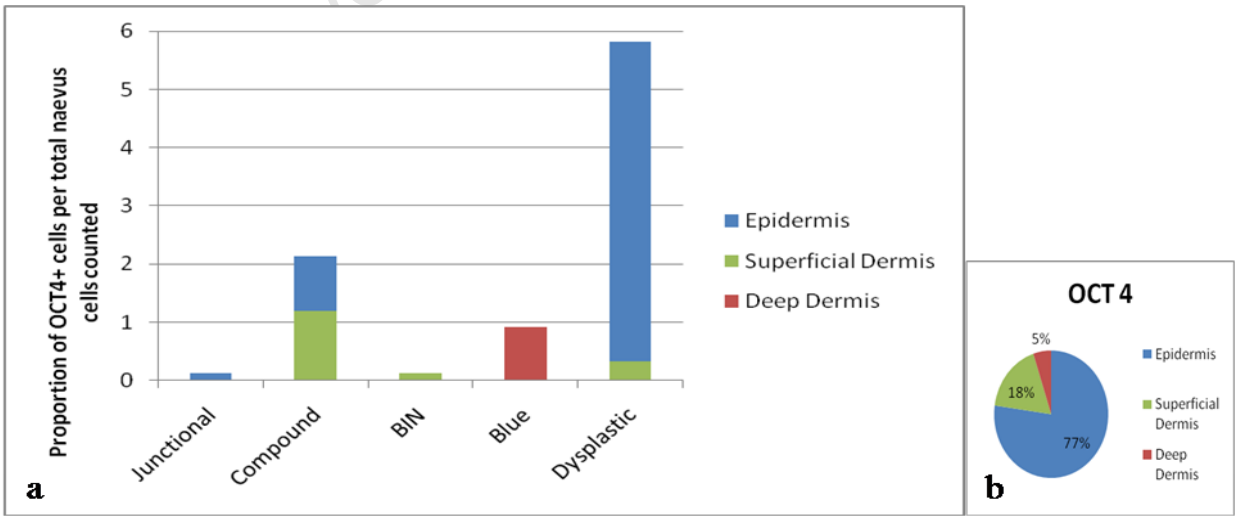

Figure 32: The proportion of OCT4+ cells per total naevus cells counted in the epidermis (blue), superficial dermis (green) and deep/reticular dermis (red), stratified according to naevus subtype (a) and cutaneous compartment (b).

3.3.3.2 NANOG

Results for NANOG immunostaining demonstrated the presence of NANOG positive (NANOG+) cells within six of the ten samples analysed (samples 2, 3, 5, 8, 9, and 10). The morphology of NANOG+ nuclei was similar to that described previously for OCT4+ nuclei and nuclei of high density iPS colonies (section 3.1.5).

In the epidermal compartment of naevi, NANOG+ cells occur predominantly as single cells and not in clusters as seen with OCT4 immunostaining (arrows Figure 33). In addition, NANOG+ cells localised to the periphery of naevus nests. No centrally located NANOG+ cells were seen in the samples analysed. In the dermal compartment of naevi, NANOG+ cells were rarely seen. Two samples (samples 9 and 10) each demonstrated a pair NANOG+ cells in the superficial dermis (Figure 34a, 34b). One sample (sample 5) demonstrated NANOG+ cells within the reticular dermis (Figure 34c). NANOG+ cells were occasionally visualised in the sebaceous glands associated with naevus tissue (not shown) and a single NANOG+ cell was seen to occur in the reticular dermis (sample 8) adjacent to naevus tissue (Figure 34d). Of interest, NANOG+ cells did not appear to co-localise with OCT4+ cells as determined by sequential section analysis.

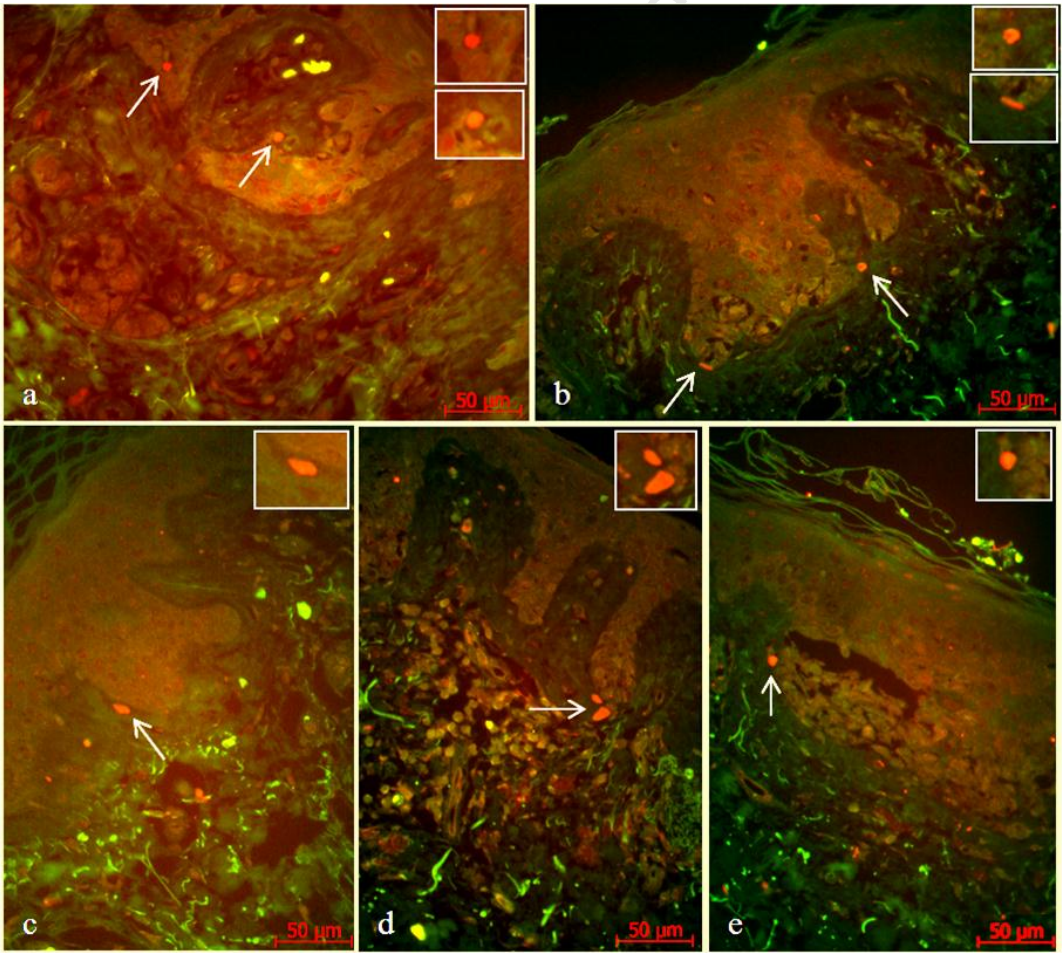

Figure 33: NANOG+ cells (red) within the epidermal compartment of naevi: a-e: NANOG+ cells (white arrows) within epidermal nests of a compound (a), dysplastic (b) and junctional (c, d, e) naevus, typically lying toward the periphery of naevus nests. Inserts: Enlarged view of NANOG+ cells.

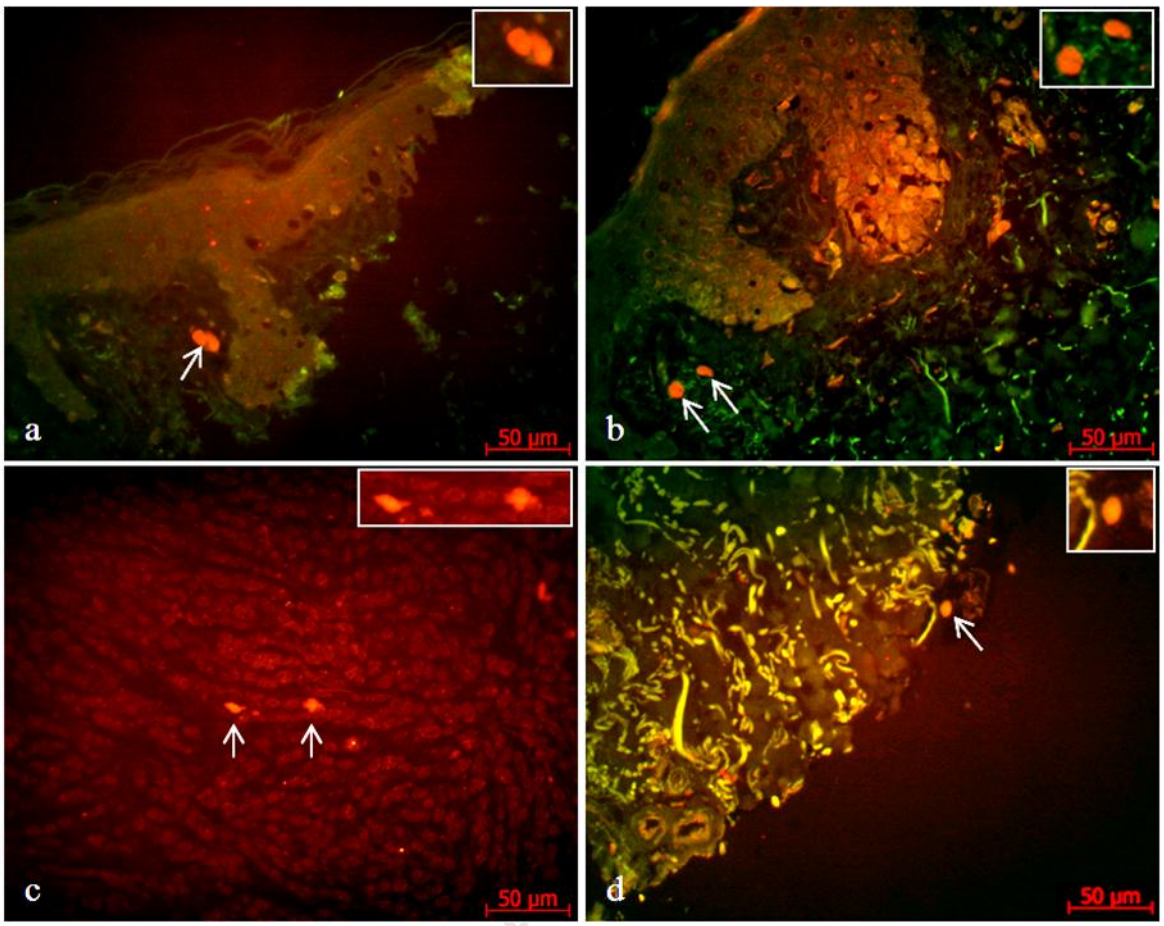

Figure 34: NANOG+ cells (red) in the dermal compartment of naevi: a, b: NANOG+ cells within the superficial/papillary dermis of a junctional naevus (white arrows), occurring commonly in pairs. c: NANOG+ cells within the reticular dermis of a BIN (white arrows). d: A NANOG+ cell in the normal adjacent normal reticular dermis of a blue naevus (arrow).

In an attempt to establish what proportion of naevus cells express NANOG, a semi-quantitative analysis was carried out as detailed in materials and methods (section 2.3.2) and previously described for Melan-A and S100 analysis (section 3.3.1). Results are shown in Figure 35. Junctional naevi and dysplastic naevi contain the highest proportion of NANOG+ cells relative to total number of cells counted (1.3% and 1.14% respectively, Figure 35a). Compound, BIN and blue naevi contain a lower proportion of NANOG+ cells (0.37%, 0.36% and 0.11% respectively), but importantly, still show NANOG positivity. Similarly to OCT4 immunostaining, of the total number of NANOG+ cells identified, the greatest proportion occur in the epidermal compartment of naevi (63.72%, Figure 35b), while a far smaller proportion occur in the superficial and deeper dermal compartments (21.95% and 14.33% respectively). Interestingly, dysplastic naevi show a greater proportion of NANOG+ cells within the superficial dermis (0.72%), as opposed to the epidermis (0.42%).

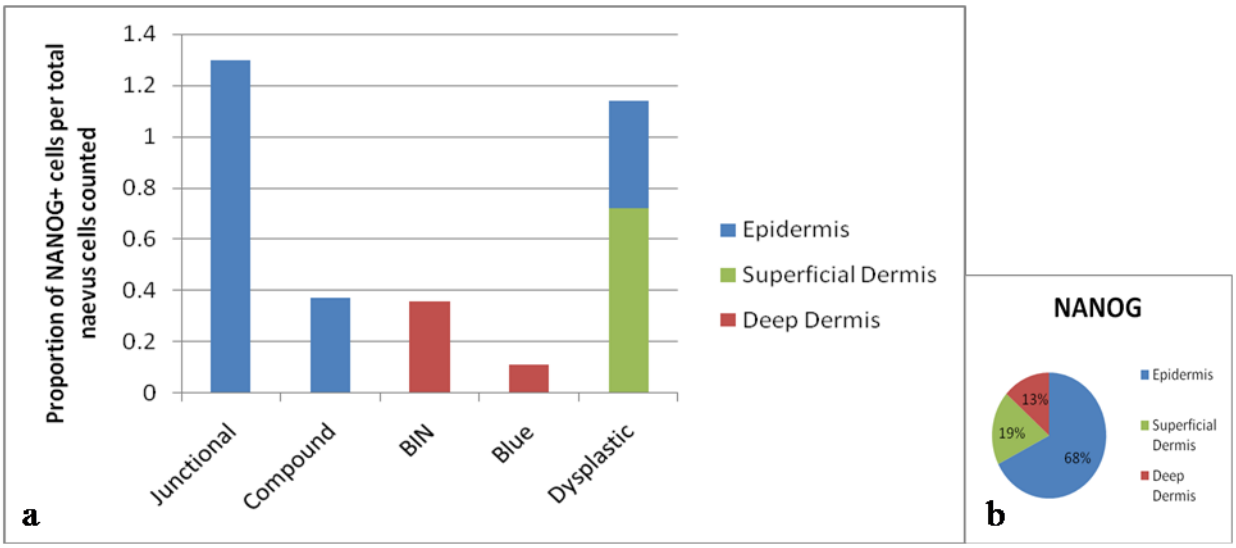

Figure 35: The proportion of NANOG+ cells per total naevus cells counted in the epidermis (blue), superficial dermis (green) and deep/reticular dermis (red), stratified according to naevus subtype (a) and cutaneous compartment (b).

3.3.4 Analysis of neural crest marker p75

To determine whether cells of a neural crest phenotype are present in naevus tissue, naevus biopsy samples were examined for the expression of the neural crest marker p75. Results for p75 immunostaining show the presence of p75 positive (p75+) cells within seven of the ten naevus samples analysed (samples 1, 2, 3, 4, 8, 9 and 10). The two benign intradermal naevi (samples 5 and 6) did not show p75 positive cells within naevus tissue in this study. P75 staining was cytoplasmic in localisation and cells were of a similar size and morphology to surrounding naevus cells.

In the epidermal compartment of naevi, p75 positive cells occurred as single cells and in clusters, usually within the centre of naevus nests. These cells showed and irregular cell border which was thought to reflect intercellular adhesions (Figures 36a, 36b). In the dermal compartment of naevi, p75+ cells had a more regular, rounded phenotype and occured as single cells (Figures 36c-f). No clusters of p75+ cells were seen. p75+ nerves were seen in the dermis of all naevus samples analysed and confirmed the adequacy of immunostaining (Figure 36g).

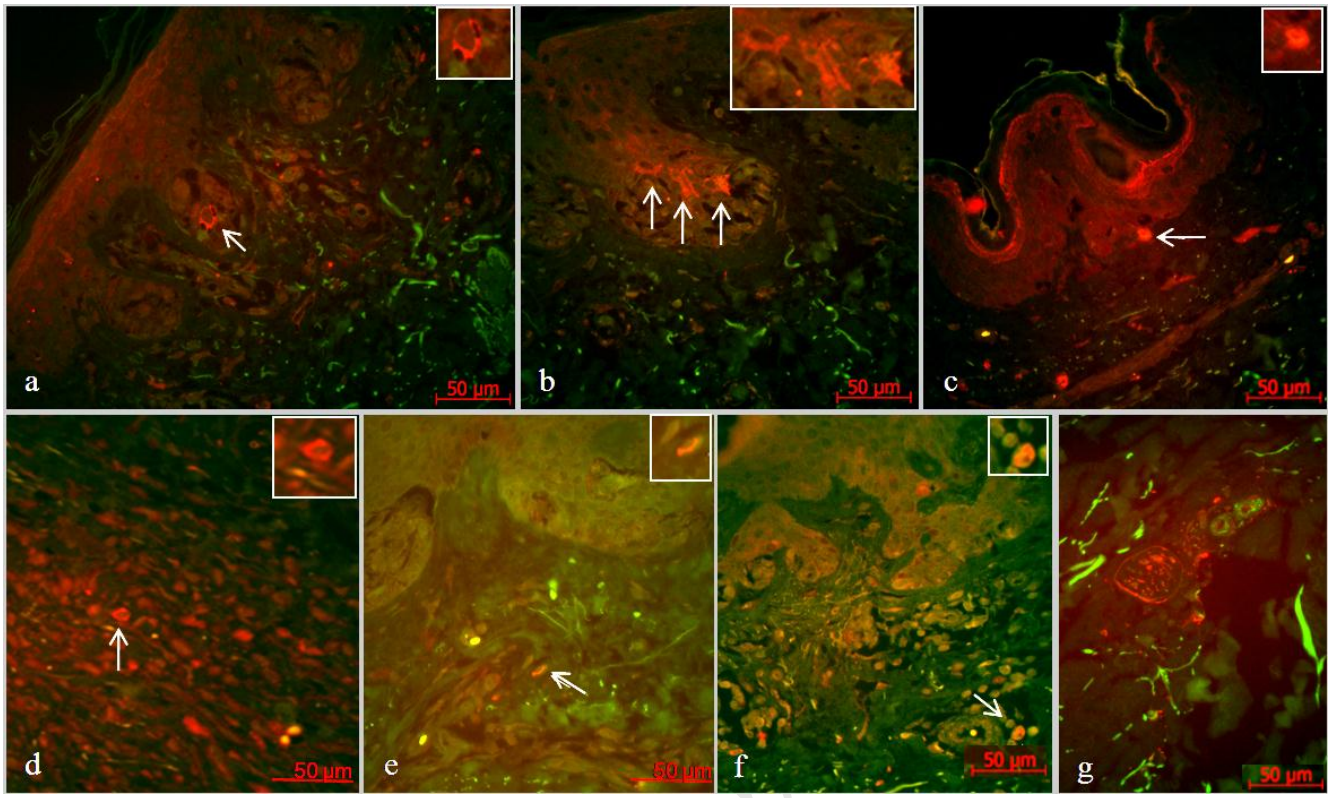

Figure 36: p75+ cells (red) within the epidermal and dermal compartment of naevi: a-c: p75+ cells within the epidermis of a junctional naevus (arrows). Staining is cytoplasmic and cells display an irregular cellular border. A more rounded, regular cell border is seen in c. d-f: p75+ cells within the dermis of a blue naevus (d) and dysplastic naevi (e, f) (arrows). Inserts: Enlarged view of p75+ cells. g: p75+ dermal nerves provided an internal positive control.

In an attempt to establish what proportion of naevus cells express p75, a semi-quantitative analysis was carried out as described in materials and methods (section 2.3.2) and previously described for Melan-A and S100 analysis (section 3.3.1). Results are shown in Figure 37. Junctional naevi showed the largest proportion of p75+ cells relative to total number of cells counted (0.62%, Figure 37a), followed by compound and dysplastic naevi (0.43% and 0.37% respectively). Blue naevi showed a smaller proportion of p75+ cells (0.13%), but did show p75 positivity. As mentioned above, BIN showed no p75+ cells in this study. As for OCT4 and NANOG immunostaining, of the total number of p75+ cells identified, the epidermis contained the greatest number (57.15%, Figure 37b), while the superficial dermis and the deep dermis contributed to a lesser extent (35.71% and 7.41% respectively). Interestingly, in dysplastic naevi the superficial compartment alone contained p75+ cells. This is similar to that reported for NANOG immunostaining above.

Overall, the epidermis contained the greatest proportion of all positively labelled precursor cells (OCT4, NANOG and p75 combined), contributing 72.72% (Figure 38a). More than half of all positive cells were observed in dysplastic naevi (Figure 38b).

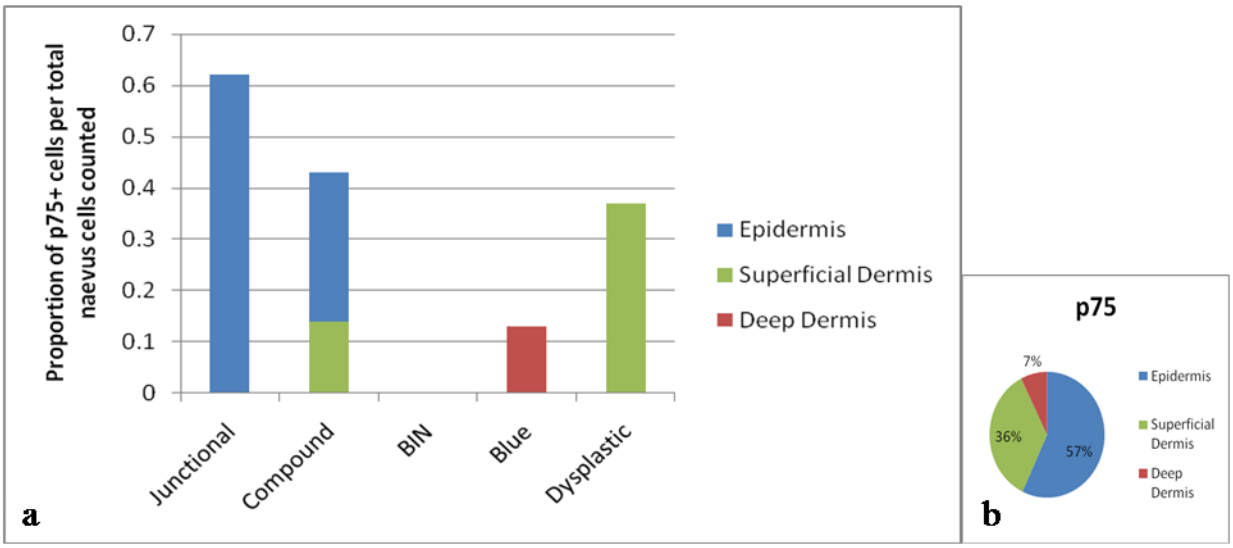

Figure 37: The proportion of p75+ cells per total naevus cells counted in the epidermis (blue), superficial dermis (green) and deep/reticular dermis (red), stratified according to naevus subtype (a) and cutaneous compartment (b).

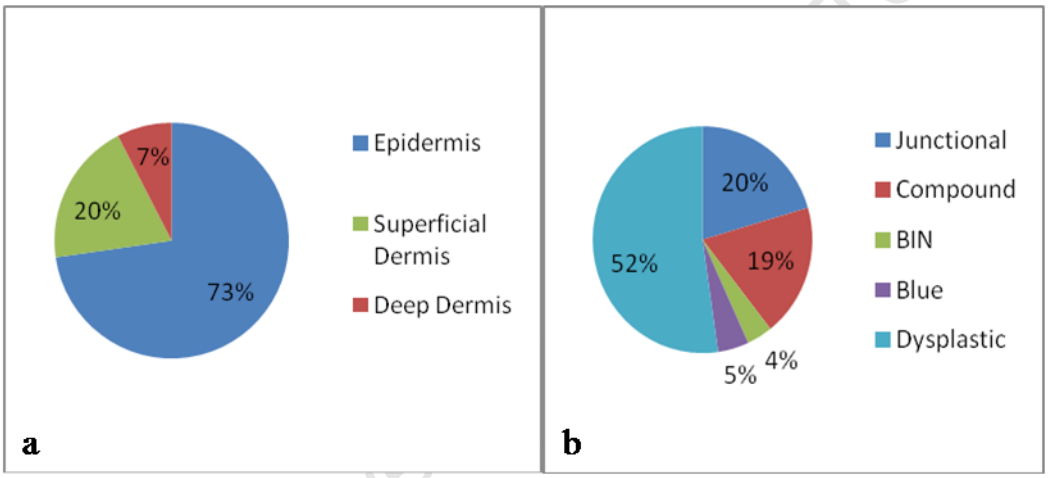

Figure 38: The combined proportion of precursor cells (OCT4+, NANOG+ and/or p75+) per total naevus cells counted, stratified according to cutaneous compartment (a) and naevus subtype (b).

4. DISCUSSION

Melanocytic neoplasia is a multifaceted process which involves a complex interplay of genetic and environmental factors. Despite recent advances, the aetiology and pathogenesis of melanocytic neoplasms remains unclear and the anatomical location and state of differentiation of the initiating cell remains to be identified. It has recently been proposed that cancer may arise from a precursor cell which persists in adult tissues, and partakes in normal tissue homeostasis and repair. It is hypothesized that, should this cell undergo a mutational event either *in utero* or postnatally, subsequent recruitment of this cell during life may result in uncontrolled proliferation and ensuing tumour formation. This is known as the tumour stem cell hypothesis and advocates that tumours arise from stem-like cells and not from mature tissue elements.

In considering the aetiology and pathogenesis of melanocytic neoplasms, and the potential role of stem cells in this process, there are two critical concepts which remain undefined and hamper our understanding of these disorders. Firstly, "naevomelanocytes" or "naevus" cells are poorly defined in current literature and, whether they represent a type of melanocyte in differing ages or stages of evolution, or whether naevus cells are a distinct cellular lineage, remains undetermined. Secondly, there is much disparity regarding the existence and phenotype of melanoma stem cells and hence the roles these tumour stem cells play in melanoma development. It has been suggested that this lack of clarity may result from variations in methodologies used to study such cells in culture, as well as *in vivo* influences such as the tumour microenvironment and immune system response, as each of these may impact on the frequency and phenotype of melanoma stem cells (as reviewed by Girouard and Murphy 2011; Gupta et al, 2009; Kennedy et al, 2007). The overall aim of this study was to evaluate the aetiology and pathogenesis of melanocytic neoplasms using the benign melanocytic naevus as a model system. First, the phenotype of a "naevus" cell was examined in order to characterise the possible lineage, and hence potential cell of origin, of these tumour cells (Section 1). Secondly, the proliferation of naevus cells was examined in order to extrapolate a possible compartment of origin of naevi (Section 2). Lastly, the hypothesis that melanocytic naevi may originate from a pluripotent or neural crest-like stem cell and not via de-differentiation from a mature epidermal melanocyte was tested (Section 3).

Section 1:

4.1 The phenotypic characterisation of a "naevus" cell

The benign melanocytic naevus is characterised histologically by proliferations of cells which arrange in defined clusters known as "nests". Benign naevus cells are thought to represent a type of melanocyte but the exact relationship between normal melanocytes and benign naevus cells remains unclear as they show important morphological differences. Consequently, the cells of a naevus have been referred to as "nevomelanocytes" or "naevus" cells and their origin and following pathogenesis remains under question. Existing hypotheses propose naevi develop from a mutated, differentiated epidermal melanocyte with the subsequent "dropping off" of these

cells into the dermis (Unna, 1893), while others propose naevi originate from a mutated precursor cell which persists in the post-natal dermis (Kawamura, 1956; Mishima, 1965 and Cramer 1984). Combining these theories, a dual origin of naevi has also been proposed where it is suggested that the epidermal component of naevi arises from a mutated epidermal melanocyte, while the intradermal component from a mutated Schwann cell (Masson, 1951).

Contributing to the uncertainty surrounding the origin of naevi, naevus tissue has been shown to stain with many melanocyte specific markers such as tyrosinase, TRP1 and Melan-A/MART-1 (Sheffield et al, 2002; Snyder and Paulino, 2002), while subsets of naevus cells have been shown to stain negatively for these melanocytic specific markers, but positively for Schwann cell markers such as S100 or p75 (Barnhill et al, 2004; Freedberg et al, 2003). To date, these studies have focused on the sensitivity of various markers in detecting naevus or melanoma cells, in order to identify a marker or panel of markers which will accurately diagnose melanoma and minimise false negative results. These studies have not, however, aimed to provide a detailed analysis of the distribution and/or overlap of markers within naevus and/or melanoma tissue which may allow for better phenotypic characterisation. This, in turn, may contribute to a better understanding of the cell of origin and subsequent pathogenesis of melanocytic neoplasms.

To re-examine the staining characteristics of naevus tissue, and to provide a thorough evaluation of naevus markers in an attempt to accurately establish the phenotype of a naevus cell, ten human naevus biopsy samples, of five different naevus subtypes, were examined for the expression of select melanocyte and/or Schwann cell differentiation markers. Melan-A positive cells, with or without S100 positivity, were designated a melanocytic phenotype. S100 positive but Melan-A negative cells were indeterminate and could be Schwann cells, other S100 positive cells such as Langerhan's cells or dermal dendritic cells, or a melanocytic cell which simply did not stain with Melan-A due to the limited sensitivity of this marker. To fully evaluate whether S100 positive but Melan-A negative cells could be Schwann cells, serial sections were examined for the expression of p75, whereby co-expression of S100 and p75 would confer a true Schwann cell identity. Furthermore, p75 positive, but S100 negative, cells would suggest a neural crest precursor phenotype (further discussed in section 3).

4.1.1 Do "naevus" cells display a melanocytic phenotype?

In this semi-quantitative analysis, 85.36% of naevus cells stained positively for Melan-A and, since Melan-A is a melanocyte differentiation antigen which is a highly sensitive and specific for skin melanocytes (Sheffield et al, 2002; Snyder and Paulino, 2002), these results were highly indicative of a melanocytic lineage. Results further showed that 84.15% of all naevus cells stained positively for S100, which shows a similar sensitivity to that seen for Melan-A. S100 has previously been considered the most sensitive marker for differentiated melanocytes, yet its lack of specificity has limited its use as a single diagnostic marker (Sheffield et al, 2002; Snyder and Paulino, 2002). This study, however, shows a comparable sensitivity in opposition to previously

reported findings. In addition, Melan-A proved a superior marker to S100 when evaluating naevus cell morphology. Melan-A showed improved cellular detail, including nuclei being more distinct, cellular borders more easily definable and dendrites, when present, more easily visualised. These results would suggest that, in formalin-fixed and paraffin-embedded naevus tissue, Melan-A is a superior maker to S100 in morphological evaluation, and displays a similar sensitivity.

Although naevus cells were shown to express melanocyte specific markers, the morphology of naevus cells was markedly different to that of normal skin melanocytes, in keeping with previous views of naevus cells being "altered" melanocytes or a melanocyte in differing stages of evolution. In this study, naevus cells showed a haphazard organisation, lying in all planes of orientation and occurring in tightly clustered nests which resulted in the loss of their normal anatomical relationships with surrounding keratinocytes and the basement membrane. Dermal naevus cells exhibited a rounded morphology, did not have dendrites and show a decrease in size at deeper dermal levels. Specimen 4 and 6 showed histological features of maturation/neurotisation in H&E analysis and in keeping with this, naevus cells were seen to align vertically in cord-like structures in the reticular dermis. The above was in keeping with previous findings but, important to our understanding of the phenotype of these cells, these results confirmed essential differences between a neavus cell and a differentiated epidermal melanocyte.

Of interest, a large proportion of naevus cells appeared to lie in pairs or "doublets". These doublets did not co-stain with Ki-67 and thus recent cellular division could not be used to explain this phenomenon. It is possible that these cells are slow-dividing cells which have previously divided but remain close together.

In contrast to banal and dysplastic naevi which showed important morphological differences to melanocytes, the cells of a cellular blue naevus showed a dermal collection of cells which more closely resembled an epidermal melanocyte. Cells of a cellular blue naevus remained as single cells, did not aggregate to form nests and retained their dendrites. Although melanin production was not evaluated in this study, the production of melanin is a known characteristic of blue naevi and it is this accumulation of dermal melanin which imparts their blue hue clinically. This would suggest that cellular blue naevi are distinct from other naevus subtypes. Cells of the epithelioid blue naevus showed a similar single cell infiltrate, however, cells were more rounded in appearance and dendrites were absent. This subtype may represent an intermediate subtype. Furthermore, the epidermal keratinocytes in both blue naevus samples surprisingly demonstrated a marked increase in Ki-67 positivity as compared to control skin and other naevus subtypes. This implies an element of epidermal proliferation exists in addition to dermal melanocytic proliferation. This may suggest discrete mechanisms are involved in the development of blue naevi and that blue naevi may well have a different aetiology and pathogenesis to other naevus subtypes. In keeping with this, Ariyanayagam-Baksh et al (2003) demonstrated the rarely occurring malignant blue naevus does not show the same genetic abnormalities as are commonly seen in malignant

melanoma. They concluded that malignant blue naevi may reflect a distinct entity with different molecular pathways of tumorigenesis to that of conventional melanoma.

4.1.2 Was there any evidence for a Schwann cell phenotype within naevi analysed?

As discussed previously, subsets of naevus cells have been shown to stain positively for Schwann cell markers such as S100 or p75, while staining negatively for melanocytic specific markers (Barnhill et al, 2004; Freedberg et al, 2003), indicating a potential Schwann cell phenotype. In this study, occasional S100+ but Melan-A- cells were identified within naevus tissue. To fully evaluate whether these S100+/Melan-A- naevus cells could be true Schwann cells, serial sections were examined for the expression of p75, where co-expression of S100 and p75 would confer a true Schwann cell identity. P75 co-expression was not noted in these S100+/Melan-A- cells, and thus a true myelinating Schwann-cell phenotype (S100+/p75+) was not observed. Due to the non-specificity of S100 staining, these S100+/Melan-A- cells could be Langerhan's cells or dermal dendritic cells which are normally present in human skin. In addition, Melan-A has been reported to be less sensitive than S100 and these S100+/Melan-A- cells may well be melanocytic cells which did simply not stain with Melan-A.

Interestingly, previous studies have shown a loss of Melan-A expression in deeper dermal naevus cells, and the retention of Schwann cells markers which suggests naevus cells in the reticular dermis may display a Schwann cell phenotype. In this study, naevus cells in the reticular dermis did not show a loss of Melan-A expression, even in the naevi which were histologically confirmed to show features of neurotisation. This indicates a melanocytic phenotype was maintained at all dermal levels, in opposition to previously reported findings (Mishima, 1965; Winnepenninkx and van den Oord, 2004).

Section 2:

4.2 The compartment of origin of naevi

Most available data on melanocytic naevi are reports from static, cross-sectional analyses from naevus biopsy specimens. Thus, the step wise evolution of naevi remains unclear and evidence to support existing hypotheses is limited. The main question is whether naevi originate from the epidermis, and whether this is from a melanocyte or a precursor cell; or whether they arise from the dermis, and similarly whether this is from a Schwann cell, a "trapped" melanocyte, or a precursor cell (Masson, 1951; Kawamura, 1956; Mishima, 1965; Unna, 1893; Cramer 1984; Grichnik et al, 2006, Grichnik, 2008 and Ross et al, 2011). It follows that if the compartment of origin of naevi can be established, the possible initiating cell may then be determined. To date, studies evaluating Ki-67 immunostaining in melanocytic neoplasms have focused on the diagnostic value of Ki-67 in assisting to differentiate between melanoma and naevus tissue. Higher proliferative rates are thought to favour a malignant diagnosis while lower proliferative rates are thought to favour a benign diagnosis (Li et al, 2000). Similarly, Ki-67 positivity in deeper dermal levels is more commonly seen within melanoma tissue and thus favours a melanoma diagnosis (Crotty et al, 1992). Ki-67 has also been utilised as a prognostic marker

whereby increased proliferative rates in melanoma biopsies are associated with an increased risk of metastases (Gimotty et al, 2005). Little data, however, exists for the qualitative description of Ki-67 positivity within naevi which may well point to an initiating or driving focus. To re-examine Ki-67 immunostaining in naevus tissue and to attempt to determine a possible compartment of origin of naevi, the same ten human naevus biopsy samples were examined using a dual labelling technique for Melan-A and Ki-67 in order to detect dividing naevus cells. It was hypothesised that areas of Ki-67 positivity may indicate foci driving naevus proliferation, and thus be a potential site of naevus initiation.

4.2.1 Which compartment drives naevus proliferation?

In this semi-quantitative analysis 76.17% of dual labelled (Melan-A+/Ki-67+) naevus cells were located in the epidermal compartment. Junctional and dysplastic naevi contained the highest proportion of dual positive cells per total Melan-A+ naevus cells counted (1.54% and 1.26%), while compound, blue and BIN showed lower proliferative rates (0.8%, 0.53% and 0.14% respectively). These results suggest that the epidermal compartment likely drives naevus proliferation and would therefore support an epidermal origin of naevi.

In support of an epidermal origin of naevi, junctional naevi are thought to arise in childhood and progress to compound and finally intradermal naevi, which may then regress. It could be expected that proliferative rates would decrease with progression through these sequential subtypes. In keeping with this, junctional naevi displayed an increased proliferative rate as compared to compound naevi, which further decreased in BIN (refer Figure 27). This would support and epidermal origin with "dropping off" of these cells into the dermis and a possible mechanistic hypothesis. In addition, dysplastic naevi, which are really atypical compound naevi, showed a proliferative rate similar to that seen in junctional naevi. It is possible that dysplastic naevi contain a mutation which limits attempted differentiation along normal melanocytic pathways and eventual cessation of proliferation. This increased proliferative drive may be associated with their tendency to change with time due to accumulation of additional mutations, as well as their increased risk of malignant transformation.

It must be considered, however, that since this is a single cross-sectional analysis, it is possible that the epidermis may drive naevus proliferation, yet not necessarily be a source of origin of the initiating cell. Thus the mechanisms of naevus development cannot be fully concluded from this study.

4.2.2 Do naevi originate from a single cell or is there evidence for multiple sites of naevus initiation?

An interesting observation when considering the origin of naevi, was that nests of naevus cells occurred as discrete clusters of cells at the tips of the rete ridges, separated by a normal intervening epidermis. This would suggest these naevi have multiple sites of initiation and the hypothesis, therefore, of a single mutated cell giving rise to, and subsequently driving, naevus proliferation cannot logically be used to explain this phenomenon. In addition, Ki-67 positivity was noted in discrete naevus nests, which further supports the idea that multiple sites

drive naevus proliferation. In opposition to this, dysplastic naevi, and some compound naevi, showed a continuous proliferation of naevus cells and merging of adjacent epidermal nests, while BIN and blue naevi showed a continuous dermal infiltration. In these subtypes, the hypothesis of a single initiating cell was more easily believable. It is possible, therefore, that different mechanisms of pathogenesis may exist for different naevus subtypes. Some may develop following a local insult, such as changes in micro-environmental signalling and the generation of multiple simultaneous foci of initiation, while others may arise from a single mutated cell.

4.2.3 Is naevus proliferation related to abnormalities in keratinocyte proliferation?

Based on the above observations of multiple sites of naevus initiation, it was questioned whether some naevus subtypes may result from a local proliferative drive, the so-called field effect, rather than a single mutated cell. It is widely accepted that melanocyte proliferation is tightly regulated by surrounding keratinocytes and this functional relationship is important for optimal functioning and differentiation of both cell types. This is supported by co-culture systems, where keratinocytes have been shown to regulate melanocyte proliferation, dendricity and melanisation by direct cell contact (cell-to-cell adhesion molecules), as well as paracrine signalling molecules such as cytokines, growth factors and hormones (Herlyn et al, 1987; Hsu et al, 2002; Shih et al, 1994). This stresses the important role of local micro-environmental signals in controlling melanocyte phenotype and proliferation. It is thus feasible that changes in local environmental signals could drive naevus proliferation within a limited area in the skin and thereby explain multiple sites of naevus initiation within this site. It has also been proposed that naevi are simply hamartomas, a benign, focal malformation of normal tissue elements, which grow at the same rate as surrounding tissue, but grow in a disorganised mass. This would imply naevi would contain proliferations of other epidermal and/or dermal elements.

Incidentally, the naevus samples analysed in this study showed a large proportion of Ki-67+ keratinocytes within the epidermis of naevus tissue (Figures 28a, 28b). This prompted the comparison of Ki-67+ keratinocytes within naevus tissue, as compared to normal skin, in order to determine whether a global proliferative effect was in fact present. The total Ki-67+ epidermal keratinocytes were determined per unit length of basement membrane in microns and this semi-quantitative analysis showed results were comparable between naevus tissue and control skin (Figure 29). This would indicate that naevi result from an isolated melanocytic drive, and does not support the hypothesis that naevi are true hamartomas. It is still possible, however, that local derangements in keratinocyte-melanocyte signalling may result in uncontrolled proliferation of cells of a melanocytic lineage. Surprisingly, however, the epidermis of blue naevi demonstrated a marked increase in Ki-67 positivity as compared to control skin and other naevus subtypes (Figure 29) and, as discussed previously, this may imply blue naevi represent a distinct group of disorders with different mechanisms of tumorigenesis.

Section 3:

4.3 Evaluation of the tumour stem cell hypothesis in melanocytic naevi

The basic steps of neoplasia involve initiation, promotion, progression and, occasionally, resolution. Tumour initiation involves a mutational event, within oncogenes or within tumour suppressor genes, which primes the cell to respond abnormally to normal growth signals or previously sub-threshold signals. It has recently been proposed that this initiating mutation may occur in a precursor cell and that this mutation may be inherited; or occur *in utero,* or postnatally. This is known as the tumour stem cell hypothesis and is based on the observation of a sub-population of cells with stem-like features within tumour cultures.

Stem cells are slow proliferating cells characterised by the ability to maintain their undifferentiated state through self renewal and to give rise to differentiated cell types. At present, four types of stem cells have been described: embryonic stem cells, cancer stem cells, adult or somatic stem cells and induced pluripotent stem (iPS) cells. The overlap between these four cell types is ill-defined and importantly, the origin of a cancer stem cell and their relationship to an adult stem cell is unclear. Whether cancer stem cells originate from a mutated adult stem cell (Reya et al, 2001), from a mutated transit amplifying cell (Clarke and Fuller, 2006), or result from de-differentiation from a terminally differentiated cell (Sun et al, 2005) remains unknown. Furthermore, not all cancer stem cells have the ability for indefinite renewal, as benign tumours such as banal naevi are known to undergo a period of growth which then stabilizes, and often regresses (Kincannon and Boutzale, 1999), implying an origin from a cell with a limited capacity for self-renewal and thus, by definition, not a true stem cell. Moreover, the occurrence of "de-differentiated" cells in malignant tissues, and the current lack of understanding as to the overlap between "de-differentiation" and "stemness", further confuses this issue.

At present, studies examining the presence and phenotype of stem cells within melanoma are based entirely on cell culture and have generated inconsistent results. Variations in methodologies used to study such cells in culture have been proposed as a cause, yet this has lead to much disagreement on the existence and/or role of stem cells in melanoma development. *In situ* studies may limit variations in study methodologies, as well as limiting the additional micro-environmental changes induced by culture conditions. However, since melanomas show histological similarities to a wide range of tumours which often makes accurate diagnosis challenging, current immunohistochemical analyses have focused on melanocytic differentiation antigens in order to accurately detect melanoma tissue and, to date, few immunohistochemical studies exist for the evaluation of stem cells or precursor cells in melanoma biopsies. As a result, to evaluate the tumour stem cell hypothesis in melanocytic neoplasms, and to do so involving limited micro-environmental changes, as well as to reduce the confusion surrounding the overlap between malignant "de-differentiation" and "stem cells", we have selected to analyse the same ten human naevus biopsy samples by direct immunofluorescence in order to determine the presence, or absence, of precursor cells and to characterise these as neural crest stem cells (p75+) or pluripotent stem cells (OCT4+ and/or NANOG+), if present.

4.3.1 Did naevi contain precursor cells?

Neural crest and pluripotent precursor markers were identified in all naevus subtypes analysed, with the exception of benign intradermal naevi which did not express p75. The majority of positively labelled cells, per total naevus cells counted, localised to the epidermal compartment (72.72%). This trend was evident for all three markers analysed: OCT4 (77.22%), NANOG (63.72%) and p75 (57.15%). It follows that naevi with an epidermal component (junctional, compound and dysplastic naevi) contained the majority of positively labelled precursor cells (a combined percentage of 91.67% of all positively labelled cells). Of these, dysplastic naevi contain more than half (52.27%) of all positive cells, and the vast majority of these expressed OCT4 (78.26%). Benign intradermal naevi and blue naevi contained fewer precursor cells, with a combined proportion of 8.33% of all positively labelled cells. Importantly, however, they did still contain precursor cells.

Interestingly, OCT4+ cells localised mainly to the epidermal compartment and were seen to occur as small clusters of positively labelled cells within the centre of naevus nests, while NANOG+ and p75+ cells occurred as single cells at the periphery of naevus nests, and were slightly more evenly distributed between the epidermis and superficial dermis. Interestingly, NANOG immunostaining did not co-localise with OCT4, as determined by sequential section analysis. In human embryos, OCT4 has been detected in early blastocysts, while NANOG expression is only detected from the 8 cell blastocyst stage onwards (Kimber et al, 2008). Similarly, in porcine embryos OCT4 expression was detected in early embryos, persisted in early blastocyst and then decreased in expression around E9.5-E10.5. NANOG, however, was only detected at later stages of embryo development (E7.5) and persisted at high expression levels at E9.5 and E10.5 (du Puy et al, 2010). It thus appears that embryonic stem cells do not co-express OCT4 and NANOG at all stages of development. It could be hypothesized that the expression of OCT4 represents an early step in tumour formation and that these cells proliferate to form clusters of OCT4+ cells. As proliferation continues, cells are pushed laterally to the outer limits of the naevus nests where it appears NANOG expression is attained and expression of OCT4 is lost or down regulated to undetectable levels.

Results of this study also showed that NANOG expression was more pronounced than OCT4 in cells in the superficial dermis. In keeping with the above line of thought, this could represent a later stage in tumour evolution, and supports the concept of an epidermal origin of naevi, with migration of cells from the epidermis to the superficial dermis. This is supported by Ki-67 staining patterns. Additionally, cells then may attempt further differentiation and gain the expression of p75. Consistent with this, p75+ cells displayed irregular cell borders which suggests the presence of intercellular adhesions (this pheomenon results from tissue distortion during procesing with widening of intercellular spaces. Intercellular adhesions are maintained and, as cells are pulled apart, they adopt an irregular, or “spiny” appearance as seen in Figures 36a, 36b). This would indicate p75+ cells are of a more differentiated phenotype as precursor cells lack intercellular adhesions. These p75+ cells did not co-express S100 and are therefore unlikely to be Schwann cells. P75 is not expressed in

melanocytes and in cells of a melanocytic lineage, is specific for a precursor phenotype. Thus, it is possible that these p75+ cells are neural crest precursors. It is also possible, however, that these p75+ cells are Merkel cells, which have been shown to express p75 in normal human skin (Lopez et al, 1998).

4.3.2 Does evidence support stem cells as the origin of melanocytic naevi?

Results of this study suggest an epidermal origin of naevi, as determined by Ki-67 immunostaining, and this is further supported by results showing naevus cells display a melanocytic phenotype, indicating origin from a cell of epidermal lineage. In addition, results demonstrated the presence of precursor cells within naevus tissue, the majority of which localise to the epidermis. Following this, the prominence of precursor cells within the epidermal compartment would suggest an association between epidermal melanocytic-lineage stem cells and naevus proliferation. This does not, however, provide evidence for the state of differentiation of the initiating cell. Whether naevus cells result from attempted differentiation of an epidermal precursor cell or from de-differentiation from an epidermal melanocyte remains questionable.

Clues as to the aetiology of naevi may be obtained from understanding normal melanocyte homeostasis; however, this remains a major challenge. A growing body of literature has established the role of stem cells in normal tissue maintenance and repair, and it is reasonable to assume that skin melanocytes are replenished from a reservoir of immature cells. It has been convincingly shown that melanocyte precursors do exist in postnatal skin. During normal hair cycling, hair follicle melanocytes are repopulated by a population of precursor cells residing in the hair follicle bulge (Nishimura et al, 2002; Sieber-Blum et al, 2004; Amoh et al, 2005; Wong et al, 2006). These quiescent bulge precursor cells have been shown to downregulate melanocyte specific markers Mitf, TRP1, TRP2 (Dct) and Tyrosinase (Nishimura et al, 2010) and consequently, since discrete melanocyte stem cell markers have not yet been identified, detection of further melanocyte precursor populations is currently difficult. Maintenance of the interfollicular keratinocyte population has been shown to involve many small “units of proliferation” (Blainpan and Fuchs, 2009), which is independent of normal hair cycling. This would suggest that melanocytes too may be replenished from an interfollicular pool of precursor cells; and this is further supported by the observation of repigmentation of glabrous skin in conditions such as vitiligo (Davids et al, 2009). However, the presence of an interfollicular niche for melanocyte stem cells has not been definitively demonstrated.

The potential for differentiated melanocytes to contribute to normal skin homeostasis is another possibility in maintaining the interfollicular melanocyte population, yet this hypothesis remains largely unexplored as dividing melanocytes have been difficult to demonstrate in samples of normal and/or wounded human skin. In this study, it was hypothesized that, should a naevus result from a precursor cell, it would require evidence for the existence of an interfollicular stem cell niche; or, should naevi result from an epidermal melanocyte, evidence that epidermal melanocytes are capable of *in vivo* cell division would be required.

4.3.2.1 Is there evidence for the existence of an interfollicular stem cell niche?

In this study, the epidermis of naevi contained the majority of proliferating naevus cells and this supports an epidermal origin of naevi. As discussed previously, 72.72% of all positively labelled precursor cells localised to the epidermal compartment of naevi and thus, if naevi originate from a precursor cell, this would imply the interfollicular epidermis is a potential precursor niche. Importantly, however, in this study only a single NANOG+ cell was identified in the basal layer of the epidermis of normal skin (Figure 16b). No further precursor cells were noted in the epidermis or dermis of normal human skin, or in the normal intervening interfollicular epidermis or dermis of naevi, as may have been expected. In keeping with this, Katona et al (2007) examined 115 cutaneous specimens, including a variety of benign and malignant epidermal neoplasms as well as normal skin, for OCT4 expression and demonstrated that all 115 specimens examined were negative for OCT4 expression as was adjacent or overlying epidermis and follicular epithelium including the bulge region. Tai et al (2005) examined a panel of 30 human normal tissue samples by immunohistochemical analysis and reported the finding of rare OCT4 positive cells within the basal layer of the epidermis. Results of this study were however unconvincing as the reported positive staining was difficult to perceive and an interfollicular niche remains to be definitively demonstrated.

From the above, one could conclude that either an interfollicular stem cell niche does not exist and precursor cells result from terminally differentiated cells when required, or that precursor cells are present but, when housed in a specific niche, known pluripotency markers such as OCT4 and NANOG are downregulated and/or other currently unidentified markers are expressed. A number of stem cell markers exist which were not examined in this study. These may serve as important phenotypic markers of stem cells in human skin and may aid in identifying an interfollicular stem cell niche.

4.3.2.2 Can normal epidermal melanocytes divide?

In order to examine whether normal epidermal melanocytes are capable of *in vivo* cell division, normal human skin biopsies were evaluated with a dual labelling technique for Melan-A and Ki-67. Two dual labelled (Melan-A+/Ki-67+) melanocytes were detected in normal skin epidermis (Figure 10). These dual labelled melanocytes were from two separate biopsy samples but interestingly, from the same patient. In addition to normal human skin, the normal epidermis adjacent to naevus tissue was examined for dual labelled cells. Dual labelled cells were occasionally present, yet because it was not possible to accurately confirm these were normal melanocytes and not distant naevus cells, they were not included in our results. The finding of Melan-A+/Ki-67+ melanocytes in normal human epidermis indicates that differentiated skin melanocytes are capable of undergoing cellular division. Thus it is entirely possible that differentiated melanocytes contribute to normal skin homeostasis and, if mutated may give rise to melanocytic neoplasms. In keeping with the above, Taylor et al (2011) showed the depletion of the overall melanocyte population in zebrafish was associated with an overall decrease in MITF and this, in turn, resulted in a significant upregulation of differentiated melanocyte division.

Also, melanocytes in culture show abilities to divide. These data, although greatly limited, support the concept that terminally differentiated melanocytes retain the ability to enter the cell cycle under certain micro-environmental changes.

It is therefore plausible that two separate pathways exist for melanocyte homeostasis, and central to this may be alterations in normal micro-environmental signals, such as MITF, which could control pathway switching. It follows that two pathways may exist for naevus development and that either precursor cells, or epidermal melanocytes, may give rise to melanocytic naevi and/or melanoma.

4.3.3 Is there an association between naevus subtype, stem cell component and risk of melanoma development?

Dysplastic naevi show histological features of architectural and/or cellular atypia, and are identified risk factors for the development of a melanoma. Of great interest, the dysplastic naevi analysed showed a very high proportion of OCT4+ cells (5.81%, Figure 32a), which was by far the greatest proportion of any precursor marker identified in this study. It is possible then that an increased stem cell component may contribute to an increased risk of malignant transformation. It can be hypothesised that cells of dysplastic naevi may have a more severe underlying mutation which may limit the cells ability to retain normal differentiation pathways and thus remain in a stem-like state. This stem-like state may result in the cellular atypia observed in these lesions, as well as confer and increased propensity to divide and therefore accumulate mutations, leading to an increased risk of malignant transformation. In keeping with this, dysplastic naevi contained a large proportion of Ki-67+ cells as compared to other naevus subtypes. The converse, however, is also feasible. It is possible that differentiated melanocytes undergo a mutational event which leads to the expression of various transcription factors resulting in an increased ability to "de-differentiate" and acquire a stem-like phenotype.

4.4 Technical aspects and limitations of study

Important in this study was the mastery of various techniques used to generate these results. The principal technique utilised was immunofluorescence and the challenge surrounded optimisation of each antibody for formalin-fixed and paraffin-embedded tissues. It is well recognized that formaldehyde fixation of tissues induces artefacts by cross-linking of amino acid residues which may lead to masking of tissue antigens and false negative results. Similarly, alteration of epitopes may lead to non-specific binding and false positive results. Many techniques have been employed to unmask these hidden epitopes and recover immunoreactivity. In this study, heat induced epitope retrieval proved the most successful method of antigen retrieval. However, complete certainty that all epitopes were detected, or not detected, is not possible. Given these limitations when performing immunohistochemistry, as well as the notorious difficulty in performing immunohistochemistry for pluripotency markers such as OCT4 and NANOG, alternative methods to validate the expression of these markers and thus validate the above data should be utilised. For example, homogenisation of naevus biopsy

samples and analysis using techniques of real time PCR could provide a sensitive alternative technique to validate the above data. Demonstration that these markers exist within the naevus tissue itself, and not within the intervening epidermis or dermis would, however, be impossible to determine. A dual approach of in situ analysis for tissue localisation and PCR for improved sensitivity and specificity would be a superior approach.

Dual labelling proved immensely difficult as tissue processing had to be balanced between optimised protocols for each antibody. This proved a time consuming task, but eventually successful dual labelling techniques for selected markers were achieved. The protocol for NANOG immunostaining was only able to be optimised for cultured cells and thus the protocols used for processed tissue may not have been optimal. Attempts to alleviate this were performed by ensuring the protocols optimised for p75 analysis in culture and in processed tissues were similar.

The main limitation of this study was the inability to draw statistical comparisons. Firstly, the sample size was limited in number due to access of biopsy samples, the volume of tissue analysed and the number of markers selected. Since this study was designed as a descriptive pilot study, a more focused analysis, using a few select markers building on the above results, would allow for an increased sample size and better statistical power. Secondly, areas for analysis were randomly selected in each high power field. This may well result in sampling error due to alteration of results should other areas have been sampled. Sampling bias was avoided by choosing the best representative area of naevus tissue in each section, regardless of staining intensity or proportion of positively labelled cells. This was continued in the same manner throughout the study and was conducted by a single observer. Lastly, a limited number of markers were utilised due to high costs of antibodies and their limited use in our laboratory. The best global marker was selected for each objective, however, a panel of markers for each objective may have provided improved results. Melanocyte precursor markers, such as MITF, c-Kit, TRP2, may have provided improved phenotypic characterization of naevus cells if used simultaneously. Similarly, additional neural crest markers, such as SOX10, TWIST and PAX3, and added pluripotency markers, such as SOX2, Alkaline phosphatase, SSEA-1 and SSEA-4, may have expanded on identification of precursor cells within naevus tissues.

4.5 Conclusions

This study demonstrates naevus cells display a melanocytic phenotype, due to the expression of melanocyte specific markers, and that this phenotype is consistent regardless of dermal depth. This strongly suggests that naevus cells arise from a melanocyte lineage. However, naevus cells show important phenotypic alterations and are morphologically distinct from differentiated melanocytes. Although studies have suggested regional variations in naevi and a possible Schwann cell lineage, there was no evidence in support of the existence of a Schwann cell phenotype of naevus cells in this study.

Secondly, this data supports an epidermal origin of naevi. Proliferating naevus cells were most numerous in the epidermal compartment and this would suggest naevi are driven by epidermal proliferation. Discrete clusters of naevus cells were noted to occur at the tips of the rete ridges, separated by a normal intervening epidermis, and this would suggest naevi may have multiple sites of epidermal initiation. An epidermal origin of naevi would imply junctional naevi precede compound and then intradermal subtypes, in keeping with traditional models of naevus evolution and, in support of this, junctional naevi displayed an increased proliferative rate as compared to compound naevi, which further decreased in intradermal subtypes. A mechanistic hypothesis can therefore be proposed with evidence in support of an epidermal origin and subsequent "dropping off" of these cells into the dermis.

It must be considered, however, that although the epidermis may drive naevus proliferation, it may not necessarily be the source of origin of the initiating cell. And, since this was a static, cross-sectional analysis, a mechanistic hypothesis cannot be credibly concluded. A dermal stem cell niche has previously been considered, based on the theory that the dermis would be less exposed to physiological or chemical stress than the epidermis (Li et al, 2009) and studies have demonstrated neural crest stem-like cells can be generated from dissociated dermis (Toma et al, 2001; Fernandes et al, 2004, 2008; Wong et al, 2006). In this study, precursor cells were present within the superficial dermis of naevus tissue and the hypothesis of an initiating cell within the superficial dermis, which subsequently migrates into the epidermis and/or reticular dermis, may also be proposed. Certain naevus samples showed merging of epidermal and dermal nests and/or a continuous dermal infiltration, without an epidermal element. Both the above would support the dermal expansion of naevus tissue from an initiating cell within the superficial dermis.

Thirdly, this study convincingly demonstrates the presence of precursor or "stem" cells within naevus tissue. These cells were of both a pluripotent and neural crest phenotype. Dysplastic naevi contained the greatest proportion of precursor cells and it is hypothesised that this increased stem cell component may confer an increased risk of malignant transformation. Interestingly, pluripotency markers OCT4 and NANOG were not co-expressed and thus pluripotent stem cells may exhibit temporal differences in the expression profiles of transcription factors *in vivo.* This may account for the discrepancies observed in previous studies of melanoma stem cells. Similarly, no OCT4 or NANOG positive cells were identified in the normal interfollicular epidermis of naevi or normal human skin. This implies that either these niche-resident cells down-regulate known stem cell markers, express other and/or currently unidentified stem cell markers, or do not exist.

It was further noted that precursor cells were most numerous within the epidermal compartment of naevi. There was therefore an association between naevus proliferation and the presence of precursor cells. It is thus plausible that precursor cells drive naevus proliferation and it may be considered then that these stem-like cells give rise to melanocytic naevi. This is in support of the tumour stem cell hypothesis for the development of melanocytic

neoplasms. It is further proposed that cells with limited mutations would retain responses to normal micro-environmental signals. Local proliferation would result in an expansion of cells which retain certain melanocytic differentiation pathways and remain within the epidermis, resulting in a junctional naevus. More severe mutations, or cumulative mutations, could result in an increased proliferative drive, a larger transit amplifying population and/or changes in adherence or response to micro-environmental signals. These cells could then migrate from the epidermis resulting in a compound, intradermal or dysplastic naevus; or a malignant melanoma. It is also plausible, however, that naevus cells result from differentiated melanocytes and, as they proliferate, they take on a more "un-differentiated" appearance and thereby resemble stem-like cells.

Regardless of the aetiology of naevi, existing hypotheses imply naevus cells are able to migrate from one cutaneous compartment to another. Yet, benign cells, by definition, do not have the capacity to metastasize. To simplify this concept, a dual origin of naevi has been proposed. However, naevus cells have been demonstrated in regional lymph nodes (Biddle et al, 2003; Fontaine et al, 2002; Howel et al, 2006; Sewart and Copeland, 1931) and in circulating blood (Argenziano et al, 2003; De Giorgi et al, 2010), and this phenomenon has been described as a benign metastatic process. It is hypothesized that a loosely adherent progenitor cell may enter the blood or lymphatic system, travel to distant sites and, if stimulated, may proliferate to form a naevus (Ross et al, 2011) (Figure 39).

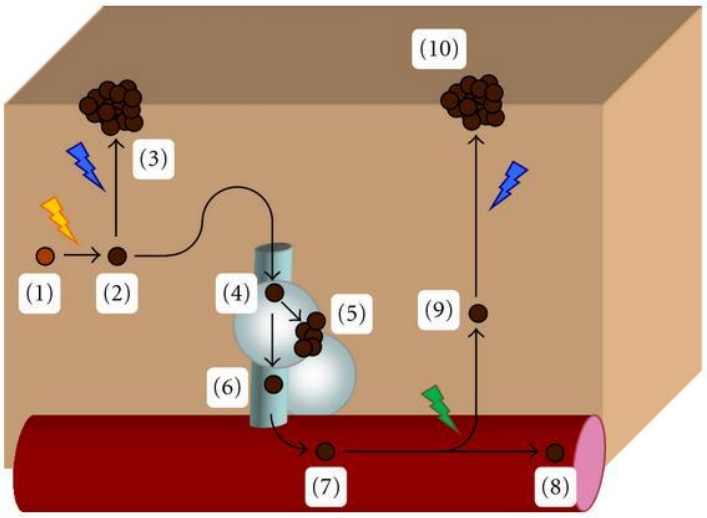

Figure 39: Model of benign metastasis. A melanocytic stem cell (1) undergoes an initiating event that transforms it into an immature naevus progenitor cell (2). This cell (2) may remain quiescent until local environmental factors stimulate it to proliferate into a naevus (3). Alternatively, this loosely adherent cell could enter the lymphatic system (4). Upon encountering a lymph node, the progenitor cell could either implant in the node and proliferate into a nodal naevus (5) or pass through without being sequestered (6) to eventually reach the circulatory system (7). The progenitor cell would continue to circulate (8) until a transforming event, like a mutation, or environmental conditions signals the cell to implant in the skin (9). The implanted naevus progenitor cell would remain quiescent in the skin until local environmental factors stimulate it to proliferate into a naevus (10) (Ross et al, 2011).

This theory has been utilised to explain the occurrence of eruptive naevi (the sudden systemic development of multiple naevi over a short period of time) and nodal naevi (benign aggregates of naevus-like cells in lymph

nodes). This theory may similarly be used to explain melanoma development, the occurrence of satellite lesions in melanoma and the metastasis of malignant cells in general. This would support the tumour stem cell model of melanoma development.

Lastly, it must be considered that not all melanocytic neoplasms necessarily originate in a similar manner. Blue naevi displayed important morphological differences to other naevus subtypes and appeared to have an associated epidermal proliferative abnormality with features more in keeping with that of a hamartoma. Junctional naevi appeared to have multiple sites of initiation, and this suggests the recruitment of many individual cells, while intradermal naevi showed a continuous infiltration of cells and was more suggestive of a single initiating cell. It is therefore possible that different mechanisms of pathogenesis may exist for different naevus subtypes. Certain subtypes may result from a local developmental abnormality, as supported by features of blue naevi and the occurrence of congenital naevi; others may develop following a local epidermal insult, such as changes in micro-environmental signalling and the generation of multiple simultaneous foci of initiation; while others may arise from a single mutated cell.

Additionally, melanomas display different subtypes where some subtypes (such as the superficial spreading melanoma) are well accepted to be causally linked to cumulative ultraviolet radiation (UVR), while the contribution of UVR to the development of other subtypes (such as those occurring on the mucosa, acral areas or congenital melanomas) is less clear. In keeping with this, malignant blue naevi display different genetic mutations to those commonly observed in melanomas. Studies examining the presence and phenotype of melanoma stem cells have generated inconsistent results with some highly suggestive of a stem cell population which drives melanoma development (Fang et al, 2005; Grichnik et al, 2006; Klein et al, 2007; Schatton and Frank, 2008; Thies et al, 2004) and others showing a lack of evidence in support of melanoma stem cells (as reviewed by Girouard and Murphy 2011; Gupta et al, 2009 and Kennedy et al, 2007; Quintana et al, 2008, 2010). It is highly plausible therefore that melanocytic neoplasms consist a heterogeneous group of disorders with altered mechanisms of initiation and development; and, while some neoplasms may originate from a mutated epidermal melanocyte and follow the traditional pathways of melanoma progression (Figure 3), others may well arise from a mutated tissue resident precursor cell, in support of the tumour stem cell hypothesis.

4.6 Future directions

This study provides strong evidence for the presence of precursor cells within naevus tissue. Their epidermal location and this association with naevus proliferation can reasonably be used to explain the development of naevi from a mutated tissue resident precursor cell, in support of the tumour stem cell hypothesis. However, this study provides only a static cross-sectional analysis of naevus tissue and the temporal development of naevi cannot be accurately concluded. It is entirely possible that these precursor cells result from differentiated melanocytes which have undergone a mutational event as described above. Further studies examining the

temporal evolution of naevi are required to fully understand the aetiology and pathogenesis of melanocytic neoplasms, however, these prove difficult to execute. Also, further studies examining the possible molecular phenotype of stem cells *in vivo*, and the location of cutaneous stem cells niches, are required. Lastly, the relationship between cancer stem cells and adult stem cells needs to be explored. Information surrounding the process of de-differentiation, in order to fully understand this concept, as well as detailed mechanisms involved, may assist in supporting or disproving this concept and thereby assist in understanding the aetiopathogenesis of melanocytic neoplasms, and specifically malignant melanoma.

5. References

Achilleos A and Trainor PA (2012). Neural crest stem cells: discovery, properties and potential for therapy. *Cell Research* 22:288-304.

Adameyko I, Lallemend F, Aquino JB, Pereira JA, Topilko P, Muller T, Fritz N, Beljajeva A, Mochii M, Liste I, Usoskin D, Suter U, Birchmeier C and Ernfors P (2009). Schwann cell precursors from nerve innervation are a cellular origin of melanocytes in skin. *Cell* 139:366–379.

Agnarsdottir M, Sooman L, Bolander A, Stromberg S, Rexhepaj E, Bergqvist M, Ponten F, Gallagher W, Lennartsson J, Ekman S, Uhlen M and Hedstrand H (2010). SOX10 expression in superficial spreading and nodular malignant melanomas. *Melanoma Research* 20:468-478.

Alberts B, Johnson A, Lewis J, Raff M, Roberts K and Walter P (2002). Molecular Biology of the Cell, 4th edition. *Garland Science* (www.ncbi.nlm.nih.gov/books/NBK26865/).

Al-Hajj M, Wicha MS, Benito-Hernandez A, Morrison SJ, Clarke MF (2003). Prospective identification of tumorigenic breast cancer cells. *Proceedings of the Natural Academy of Sciences* 100:3983-3988.

Amoh Y, Li L, Katsuoka K, Penman S and Hoffman RM (2005). Multipotent nestin-positive, keratin negative hair follicle bulge stem cells can form neurons. *Proceedings of the Natural Academy of Sciences* 102:5530-5534.

Andersson DJ (1997). Cellular and molecular biology of neural crest cell lineage determination. *Trends in Genetics* 13:276-280.

Argenziano G, Soyer HP, Chimenti S, Talamini R, Corona R, Sera F, Binder M, Cerroni L, De Rosa G, Ferrara G, Hofmann-Wellenhof R, Landthaler M, Menzies SW, Pehamberger H, Piccolo D, Rabinovitz HS, Schiffner R, Staibano S, Stolz W, Bartenjev I, Blum A, Braun R, Cabo H, Carli P, De Giorgi V, Flemming MG, Grichnik JM, Grin CM, Halpern AC, Johr R, Katz B, Kenet RO, Kittler H, Kreusch J, Malvehy J, Mazzocchetti G, Oliviero M, Ozdemir F, Peris K, Perotti R, Perusquia A, Pizzichetta MA, Puig S, Rao B, Rubegni P, Saida T, Scalvenzi M, Seidenari S, Stanganelli I, Tanaka M, Westerhoff K, Wolf IH, Braun-Falco O, Kerl H, Nishikawa T, Wolff K and Kopf AW (2003). Dermoscopy of pigmented skin lesions: results of a consensus meeting via the internet. *Journal of the American Academy of Dermatology* 48:679–693.

Ariyanayagam-Baksh SM, Baksh FK, Finkelstein SD, Swalsky PA, Abernethy J and Barnes EL (2003). Malignant blue nevus: a case report and molecular analysis. *American Journal of Dermatopathology* 25:21-27.

Barnhill RL, Piepkorn J and Busum KJ (2004). Pathology of Nevi and Malignant Melanoma. *Springer* 148-198.

Belicchi M, Pisati F, Lopa R, Porretti L, Fortunato F, Sironi M, Scalamogna M, Parati EA, Bresolin N and Torrente Y (2004). Human skin-derived stem cells migrate throughout forebrain and differentiate into astrocytes after injection into adult mouse brain. *Journal of Neuroscience Research* 77:475–486.

Biddle DA, Evans HL, Kemp BL, El-Naggar AK, Harvell JD, White WL, Iskandar SS and Prieto VG (2003). Intraparenchymal nevus cell aggregates in lymph nodes: a possible diagnostic pitfall with malignant melanoma and carcinoma. *The American Journal of Surgical Pathology* 27:673-681.

Blanpain C and Fuchs E (2009). Epidermal homeostasis: a balancing act of stem cells in the skin. *Nature Reviews Molecular Cell Biology* 10:207–217.

Boenisch T, Farmilo AJ, Stead RH, Key M, Welcher R, Harvey R and Atwood K (2001). Immunohistochemical staining methods. 3rd Edition. *DakoCytomation* 18-22.

Bonnet D and Dick JE (1997). Human acute myeloid leukemia is organized as a hierarchy that originates from a primitive hematopoietic stem cell. *Nature Medicine* 3:730-737.

Brandl C, Florian C, Driemel O, Weber BH and Morsczeck C (2009). Identification of neural crest stem cell-like cells from the corneal limbus of juvenile mice. *Experimental Eye Research* 89:209-217.

Bremer M, Frob F, Kichko T, Reeh P, Tamm ER, Suter U and Wegner M (2011). Sox10 is required for Schwann-cell homeostasis and myelin maintenance in the adult peripheral nerve. *Glia* 59:1022-1032.

Carlson JA, Ross, JS and Slominski AJ (2009). New techniques in dermatopathology that help to diagnose and prognosticate melanoma. *Clinics in Dermatology* 27:75-102.

Chambers I, Colby D, Robertson M, Nichols J, Lee S, Tweedie S and Smith A (2003). Functional Expression Cloning of Nanog, a Pluripotency Sustaining Factor in Embryonic Stem Cells. *Cell* 113:643-655.

Chen TR (1977). In situ detection of mycoplasma contamination in cell cultures by fluorescent Hoechst 33258 stain. *Experimental Cell Research* 104:255-262.

Clark WH Jr, Elder DE, Guerry D 4th, Epstein MN, Greene MH and Van Horn M (1984). A study of tumour progression: the precursor lesions of superficial spreading and nodular melanoma. *Human Pathology* 15:1147-1165.

Clarke MF and Fuller M (2006). Stem cells and cancer: two faces of eve. *Cell* 124:1111-1115.

Cotran RS, Kumar V, Robbins SL (1994) Robbin's pathological basis of disease. 5th Edition. *WB Saunders Company*.

Cramer SF (1984). The histogenesis of acquired melanocytic nevi. Based on a new concept of melanocytic differentiation. *The American Journal of Dermatopathology* 6:*289-298.*

Crotty KA, McCarthy SW, Palmer AA, Ng AB, Thompson JF, Gianoutsos MP and Shaw HM (1992). Malignant melanoma in childhood: a clinicopathological study of 13 cases and comparison with Spitz naevi. *World Journal of Surgery* 16:179-185.

Darr H, Mayshar Y and Benvenisty N (2006). Overexpression of NANOG in human ES cells enables feeder-free growth while inducing primitive ectoderm features. *Development* 133:1193-1201.

Davids LM, du Toit E, Kidson SH and Todd G (2009). A rare repigmentation pattern in a vitiligo patient: A clue to an epidermal stem-cell reservoir of melanocytes? *Clinical and Experimental Dermatology* 34:246-248.

De Giorgi V, Pinzani P, Salvianti F, Grazzini M, Orlando C, Lotti T, Pazzagli M and Massi D (2010). Circulating benign nevus cells detected by ISET technique: warning for melanoma molecular diagnosis. *Archives of Dermatology* 146:1120-1124.

du Puy L, Lopes SM, Haagsman HP and Roelen BA (2010). Analysis of co-expression of OCT4, NANOG and SOX2 in pluripotent cells of the porcine embryo, in vivo and in vitro. *Theriogenology* 75:513-526.

Dupin E, Calloni G, Real C, Goncalves-Tretin A and Le Douarin NM (2007). Neural crest progenitors and stem cells. *Comptes Rendus des Seances de la Societe de Biologie et de ses Filiales* 330:521-529.

Ernfors P (2010). Cellular origin and developmental mechanisms during the formation of skin melanocytes. *Experimental Cell Research* 316:1397-1407.

Evans M and Kaufman M (1981). Establishment in culture of pluripotent cells from mouse embryos. *Nature* 292: 155-156.

Fang D, Nguyen TK, Leishear K, Finko R, Kulp AN, Hotz S Van Belle PA, Xu X, Elder DE and Herlyn M (2005). A tumorigenic subpopulation with stem cell properties in melanomas. *Cancer Research* 65:9328–9337.

Fernandes KJ, Mckenzie IA, Mill P, Smith KM, Akhavan M, Barnabe-Heider F, Biernaskie J, Junek A, Kobayashi NR, Toma JG, Kaplan DR, Labosky PA, Rafuse V, Hui C and Miller FD (2004). A dermal niche for multipotent adult skin-derived precursor cells. *Nature Cell Biology* 6:1082-1093.

Fernandes KJ and Miller FD (2009). Isolation, expansion, and differentiation of mouse skin-derived precursors. *Methods in Molecular Biology* 482:159-170.

Fernandes KJ, Toma JG and Miller FD (2008). Multipotent skin-derived precursors: adult neural crest-related precursors with therapeutic potential. *Philosophical Transactions of the Royal Society of London. Series B, Biological Sciences* 363:185-198.

Fitzpatrick TB and Breathnach AS (1963). [The epidermal melanin unit system]. *Dermatologische Wochenschrift* 18:481-489.

Fontaine D, Parkhill W, Greer W and Walsh N (2002). Nevus cells in lymph nodes: an association with congenital cutaneous nevi. *The American Journal of Dermatopathology* 24:1-5.

Fox MJ (1949). Analysis of some phases of melanoblast migration in the barred Plymouth Rock embryos. *Physiological Zoology* 22:1-22

Freedberg PM, Eisen AZ, Wolf K, Austen KF, Goldsmith LA and Katz SI (2003). Fitzpatrick's dermatology in general medicine. 6th Edition, volume I. *McGraw Hill.*

Freedberg PM, Eisen AZ, Wolf K, Austen KF, Goldsmith LA and Katz SI (2003). Fitzpatrick's dermatology in general medicine. 6th Edition, volume II. *McGraw Hill.*

Gilbert SF (2000). The Neural Crest. Developmental Biology. 6th edition. *Sunderland (MA): Sinauer Associates.* (http://www.ncbi.nlm.nih.gov/books/NBK10065/).

Gimotty PA, Van Belle P, Elder DE, Murry T, Montone KT, Xu X, Hotz S, Raines S, Ming ME, Wahl P and Guerry D (2005). Biologic and prognostic significance of dermal Ki-67 expression, mitoses, and tumorigenicity in thin invasive cutaneous melanoma. *Journal of Clinical Oncology* 23:8048-8056.

Girouard SD and Murphy GF (2011). Melanoma stem cells: not rare, but well done. *Laboratory Investigation* 91:647-664.

Gleason BC, Crum CP and Murphy GF (2008). Expression patterns of MITF during human cutaneous embryogenesis: evidence for bulge epithelial expression and persistence of dermal melanoblasts. *Journal of Cutaneous Pathology* 35:615-622.

Graham A, Fuller A, Murphy M, Jones M, Forman D and Swerdlow AJ (1999). Maternal and child constitutional factors and the frequency of melanocytic naevi in children. *Paediatric and Perinatal Epidemiology* 13:316-324.

Green A and Swerdlow AJ (1989). Epidemiology of melanocytic nevi. *Epidemiologic Reviews* 11:204-220.

Grichnik JM, (2008). Melanoma, Nevogenesis, and Stem Cell Biology, *Journal of Investigative Dermatology* 128: 2365-2380.

Grichnik JM, Burch JA, Schulteis RD, Shan S, Liu J, Darrow TL Vervaert CE and Seigler HF (2006) Melanoma, a tumor based on a mutant stem cell*? Journal of Investigative Dermatology* 126:142–153.

Gupta PB, Chaffer CL and Weinberg RA (2009). Cancer stem cells: mirage or reality? *Nature Medicine* 15:1010-1012.

Herlyn M, Clark WH, Rodeck U, Mansiati ML, Jambrosic J and Koprowski H (1987). Biology of Tumor progression in human melanocytes. *Laboratory Investigation* 56:461-474.

Herlyn M, Guerry D and Kaprowski H (1985). Recombinant y-interferon induces changes in expression and shedding of antigens associated with normal human melanocytes, nevus and primary metastatic melanoma cells. *Journal of Immunology* 134: 4226-4231.

Ho MM, Ng AV and Hung JY (2007). Side population in human lung cancer cell lines and tumors is enriched with stem-like cancer cells. *Cancer Research* 67:4827-4833.

Holbrook KA, Underwood RA, Vogel AM, Gown AM and Kimball H (1989). The appearance, density and distribution of melanocytes in human embryonic and fetal skin revealed by the anti-melanoma monoclonal antibody, HMB-45. *Anatomy and Embryology* 180:443-455.

Howel BG, Lipa JE and Ghazarian DM (2006). Intracapsular melanoma: a new pitfall for sentinel lymph node biopsy. *Journal of Clinical Pathology* 59:891-892.

Hsu MY, Meier F and Herlyn M (2002). Melanoma development and progression: a conspiracy between tumor and host. *Differentiation* 70:522-536.

Hu DN, Savage H and Roberts JE (2002). Uveal melanocytes, ocular pigment epithelium ad Mueller cells in culture: in vitro toxicology. *International Journal of Toxicology* 21:465-472.

Hui P, Perkins A and Glusac E (2001). Assessment of clonality in melanocytic nevi. *Journal of Cutaneous Pathology* 28:140–144.

Hulley PA, Stander CS and Kidson SH (1991). Terminal migration and early differentiation of melanocytes in embryonic chick skin. *Developmental Biology* 145:182-194.

Jaenisch R and Young R (2008). Stem cells, the molecular circuitry of pluripotency and nuclear reprogramming. *Cell* 132:567-582.

Katona TM, Billings SD, Montironi R, Lopez-Beltran A and Cheng L (2007). Expression of OCT4 transcription factor in cutaneous neoplasia. *Applied Immunohistochemistry and Molecular Morphology* 15:359-362.

Kawamura T (1956). [Pathogenesis of evus cells and genetic relationship between nevus pigmentosus, blue nevus and Recklinghausen's phakomatosis]. *Der Hautarzt* 7:7-14.

Kelly JW, Yeatman JM, Regalia C, Mason G and Henham AP (1997). A high incidence of melanoma found in patients with multiple dysplastic naevi using photographic surveillance. *The Medical Journal of Australia* 167:191-194.

Kennedy JA, Barabe F, Poeppl AG, Wang JCY and Dick JE (2007). Comment on 'Tumour growth need not be driven by rare cancer stem cells'. Author reply. *Science* 318:1722.

Kimber SJ, Sneddon SF, Bloor DJ, El-Bareg AM, Hawkhead JA, Metcalfe AD, Houghton FD, Leese HJ, Rutherford A, Lieberman BA and Brison DR (2008). Expression of genes involved in early cell fate decisions in human embryos and their regulation by growth factors. *Reproduction* 135:635-647.

Kincannon J and Boutzale C (1999). The Physiology of Pigmented Nevi. *Pediatrics* 104:1042-1045.

Kitajima H, Yoshimura S, Kokuzawa J, Kato M, Iwama T, Motohashi T, Kunisada T and Sakai N (2005). Culture methods for the induction of neurospheres from mouse embryonic stem cells by co-culture with PA6 stromal cells. *Journal of Neuroscience Research* 80:467-474.

Klein WM, Wu BP, Zhao S, Wu H, Klein-Szanto AJ and Tahan SR (2007). Increased expression of stem cell markers in malignant melanoma. *Modern Pathology* 20:102–107.

Kodama HA, Amagai Y, Koyama H and Kasai A (1982). Hormonal responsiveness of a preadipose cell line derived from newborn mouse calvaria. *Journal of Cellular Physiology* 112:83-88.

Kondo T, Setoguchi T and Taga T (2004). Persistence of a small population of cancer stem cells in the C6 glioma cell line. *Proceedings of the Natural Academy of Sciences* 101:781-786.

Larsson B (1993). Interaction between chemicals and melanin. *Pigment Cell Research* 6:127-133.

Le Douarin NM, Calloni GW and Dupin E (2008). The stem cells of the neural crest. *Cell Cycle* 7:1013-1019.

Levy C, Khaled M and Fisher DE (2006). MITF: master regulator of melanocyte development and melanoma oncogene. *Trends in Molecular Medicine* 12:406-414.

Lewin GR and Baarde YA (1996). Physiology of the neurotrophins. *Annual Review of Neuroscience* 19:289-317.

Li L, Crotty K, McCarthy SW, Palmer AA and Kril JJ (2000). A zonal comparison of MIB1-Ki-67 immunoreactivity in benign and malignant melanocytic lesions. *The American Journal of Dermatopathology*, 22:489-495.

Li L, Fukunaga-Kalabis M, Yu H, Xu X, Kong J, Lee JT and Herlyn M (2009). Human dermal stem cells differentiate into functional epidermal melanocytes. *Journal of Cell Science* 123:853-860.

Li C, Heidt DG, Dalerba P, Burant CF, Zhang L, Adsay V, Wicha M, Clarke MF and Simeone DM (2007). Identification of pancreatic cancer stem cells. *Cancer Research* 67:1030-1037.

Liang Y and Johansson O (1998). Light and electron microscopic demonstration of the p75 nerve growth factor receptor in normal human cutaneous nerve fibres: new vistas. *Journal of Investigative Dermatology* 111:114-118.

Lopez SM, Perez-Perez M, Marquez JM, Naves FJ, Represa J and Vega JA (1998) P75 and TrkA neurotrophin receptors in human skin after spinal cord and peripheral nerve injury, with special reference to sensory corpuscles. *The Anatomical Record* 251:371-383.

Lucas CR, Sanders LL, Murray JC, Myers SA, Hall RP and Grichnik JM (2003). Early melanoma detection: non-uniform dermoscopic features and growth. *Journal of the American Academy of Dermatology* 48:663–671.

Martin GR (1981). Isolation of a pluripotent cell line from early mouse embryos cultured in medium conditioned by teratocarcinoma stem cells. *Proceedings of the Natural Academy of Sciences* 78:7634-7638.

Masson P (1951). My conception of Cellular Nevi. *Cancer* 4:9–38.

Matsuda T, Nakamura T, Nakao K, Arai T, Katsuki M, Heike T and Yokota T (1999). STAT3 activation is sufficient to maintain an undifferentiated state of mouse embryonic stem cells. *The EMBO Journal* 18:4261-4269.

McKee PH, Colonje E and Granter SR (2005). Pathology of the skin. 3rd Edition, volume II. *Elsevier Mosby*.

Miller AJ and Mihm MC Jr. (2006). Melanoma. *The New England Jounal of Medicine* 355:51-65 (diagram).

Mishima Y (1965). Macromolecular Changes in Pigmentary Disorders. *Archives of Dermatology* 91:519-557

Murisier F, Guichard S and Beermann F (2007). The tyrosinase enhancer is activated by Sox10 and Mitf in mouse melanocytes. *Pigment Cell Research* 20:173-184.

Nichols J, Zevnik B, Anastassiadis K, Niwa H, Klewe-Nebenius D, Chambers I, Scholer H and Smith A (1998). Formation of pluripotent stem cells in the mammalian embryo depends on the POU transcription factor Oct4. *Cell* 95:379-391.

Nishimura EK, Jordan SA, Oshima H, Yoshida H, Osawa M, Moriyama M, Jackson IJ, Barrandon Y, Miyachi Y and Nishikawa SI (2002). Dominant role of the niche in melanocyte stem-cell fate determination. *Nature* 416:854–860.

Nishimura EK, Suzuki M, Igras V, Du J, Lonning S, Miyachi Y, Roes J, Beermann F and Fisher DE (2010). Key roles for transforming growth factor beta in melanocyte stem cell maintenance. *Cell Stem Cell* 6:130-140.

Niwa H, Miyazaki J and Smith AG (2000). Quantitative expression of Oct-3/4 defines differentiation, dedifferentiation or self-renewal of ES cells. *Nature Genetics* 24:372-376.

Nordlund JJ, Boissy RE, Hearing VJ, King RA, Oetting WS, Ortonne JP (2006). The pigmentary system: physiology and pathophysiology. 2nd Edition. *Blackwell Publishers.*

O'Brien CA, Pollett A, Gallinger S and Dick JE (2007). A human colon cancer cell capable of initiating tumour growth in immunodeficient mice. *Nature* 445:106-110.

Orkin SH (2005). Chipping away at the embryonic stem cell network. *Cell* 122:828–830.

Quintana E, Shackleton M, Foster HR, Fullen DR, Sabel MS, Johnson TM and Morrison SJ (2010). Phenotypic heterogeneity among tumorigenic melanoma cells from patients that is reversible and not hierarchically organized. *Cancer Cell* 18:510-523.

Quintana E, Shackleton M, Sabel MS, Fullen DR, Johnson TM and Morrison SJ (2008). Efficient tumour formation by single human melanoma cells. *Nature* 456:593-598.

Reya T, Morrison SJ, Clarke MF and Weissman IL (2001). Stem cells, cancer, and cancer stem cells. Nature 414:105-111.

Ricci-Vitiani L, Lombardi DG, Pilozzi E, Biffoni M, Todaro M, Peschle C and De Maria R (2007). Identification and expansion of human colon-cancer-initiating cells. *Nature* 445:111-115.

Rippey JJ (1994). General pathology: illustrated lecture notes. *Witwatersrand University Press.*

Robertson E (1987). Teratocarcinomas and embryonic stem cells: a practical approach (Oxford: IRL Press).

Ross AL, Sanchez MI, Grichnik JM (2011). Molecular Nevogenesis. *Dermatology Research and Practice*

Sakai D and Wakamatsu Y (2005). Regulatory mechanisms of neural crest formation. Cells Tissues Organs 179:24-35 (http://www.dev-neurobio.med.tohoku.ac.jp/en/?cat=15)

Savin C (1965). The blood vessels and pigmentary cells of the inner ear. *Annals of Otology, Rhinology and Laryngology* 74:611-623.

Schatton T and Frank MH (2008). Cancer stem cells and malignant melanoma. *Pigment Cell and Melanoma Research* 21:39-55.

Schwartz CM, Spivak CE, Baker SC, McDaniel TK, Loring JF, Nguyen C, Chrest FJ, Wersto R, Arenas E, Zeng X, Freed WJ and Rao MS (2005). NTera2: a model system to study dopaminergic differentiation of human embryonic stem cells. *Stem Cells and Development* 14:517-534.

Sheffield MV, Yee H, Dorvault CC, Weilbaecher KN, Eltoum IA, Siegal GP, Fisher DE and Chhieng DC (2002). Comparison of five antibodies as markers in the diagnosis of melanoma in cytologic preparations. *American Journal of Clinical Pathology* 118:930-936.

Shih IM, Elder DE, Hsu MY and Herlyn M (1994). Regulation of Mel-CAM/MUC18 expression on melanocytes of different stages of tumour progression by normal keratinocytes. *American Journal of Pathology* 145:837-845.

Sieber-Blum M, Grim M, Hu YF and Szeder V (2004). Pluripotent neural crest stem cells in the adult hair follicle. *Developmental Dynamics* 231:258-269.

Sieber-Blum M and Hu Y (2008). Mouse epidermal neural crest stem cell (EPI-NCSC) cultures. *Journal of Visualised Experiments* 9:772.

Sieber-Blum M, Schnell L, Grim M, Hu F, Schneider R and Schwab ME (2006). Characterisation of epidermal neural crest stem cell (EPI-NCSC) grafts in the lesioned spinal cord. *Molecular and cellular Neuroscience* 32:67-81.

Singh SK, Clarke ID, Terasaki M Bonn VE, Hawkins C, Squire JA and Dirks PB (2003). Identification of a cancer stem cell in human brain tumors. *Cancer Research* 63:5821-5828.

Singh SK, Hawkins C, Clarke ID, Squire JA, Bayani J, Hide T, Henkelman RM, Cusimano MD and Dirks PB (2004). Identification of human brain tumor initiating cells. *Nature* 432:396-401.

Snyder ML and Paulino AFG (2002) Melan-A as a useful diagnostic immunohistochemical stain for the diagnosis of primary sinonasal melanomas. *Head and Neck* 24:52-55.

Stewart FW and Copeland MM (1931). Neurogenic sarcoma. *American Journal of Cancer* 15:1235-1320.

Sun B, Chen M, Hawkes CL, Pereira-Smith OM and Hornsby PJ (2005). The minimal set of genetic alterations required for conversion of primary human fibroblasts to cancer cells in the subrenal capsule assay. Neoplasia 7:585-593.

Tai MH, Chang CC, Kiupel M, Webster JD, Olson LK and Trosko JE (2005). Oct4 expression in adult human stem cells: evidence in support of the stem cell theory of carcinogenesis. *Carcinogenesis* 26:495-502.

Taylor KLLister JA, Zeng Z, Ishizaki H, Anderson C, Kelsh RN, Jackson IJ and Patton EE (2011). Diferentiated melanocyte cell division occurs in vivo and is promoted by mutations in MITF. *Development* 138:3579-3589.

Thies A, Schachner M, Berger J, Moll I, Schultz HJ, Brunner G and Schumacher U (2004). The developmentally regulated neural crest-associated glycotope HNK-1 predicts metastasis in cutaneous malignant melanoma. *Journal of Pathology* 203:933-939.

Thomas S, Thomas M, Winker P, Babarit C, Xu, P, Speer MC, Munnich A, Lyonnet S, Vekemans M and Etchevers HC (2008). Human neural crest cells display molecular and phenotypic hallmarks of stem cells. *Human Molecular Genetics* 17:3411-3425.

Tolleson WH (2005). Human melanocyte biology, toxicology, and pathology. *Journal of Environmental Science and Health. Part C, Environmental Carcinogenesis and Ecotoxicology Reviews* 23:105–161.

Toma JG, Akhavan M, Fernandes KJL, Barnabe-Heider F, Sadikot A, Kaplan DR and Miller FD (2001). Isolation of multipotent adult stem cells from the dermis of mammalian skin. *Nature Cell Biology* 3:778-784.

Toma JG, McKenzie IA, Bagli D and Miller FD (2005). Isolation and characterization of multipotent skin-derived precursors from human skin. *Stem Cells* 23:727-737.

Trejo O, Reed JA and Prieto VG (2002). Atypical cells in human cutaneous re-excision scars for melanoma express p75NGFR, C56/N-CAM and GAP-43: evidence of early Schwann cell differentiation. *Journal of Cutaneous Pathology* 29:397-406.

Tucker MA, Fraser MC, Goldstein AM, Struewing JP, King MA, Crawford JT, Chiazze EA, Zametkin DP, Fontaine LS and Clark WH Jr. (2002). A natural history of melanomas and dysplastic nevi: An atlas of lesions in melanoma-prone families. *Cancer* 94:3192-3209.

Unna P (1893). Naevi and Naevocarcinoma. Klinische Wochenschrift (Berlin) 30*:14*.

Weicker TS, Luther H, Buettner P, Bauer J and Garbe C (2003). Moderate sun exposure and nevus counts in parents are associated with development of melanocytic nevi in childhood. Cancer 97:628-638.

Widera D, Zander C, Heidbreder M, Kasperek Y, Noll T, Seitz O, Saldamli B, Sudhoff H, Sader R, Kaltschmidt C and Kaltschmidt B (2009) Adult palatum as a novel source of neural crest-related stem cells. Stem Cells 27:1899-1910.

Winnepenninkx V and van den Oord JJ (2004). Immunophenotype and possible origin of nevi with phenotypical heterogeneity. *Archives of Dermatological Research* 296:49-53.

Wong CE, Paratore C, Rochat A, Pietri T, Suter U, Zimmermann DR, Dufour S, Thiery JP, Meijer D, Beermann F, Barrandon Y and Sommer L (2006). Neural crest–derived cells with stem cell features can be traced back to multiple lineages in the adult skin. *Cell* 175:1005-1015

Wulf GG, Wang RY, Kuenle I, Weidner D, Marini F, Brenner MK et al (2001). A leukemic stem cell with iontrinsic drug efflux capacity in acute myeloid leukemia, *Blood* 98:1166-73

Zimmerman AA and Becker SW (1959). Melanoblasts and melanocytes in fetal negro skin. *Ill Mongolian Medical Science Journal* 6:1.

6. Appendix A: Anatomical pathology reports

Naevus sample 1

Clinical details:
? Melanoma. ? Naevus.

Macroscopic:
Specimen labelled "R side" consisting of an ellipse of skin measuring 12x7x7 mm. there is a pigmented macule measuring 5 mm in greatest dimension. The closest resection margin is less than 2 mm.

Anatomical site: thigh
Lesions greatest dimension: 5 mm, additional dimension 0 mm
Pigmentation: diffuse
Edge: regular
Satellite nodule (s): absent

Microscopic:
Sections show skin with only junctional nests of naevoid cells and focal basal hyperpigmentation. The papillary dermis shows mild mononuclear perivascular inflammation abundant melanin incontinence with scattered melanophages. There is no evidence of dysplasia or malignancy present.

Diagnosis:
Skin of thigh, excisional biopsy – Junctional naevus.

Naevus sample 2

Clinical details
64 year old female. Naevus on back (left) – dark lesion, irregular border. Removed under LA.

Macroscopic:
Specimen labelled "back naevus" consists of a small ellipse of skin measuring 7x4x4 mm. There is a surface flat pigmented lesion approximately 3 mm in greatest dimension. It has an irregular edge. Specimen bisected.

Microscopic:
Sections of the skin biopsy show thin skin with occasional elongated rete ridges containing nests of bland melanocytes. Bridging of occasional rete ridges is also present. In addition, fibroplasia is noted. There is no pagetoid extension of the melanocytes.

Diagnosis:
Skin of back, excisional biopsy - features compatible with a Junctional naevus with mild atypia.

Naevus sample 3

Clinical details:
(L) thigh.

Macroscopic:
Specimen labelled "left" thigh consists of an ellipse of skin measuring 18x10x4 mm with long suture superior, short suture medial. A 4 mm in diameter pigmented flat, non-ulcerated, rectangular lesion is present centrally, 2 mm from superior margin and 6 mm from the medial margin. Superior inked green and inferior black. Serially sliced into 3 mm slices from medial to lateral.

Microscopic:
Sections show a symmetrical melanocytic lesion with epidermal and intradermal nests of melanocytes. No atypia or dermal mitoses were seen. Melanocyte maturation is present toward the base of the lesion. The features are those of a benign compound naevus. The lesion is fully excised.

Diagnosis
Skin of (L) thigh, excisional biopsy - Compound naevus.

Naevus sample 4

Clinical details:
? Benign naevus. ? Early melanoma.

Macroscopic:

Topographically unlabelled specimen consists of an ellipse of skin measuring 10x6x3 mm. The centre is hyperpigmented with a thin white rim.

Microscopic:
Sections of skin show nests of melanocytes in the dermis, with very scanty epidermal melanocytic nests. Maturation is seen deeper in the lesion. No atypia or mitoses are present. The lesion is completely excised.

Diagnosis
Skin of foot, excisional biopsy - Benign compound naevus.

Naevus sample 5

Clinical details:
Naevus of (R) buttock. ? Malignant melanoma.

Macroscopic:
Specimen labelled "biopsy" consists of a diamond of skin measuring 20x13x8 mm. A 6 mm pigmented lesion is visible on the surface. There is no suture to orientate the specimen.

Microscopic:
Sections of the buttock skin show:

- A melanocytic lesion situated in the dermis
- No junctional activity
- Composed of benign appearing melanocytes
- Melanin pigment in the neoplastic melanocytes and melanophages
- A single mitosis is present

Diagnosis:
Skin of buttock, excisional biopsy - Benign intradermal naevus

Naevus sample 6

Clinical details:
Tiny mole on anterior abdominal wall. Itch and increase in size recently.

Macroscopic:
Specimen consists of an ellipse of skin measuring 20x10 mm with underlying subcutaneous tissue measuring 20 mm in depth. A central 3 mm pigmented lesion is present 2 mm from the closest resection margin.

Microscopic:
Sections show a symmetrical lesion, composed of nests of naevus cells, predominantly in the dermis, with focal junctional activity. The dermal naevus cells show maturation toward the base of the lesion. No atypia or mitotic activity is present.

The features are those of a predominantly intra-dermal naevus. The lesion is completely excised.

Diagnosis
Skin of anterior abdominal wall, excision biopsy – Benign intradermal naevus.

Naevus sample 7

Clinical details:
? Melanoma. History of pencil lead / foreign body since childhood.

Macroscopic:
Specimen consists of skin excision right forearm
State of specimen: fixative
Dimensions of specimen: 12x7x3 mm
Pigmented lesion: Regular, 5 mm circular
Maximum diameter of dominant nodule: 5 mm
Intactness of skin over the dominant nodule
Minimum distance between the edge of the lesion and nearest resection margin: <1 mm

Microscopic:
Sections show a single fragment of skin with a dermal melanocytic lesion which is composed of dendritic melanocytes surrounded by dense collagen in the mid and upper dermis. There are some associated melanophages.
There are no atypical cells or mitotic figures present.

Diagnosis

Skin of right forearm, excisional biopsy - Blue naevus

Naevus sample 8

Clinical details:
Pigmented lesion tip of nose.

Macroscopic:
Specimen consists of a pigmented nodular lesion with a diameter of 5 mm. specimen bisected.

Microscopic:
Section shows a cellular and heavily pigmented (requiring melanin bleach) dermal lesion composed of epithelioid and spindle/dendritic melanocytes which expand the dermis. The lesion is symmetrical and there are no features of ulceration or junctional melanocytic activity. No mitotic figures and no necrotic foci are identified. The Ki-67 immunochemical stain does not display significant nuclear immunoreactivity. The closest resection margin is 1 mm.

There is no malignancy.

Diagnosis
Skin of nose, excision biopsy - Features compatible with a (epithelioid) blue naevus.

Naevus sample 9

Clinical details:
Excision biopsy (R) abdomen. Marker medial.

Macroscopic:
Topographically unlabelled specimen consisting of an ellipse of skin measuring 15x8x3 mm with central pigmented lesion. The central lesion has an irregular edge measuring 9 mm in greatest dimension approximately 1 mm from the short resection margin. No marker is present.

Microscopic:
Multiple levels on this biopsy show collections of melanocytes in an atrophic epidermis and underlying superficial dermis. The nests are confined to the basal layer with no pagetoid spread. A small shoulder is present at the edge of the lesion. Rete pegs are fused with superficial lamellar dermal fibrosis. The dermal collections of melanocytes show pleomorphism, occasional atypical cells with prominent nucleoli. No mitotic figures could be found.

Diagnosis
Skin of (R) abdomen, excisional biopsy - The features are of a dysplastic (= atypical) naevus.

Naevus sample 10

Clinical details:
Atypical naevus (L) calf.

Macroscopic:
Topographically unlabelled specimen received in fixative measuring 10x7x7 mm. pigmented lesion measures 9x6 mm. no dominant nodule. Intactness of skin over the nodule. Apices involved, side margins 0.5 mm. Bisected longitudinally.

Microscopic:
Histology shows intraepidermal lentiginous hyperplasia of melanocytes, occurring as single cells and in nests. There is hyperplasia and fusion of the rete pegs, often involving several pegs, and associated lamellar fibroplasias of the papillary dermis. There is a low grade cytological atypia of the epidermal melanocytes represented by focal hyperchromasia and nucleomegaly. The junctional component extends to the one apical resection margin.

There is a dermal component of melanocytes that show poor maturation and similar low grade cytological atypia. The junctional activity extends beyond the dermal component (shoulder effect). No mitosis are seen. Melanin pigment is preset in the dermis and associated with dermal melanocytes.

Diagnosis
Skin of (L) calf, excisional biopsy - Compound dysplastic naevus.

7. Appendix B – Ethics approval

UNIVERSITY OF CAPE TOWN

Health Sciences Faculty
Human Research Ethics Committee
Room E52-24 Groote Schuur Hospital Old Main Building
Observatory 7925
Telephone [021] 406 6626 • **Facsimile** [021] 406 6411
e-mail: shuretta.thomas@uct.ac.za

17 November 2010

HREC REF: 553/2010

Prof S Kidson
Human Biology

Dear Prof Kidson

PROJECT TITLE: STEM CELLS AND NEOPLASIA: A STUDY OF ACQUIRED MELANOCYTIC NAEVI.

Thank you for submitting your study to the Faculty of Health Sciences Human Research Ethics Committee for review.

It is a pleasure to inform you that the Ethics Committee has **formally approved** the above-mentioned study.

Approval is granted for one year till the 30th November 2011.

Please submit an annual progress report (FHS016) if the research continues beyond the approval period. Please submit a brief summary of findings if you complete the study within the approval period so that we can close our file.

Please note that the ongoing ethical conduct of the study remains the responsibility of the principal investigator.

Please quote the REC. REF in all your correspondence.

Yours sincerely

pp **PROFESSOR M BLOCKMAN**
CHAIRPERSON, HSF HUMAN ETHICS
Federal Wide Assurance Number: FWA00001637.
Institutional Review Board (IRB) number: IRB00001938

S Thomas

Western Cape Government
Health

STRATEGY & HEALTH SUPPORT
healthres@pgwc.gov.za
Tel: +27 21 483 9905; Fax: +27 21 483 9895
1e Floor, Norton Rose House, 8 Riebeek Street, Cape Town, 8001
www.capegateway.gov.za

REFERENCE: RP 159/2011
ENQUIRIES: Dr V Appiah-Balden

Department of Human Biology,
6th Floor Anatomy Building,
Medical campus.
University of Cape Town,
Anzio Road.
Observatory,
7935

For attention: Professor S.H. Kidson, Professor G. Todd,
Dr A. Bonthuys

Re: Stem cells and Neoplasia: A study of acquired Melanocytic naevi.

Thank you for submitting your proposal to undertake the above-mentioned study. We are pleased to inform you that the department has granted you approval for your research.
Please contact the following people to assist you with any further enquiries.

Victoria Hospital	**Dr N Peer**	**(021) 7978065**

Kindly ensure that the following are adhered to:

1. Arrangements can be made with managers, providing that normal activities at requested facilities are not interrupted.
2. Researchers, in accessing provincial health facilities, are expressing consent to provide the department with an electronic copy of the final report within six months of completion of research. This can be submitted to the provincial Research Co-ordinator (healthres@pgwc.gov.za).
3. The reference number above should be quoted in all future correspondence.

Yours sincerely,

DR T NALEDI
DIRECTOR: HEALTH IMPACT ASSESSMENT
DATE: 12/12/2011

CC **MR B MASHEDI** **CEO: VICTORIA HOSPITAL**

Page 1 of 1

8. Appendix C – Immunofluorescence protocol

Protocol for immunofluorescence of formalin-fixed paraffin embedded skin samples

1. Place sections on hot plate for 15 minutes, or until was thoroughly melted
2. Rehydrate sections according to standard protocol as follows:
    i. Xylol 2x 10 min
    ii. 100% alcohol 3x 3min
    iii. 90% alcohol 1x 1min
    iv. 70% alcohol 1x 1min
    v. Running tap water 1x 1min
3. Antigen retrieval: Heat induced antigen retrieval (HIER) in pressure cooker
    i. Pre-heat pressure cooker, using water
    ii. Place 50 ml buffer solution in a coplin jar containing processed slides (≤ 4 slides per jar)
    iii. Place coplin jars in pre-heated pressure cooker:
        i. 0.01 M Citrate buffer (pH 6) for 20 minutes. Allowed to cool for 10 minutes.
        ii. 1 mM EDTA (pH 8) for 5 minutes . Allowed to cool for 10 minutes
4. Wash slides in PBS 2x 5min
    i. Here washes in 1x PBS-Tween20 and 1x PBS-TritonX 100 may be tried if sub-optimal staining
5. Dry slides and placed in incubation chamber
6. Block with 1% BSA in 1x PBS for 2 hours at room temperature
7. Remove blocking solution and apply primary antibody
    i. Primary antibodies diluted in blocking solution (1% BSA in 1x PBS)
    ii. Dilutions optimised for each antibody
    iii. Dual staining – apply cocktail of primary antibodies, ensure end concentration of each antibody is correct
    iv. Incubate at 4 °C overnight in an incubation chamber
8. Following day, wash slides in PBS 3x 5min
9. Dry slides and apply secondary antibody
    i. Secondary antibodies diluted in blocking solution (1% BSA in 1x PBS)
    ii. Dilutions optimised for each secondary antibody (1:500 Alexa and 1:1000 Cy3)
    iii. Dual staining – apply cocktail of secondary antibodies, ensure end concentration of each antibody is correct
10. Incubate at room temperature for 2 hours in an incubation chamber, in the dark
11. Wash slides in PBS 3x 5min, in the dark
12. Dry slides and mount using Mowiol
13. Allow to dry at room temperature for a minimum of 1 hour, in the dark
14. Store slides at 4 °C in the dark until viewed